

Cocrystal Formation

- Thermodynamics and Kinetics -

DISSERTATION

zur Erlangung des
Doktorgrades der Ingenieurwissenschaften (Dr.-Ing.)
des
des Zentrums für Ingenieurwissenschaften
der
Martin-Luther-Universität Halle-Wittenberg,

vorgelegt

von Frau M. Sc. Kyeongsill Lee
geb. am 04.10.1984 in Daejeon, South Korea

Referee:

- 1) Prof. Dr. Dr. h.c. Joachim Ulrich
- 2) Prof. Dr.-Ing. Kwang-Joo Kim
- 3) Prof. Dr. Izumi Hirasawa

Tag der öffentlichen Verteidigung: 26.11.2015

Halle (Saale), den 30.11.2015

DEDICATED TO

My Parents

Mr. Hanchul Lee

Mrs. Hyunja Shin

My elder sister & younger brother

Acknowledgement

This research work was carried out at the chair of Thermal Process Technology, Center of Engineering at Martin Luther University Halle-Wittenberg, Germany and partly at Hanbat National University, Korea between 2010 and 2015 as PhD student.

I wish to express my deepest gratitude to my supervisor Prof. Joachim Ulrich for the opportunity to join his group. His dedication, enthusiasm, and passion for research motivated me to pursue a PhD under his guidance throughout the work. The training, support, and encouragement he has given me during my years will be remembered forever. In this context I would like to specially acknowledge my supervisor at Hanbat National University, Prof. Kwang-Joo Kim who has continuously supported, encouraged, and inspired me in more than just the subject of this thesis. Both supervisors, Prof. Joachim Ulrich and Prof. Kwang-Joo Kim, allowed me to achieve my tasks and aims.

This thesis was made possible by a scholarship of Germany Government of Sachsen-Anhalt GradFC. I am grateful to the Germany Government for the scholarship from Graduiertenförderungsgesetz Programme which enabled me to undertake a PhD program at Martin Luther University Halle-Wittenberg.

Co-workers in the TVT and CPEL are thanked for creating a motivating working environment, their support, help and moment we spent together I will remember forever. First of all I want to special thank you goes to my TVT colleagues Sandra, Lydia, Viviana, Dan, Anke, Robert, Patrick and Phuong who have helped me feel at home through their support and kindness especially during my years of stay in Germany. Furthermore, a special thank you goes to the students which were under my supervision: Dang, Owusu, Tung, Tacky, Hyojun, Chaeho and Inkue. Especially I would like to thank Dang for making my work place such a pleasant place to be. I will always remember your enthusiasm, encouragement and kindness.

A big thank you also goes to my friends for all the fun times and being there for me. In particular, Hojin, Kabshin, Boseob, Sanghoon and Hyeran are thanked for their friendship throughout my studies.

Where I am today is because of my family, and this dissertation is a reflection of the love and support that my family has given me throughout my life. This journey would have been difficult without their support, patience and sacrifices. I specially thank my mother, Mrs. Shin, who never gives up believing me. She has inspired me to work hard in order to achieve my

goals. I would also like to acknowledge my sister and little brother, Hyojin and Pyeongik, who has supported me to keep moving through difficult times. Their care and patience has been a tremendous source of strength for me throughout my studies.

Kyeongsill Lee

Table of Contents

ACKNOWLEDGEMENT	I
TABLE OF CONTENTS.....	III
1. INTRODUCTION	1
2. FUNDAMENTALS	3
2.1 COCRYSTAL DEFINITION	3
2.2 DESIGN OF COCRYSTALS.....	4
2.3 SCREENING OF COCRYSTALS	5
2.4 COCRYSTAL PHASE DIAGRAMS	7
3. AIM OF RESEARCH.....	10
4. MATERIALS AND METHODS	12
4.1 MODEL SYSTEMS.....	12
4.2 CHEMICALS	12
4.3 METHODS	14
4.4 SOLID-STATE AND ANALYTICAL INSTRUMENTATION.....	15
4.4.1 Powder X-ray diffraction	16
4.4.2 Differential scanning calorimetry	16
4.4.3 Scanning electron microscopy.....	16
4.4.4 Raman spectroscopy	16
4.4.5 FT-IR spectroscopy.....	17
4.4.6 Single crystal diffraction	18
5.1 N-H...O, O-H...O HYDROGEN BONDED SUPRAMOLECULAR FORMATION IN THE COCRYSTAL OF SALICYLIC ACID WITH N-CONTAINING BASES	19
5.1.1 Preparation of cocrystals.....	21
(1) Salicylic acid/ 4,4'dipyridyl (2:1)	21
(2) Salicylic acid/ nicotinamide (1:1)	22
(3) Salicylic acid/ isonicotinamide (1:1).....	22
(4) Salicylic acid/ piperazine (1:0.5).....	22
(5) Salicylic acid/ N,N'-diacetylpiperazine (2:1)	23
5.1.2 Results and discussion.....	23
5.1.2.1 Thermal analysis of cocrystals.....	24

Table of Contents

5.1.2.2 X-ray powder diffraction	25
5.1.2.3 SEM analysis	27
5.1.2.4 Crystal structures	28
(1) Salicylic acid/4,4'dipyridyl (2:1)	28
(2) Salicylic acid/nicotinamide (1:1)	29
(3) Salicylic acid/isonicotinamide (1:1)	30
(4) Salicylic acid/piperazine (1:0.5)	30
(5) Salicylic acid/N,N'-diacetylpiperazine (2:1)	31
5.1.2.5 Raman spectroscopy	32
5.1.3 <i>Monitoring cocrystal formation by raman spectroscopy</i>	33
5.1.4 <i>Property of cocrystal</i>	35
5.1.5 <i>Conclusions</i>	36
5.2 IN-SITU MONITORING OF THE FORMATION OF A SALICYLIC ACID-4,4'DIPYRIDYL COCRYSTAL USING RAMAN SPECTROSCOPY	38
5.2.1 <i>Identification of ASA-4,4'-bipy cocrystals</i>	38
5.2.1.1 Single-crystal x-ray crystallography	38
5.2.1.2 XRD analysis	41
5.2.1.3 DSC analysis	43
5.1.2.4 SEM analysis	45
5.2.1.5 Raman spectroscopy analysis	45
5.2.1.6 FTIR spectroscopy analysis	46
5.2.2 <i>In-situ monitoring during formation of cocrystals using Raman spectroscopy</i>	48
5.2.3 <i>Conclusion</i>	54
5.3 SUPRAMOLECULAR REAGGREGATION OF ASPIRIN-4,4'DIPYRIDYL COCRYSTALS FROM COCRYSTALS OF SALICYLIC ACID-4,4'DIPYRIDYL	55
5.3.1 <i>Cocrystal preparation</i>	56
5.3.2 <i>Identification of cocrystals</i>	56
5.3.3 <i>In-situ measurement in cooling crystallization (Solid-state)</i>	59
5.3.3.1 Optical microscope	59
5.3.3.2 Powder x-ray diffraction	61
5.3.3.3 Raman spectroscopy	62
5.3.3.4 Thermal analysis (DSC)	63
5.3.4 <i>In-situ monitoring the transformation of cocrystals using Raman spectroscopy (in solution)</i>	64

Table of Contents

5.3.5 Formation and transformation of cocrystals.....	68
5.3.6 Conclusions	69
5.4 FORMATION OF SALICYLIC ACID/4,4'DIPYRIDYL COCRYSTALS BASED ON THE TERNARY PHASE DIAGRAM.....	70
5.4.1 Experimental methods	70
5.4.1.1 Construction of the ternary phase diagram	70
5.4.1.2 Determination of solubility.....	70
5.4.2 Solubility curves.....	71
5.4.3 The ternary phase diagram	73
5.4.4 Solid-state characterization	74
5.4.5 The formation of cocrystals: the thermodynamic and the kinetic effect.....	79
5.4.6 Conclusions	83
6. SUMMARY OF THE CONCLUSIONS.....	84
7. SUMMARY	86
8. ABBREVIATIONS AND SYMBOLS	88
9. REFERENCES	90
10. DECLARATION	101
CURRICULUM VITAE	102

1. Introduction

The selection of appropriate crystalline forms of active pharmaceutical ingredients, APIs, is an important decision for drug development. Drug molecules in a solid form are in either crystalline or amorphous state. Most drugs are formulated in the crystalline state due to the instability of an amorphous state [Vip01]. Crystalline solids can show polymorphs, solvates and if water is the solvent hydrates or cocrystals. Figure 1.1 shows a classification of API solid form based on structure and composition. A solid can be crystallized with solvent molecules to form hydrates or solvates. It can also form multicomponent molecular crystals with compounds other than solvents. The cocrystals can also show hydrate or solvate forms and all multicomponent crystals can form polymorphs. The API solid form is affected in its physic-chemical properties such as solubility, dissolution rates, hygroscopicity, physical and chemical stability, and mechanical properties as a consequence of differences in molecular interactions, structure and composition that result in different energetic [Vip01, Cui07].

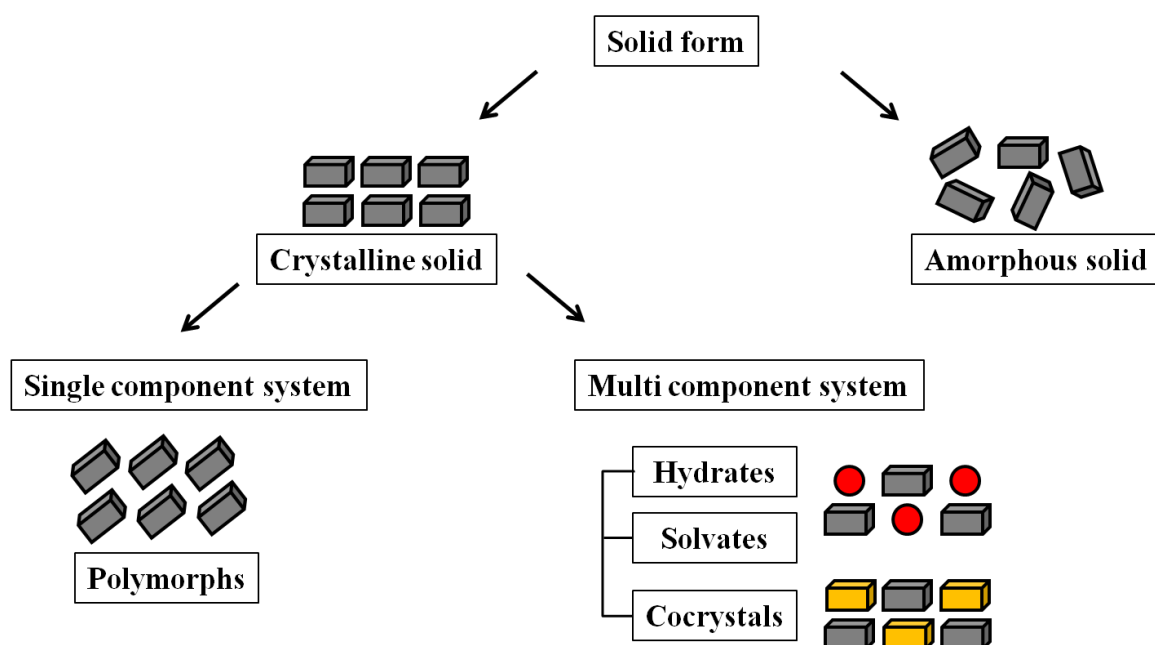


Figure 1.1: Classification of API solid forms based on structure and composition. Gray, red, blue, and yellow represent drug, water/solvent, and coformer molecules, respectively.

As a result, solid form screening is a common element embedded in the search for materials with optimal properties for drug development [Cho08].

1. Introduction

Cocrystals have recently emerged as an interesting alternative solid form for producing a large diversity of solid forms of drug substances exhibiting the proper balance of important properties for development into a viable and effective drug product [Fle03, Aak07]. Until now, numerous APIs have been cocrystallized with different co-formers and new solid forms of cocrystals are on the rise [Chi07, Chi07]. In spite of the successful application of cocrystallization to manipulate the physical properties of a drug, no marketed drug products utilize cocrystals. One reason for this may be related to concern about the thermodynamic stability of cocrystals [Sch09]. Metastable crystal forms have a risk to change to different forms during the shelf life of the product, hence pharmaceutical companies reluctant to develop metastable forms. Therefore, an understanding of the thermodynamics that will support cocrystal formation would be useful.

2. Fundamentals

2.1 Cocrystal definition

To date, the term cocrystal is still under debate in the academic literature [Bon07, Cun03, Des03]. Cocrystals can be defined in a number of ways [Sch09, Sha08]. However, everyone can agree that a cocrystal is a crystalline form that comprised of at least two different components (commonly called multicomponent crystals). A restrictive definition utilised is that a crystal that is built up of a structurally homogeneous crystalline material in which two or more component's molecules are present in a well-defined stoichiometric ratio [Aak07]. A cocrystal in definition of a pharmaceutical is a single crystalline solid that incorporates two neutral molecules at ambient temperature. One being an API and the other is the excipient or another drug which is called coformer [Cui07, Fle03, Chi07, Bon07, Aak05, Vis06, Tra05]. The definition of a cocrystal is important because of intellectual property implications, since cocrystals are novel, useful and non-obvious form of drugs [Tra07].

The structural differences between salts and cocrystals have been under discussions for a long time [Aak07]. The understanding of the fundamental difference between a salt formation and a cocrystal is very important to both pro-formulation activities and chemical/pharmaceutical development aspects. A pharmaceutical cocrystal is formed by a neutral API and a coformer through noncovalent interactions. For cocrystals, there is no transfer or only a partial transfer, whereas a salt is formed by an ionic API and an acid with a proton completely transferred [Aak07, Vis06]. The difference between a salt and a cocrystal is that whether a proton transfer has happened or not. A proton transfer is thought mainly to depend on the pKa values of the components which could help to guide the eventual formation of a salt or a cocrystal [Chi07, Ste10].

There is sometimes a confusion between cocrystals and solvates/hydrates. The main difference between solvate/hydrate and cocrystals is the physical state of the isolated pure components. If one component is a liquid at room temperature, the crystals are designated as solvates or hydrates. If both components are solids at room temperature, the crystals are designated as cocrystals [Bic11]. Hydrates and solvates of an API similarly impact on the biopharmaceutical properties. API hydrates have lower aqueous solubilities, while solvates have higher aqueous solubilities when compared to anhydrous crystalline phases [Zhu96, Zhu97, Gho95].

2.2 Design of cocrystals

Cocrystal design is based on crystal engineering principles with intention to improve the solid-state properties of an API without affecting its intrinsic structure. Crystal engineering defined as the understanding of intermolecular interactions in the context of crystal packing and in the utilization of such understanding in the design of new solids with desired physical and chemical properties by Desiraju [Des03]. Cocrystals are constructed synthons that are basic structural units formed with non-covalent interaction such as van der Waals interactions, π - π stacking interactions, and hydrogen bonds between the functional groups in the molecules [He08, Kav10, Des95, Des02]. Most often the synthons involve hydrogen bonds in crystal engineering utilized in cocrystal in pharmacy [Sve99], because of their strength, directionality and frequency of occurrence [Fle03, Chi07, Tra05, Tra06, Ett90, Ett89, Ett91]. Figure 2.1 shows some examples of commonly occurring synthons in the crystal structures of single and multicomponent materials.

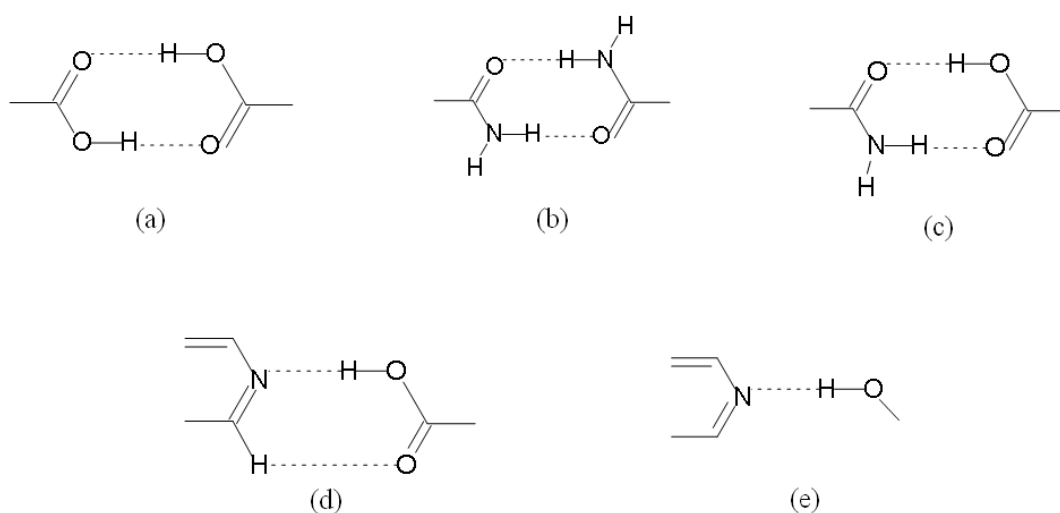


Figure 2.1: Typical hydrogen bonds utilized in crystal engineering are; (a) acid-acid, (b) amide-amide homosynthons, (c) amide-acid, (d) pyridine-acid and (e) pyridine-hydroxyl.

The basis of packing motifs and hydrogen bond patterns in the crystal structure are followed by hydrogen bonding rules for organic compounds proposed by Etter [Ett91, Ett90].

- (i) All good proton hydrogen bond acceptors will be used when there are available hydrogen bond donors.
- (ii) All acidic hydrogens in molecules will be used for hydrogen bond formation.

3. Aim of Research

- (iii) The best proton donors and acceptors remaining after intramolecular hydrogen bond formation form intermolecular hydrogen bonds to one another.

Using these rules, hydrogen bond and synthon formation between functional groups can be predicted [Lei69, Lei76, Ett85], and a more detailed strategy for cocrystal design can be derived.

The molecular structure of salicylic acid (Figure 2.2) shows two functional groups, a carboxylic acid (-COOH) and an alcohol (-OH) that has one hydrogen bond and two acceptors.

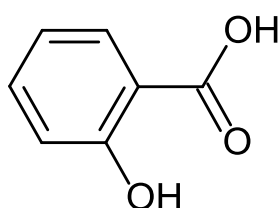


Figure 2.2: *Molecular structure of salicylic acid.*

2.3 Screening of cocrystals

As pharmaceutical cocrystals have rapidly emerged as a new class of API solids, much work has focused on exploring the crystal engineering and design strategies. The ability of an API to form a cocrystal is dependent on various parameters including the types of the coformer, the solvents, the stoichiometric ratio of API/coformer, the crystallization method, etc. The schematic of the strategies for preparation of cocrystals is shown in Figure 2.3.

In order to obtain a desired cocrystal, the study of the structure of the target API molecule and the functional group which is capable of forming supramolecular crystal with a coformer should have priority.

The next step is the selection of cofomers that are compatible with a particular API. The coformer has to be a pharmaceutically acceptable/approved compound classified as generally recognized as safe (GRAS) for use as food additives.

Cocrystal screening is the next step to determine if a particular coformer candidate is able to cocrystallize with a targeted API. Cocrystal screening can be accomplished via a number of methods, including a slow solvent evaporation crystallization, a solvent-reduction (slurring,

3. Aim of Research

solvent-drop grinding), a solvent free (grinding, hot-stage thermal microscopy) techniques [Hab09, Lee10, McN06, Ber08, Zha07].

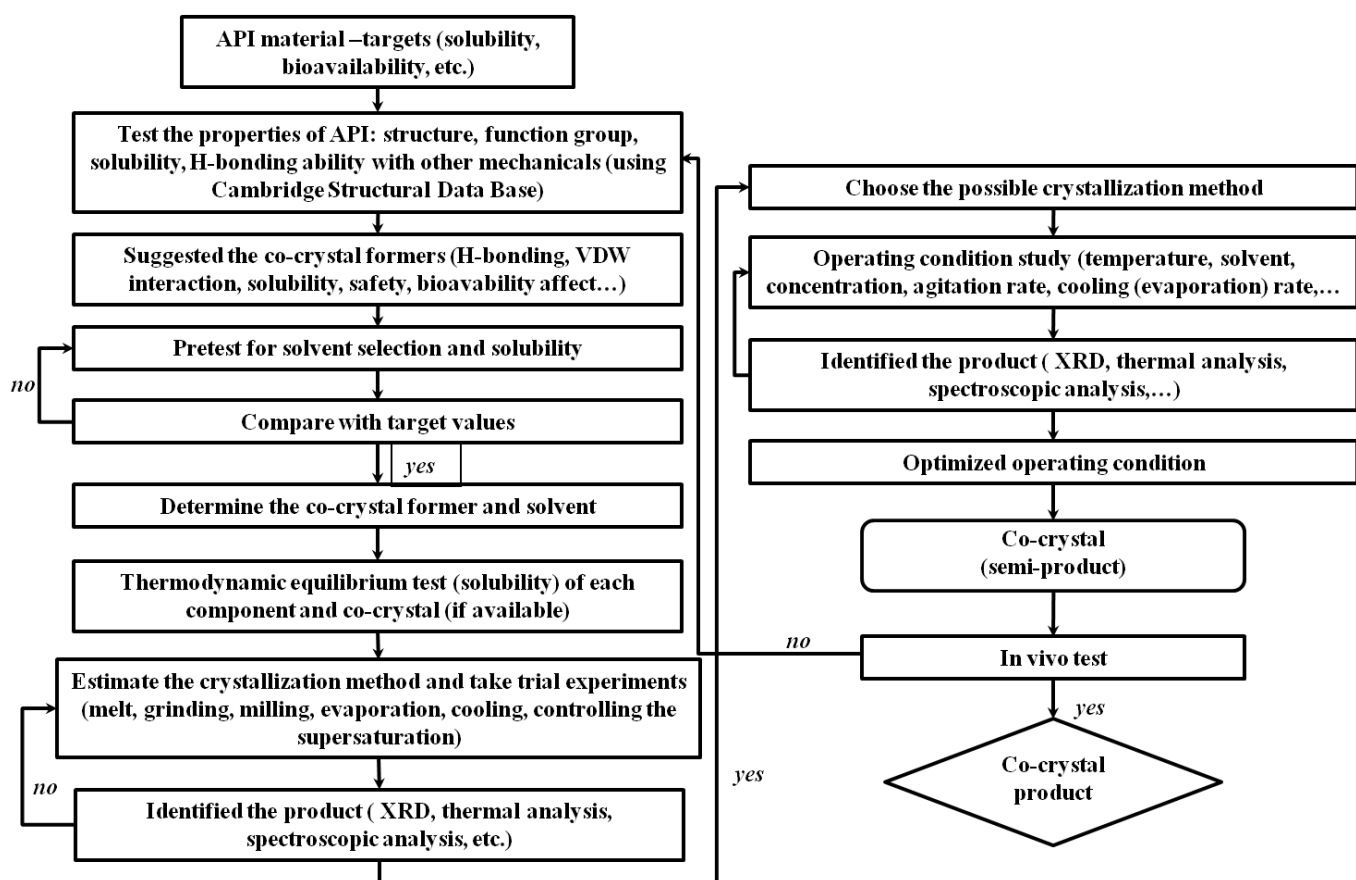


Figure 2.3: Steps for cocrystal design and preparation strategies.

To date, many ways of methods and tools have been proposed for the preparation of cocrystals in line with an increased interest in that area. Cocrystals involving supramolecular synthons are usually synthesized by slow evaporation from a solution that contains stoichiometric amounts of the components. Also sublimation, growth from the melt, slurries, and grinding two solid cocrystal formers in a ballmill are suitable methodologies. Table 2.1 presents different methods to prepare cocrystals [Moh11].

3. Aim of Research

Table 2.1: *Cocrystal formation methods involving solid-based and liquid-based methods.*

Liquid-based method	Evaporative crystallization, slurry conversion, reaction cocrystallization, cooling crystallization, liquid-assisted grinding, sonication, supercritical fluid crystallization, and spray drying.
Solid-based method	Melt crystallization (hot stage microscopy and differential scanning calorimetry), solid-state grinding, and twin screw extrusion.

The most obvious way to prepare pharmaceutical cocrystal is to simply crystallize by slow evaporation of supersaturated solutions in the presence of the cocrystal former. Most commonly supersaturation is achieved by slowly cooling/evaporation an undersaturated mixture until the solubility limit is passed. Solution crystallization offers the possibility to obtain single crystals for structure determination. This is of great importance since most of the cocrystals which qualify for single X-ray diffraction testing, can only be prepared through this method.

2.4 Cocrystal phase diagrams

Binary phase solubility diagrams (PSDs) and ternary phase diagrams (TPDs) have recently been used to explain the solubility and stability of cocrystals in solution [Chi07, Neh05]. PSDs have been used for studies of the solution concentration at equilibrium with solid phases and the relative thermodynamic stability of cocrystals. TPDs show the total composition of solid phases and liquid phases at equilibrium and comparative region for effective cocrystallization processes.

The key source of information for the experimental design is the ternary phase diagrams (TPD) [Chi07, Ain09, Mah09], which demonstrates the thermodynamic stability regions and predicts the transformation of the phase of a compound at a given temperature, pressures and composition [Rag09]. If the ternary phase diagram of a system is known, crystallization experiments to acquire the cocrystal can be efficiently designed and the outcome can be predicted. In addition, such phase information can provide insights into the existence of metastable states and potential dissolution pathways [Chi07, Neh05, Cha09, Rod06]. Ternary phase diagrams are equilateral triangles with each side as a scale of the mole or

3. Aim of Research

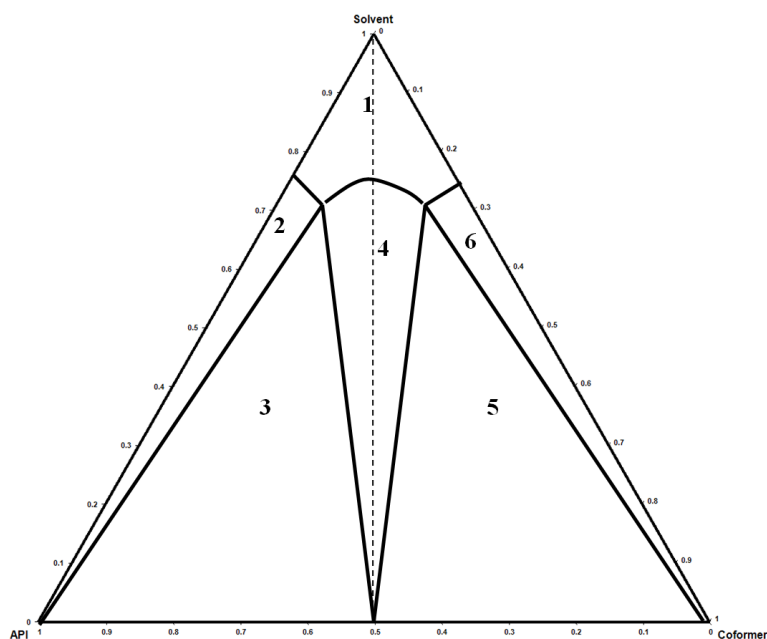
weight fraction. Each corner in the triangle represents a pure compound A, B and C. The triangle's sides represent the binary systems A+B, A+C and B+C. In the specific case of cocrystal phase diagrams, the three components are the solvent, the API and the coformer.

The relative solubility of two components affects highly the ternary phase diagram. A cocrystal may be defined as a congruent or incongruent depending on how it dissolves in a solvent system [Coq14]. Figure 2.4a shows a schematic ternary phase diagram for two components of similar solubility in the given solvent. The dotted line joining 'A' to solvent intersects the stable solubility curve. It is easy to crystallize 'A' by mixing API and conformer in stoichiometric amounts [Lor01, Fri09]. The diagram shown in Figure 2.4b is more complicated and represents the case in which the components have very different solubilities. The dotted line segment intersects the metastable solution curve of 'A' [Chi07].

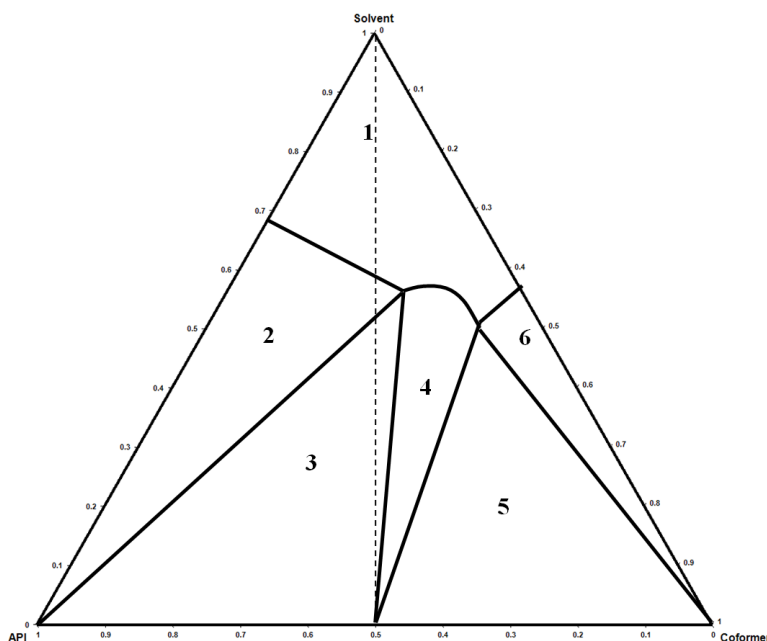
The diagram is divided into several areas with different composition and phases as summarized in Figure 2.4. There are six zones in a typical TPD for a system with one cocrystal for an API and a coformer. Domain 1 is the solution phase region where all materials are dissolved and only a homogeneous liquid phase is presented. Also it is bounded by solubility curves of the API, the cocrystal, and the coformer. In zone 2 and 6 there is the solid API compound and the coformer and the liquid phase, respectively. In zone 3 there is the solid compound API, the solid cocrystal and a liquid phase. Zone 4 represents the pure solid cocrystal in equilibrium with the liquid. Zone 5 is like zone 3 the coformer with the solid compound B, the solid cocrystal and a liquid phase.

The TPD can be constructed if the equilibrium between the API and coformer, the cocrystal and the solution is determined by measuring and calculating the solubility curves of the API, the coformer, and the cocrystal in solvent.

3. Aim of Research



(a)



(b)

Figure 2.4: Schematic ternary phase diagram, which shows a 1:1 cocrystal, (a) similar solubilities between two components (API and coformer) in a solvent and (b) different solubilities of API and coformer, i.e., when the solubility of API is much lower than that of the coformer. Figure adapted from Rager and Hilfiker [Rag09].

3. Aim of research

Considering the entire field of cocrystals in pharmacy there are still many questions which need to be answered. In order to investigate how cocrystals for pharmaceutical uses can be improved in their solubility and how the dissolution properties of poorly water soluble drugs can be improved under different environments. A fundamental understanding of the formation mechanisms, solution behaviour and solid-state properties of cocrystals with pharmaceutical substances has to be found. Main important items should be found by a case study in the following steps.

- Identify the parameters for the formation and the characterization of five pharmaceutical cocrystals of the poorly water soluble drug of salicylic acid (SAA), which are salicylic acid/ 4,4'dipyridyl (2:1), salicylic acid/ nicotinamide (1:1), salicylic acid/ isonicotinamide (1:1), salicylic acid/ piperazine (1:0.5), and salicylic acid/ N,N'-diacetylpiperazine (2:1) with N-containing bases.
- Establish a screening for cocrystal formation using Raman spectroscopy for an in-situ monitoring. Apply this method to determine cocrystal formation mechanisms during solution crystallization.
- Identify two different cocrystals (salicylic acid/ 4,4'dipyridyl cocrystal and aspirin/4,4'dipyridyl cocrystal) and investigate the transformation behavior in a solution medium using Raman spectroscopy for the in-situ monitoring.
- Investigate the effect of kinetics and thermodynamics such as cooling rate and temperature on formation of cocrystals based on the ternary phase diagram.
- Gain a fundamental understanding of the solubility behaviour of cocrystals and provide insights into the solubility advantage offered by cocrystals.

Subsequent chapters in this thesis will address the above objectives. This thesis is organized in 10 chapters. A short overview of the state of the art is given in the second chapter. In the second chapter an overview of pharmaceutical cocrystals, their definitions and basic theories are summarized. Model APIs and cofomers and analytical approaches used in this study are specified in chapter 4. The principles and experimental set-up of all analytical techniques were given in this chapter. Findings of the novel cocrystals are presented in the "results and disussion" chapter. Chapter 5 examines all characterised

3. Aim of Research

cocrystals with different stoichiometric molar ratio under different conditions. All of the resulting cocrystals-forms of the case studies- salicylic acid/ 4,4'dipyridyl (2:1), salicylic acid/ nicotinamide (1:1), salicylic acid/ isonicotinamide (1:1), salicylic acid/ piperazine (1:0.5) and salicylic acid/ N,N'-diacetylpiperazine (2:1) (derived from the reaction between aspirin and piperazine) will be given. The key element to form cocrystals which is hydrogen bonding in intermolecular interaction is presented in this chapter. The molecular structures of all of the cocrystals were also presented. In chapter 5.2 the method to monitor the formation of cocrystals during solution crystallization was established. After the identification of the cocrystals of the selected systems the screening of the formation of cocrystals was investigated in real time by means of Raman spectroscopy. Chapter 5.3 investigated the mechanism of transformation of cocrystals (salicylic acid/ 4,4'dipyridyl cocrystal and aspirin/4,4'dipyridyl cocrystal) in real time. The solubility of cocrystals and physical properties were studied and compared. Chapter 5.4 focuses on the mechanism of cocrystal formation based on ternary phase diagram. The effects of thermodynamic and kinetic factors in formation are presented in this chapter. The formation of salicylic acid/ 4,4'dipyridyl cocrystal and aspirin/4,4'dipyridyl cocrystal in dependence on kinetic and thermodynamic parameters in specific region are presented. Chapter 6 summarized the presented work and results obtained from this work.

4. Materials and methods

4.1 Model systems

The materials and analytical methods used in this study were introduced in this chapter. The selection of model substances was governed by the intention to form cocrystal depending upon the crystallization conditions of the main compound.

4.2 Chemicals

All materials were used as received without further purification.

Table 4.1: Summary of raw materials for the experiments.

Materials	Formula	Purity/grade	Manufacturer
Acetylsalicylic acid	$C_9H_8O_4$	$\geq 99.0\%$	Sigma-Aldrich (USA)
4,4'-bipyridine	$C_{10}H_8N_2$	98.0%	Acros (USA)
Nicotinamide	$C_6H_6N_2O$	99.0%	Samchun (Korea)
Isonicotinamide	$C_6H_6N_2O$	99.0%	Sigma-Aldrich (France)
Piperazine	$C_4H_{10}N_2$	99.0%	Sigma-Aldrich (Netherlands)
Ethanol	CH_3CH_2OH	$\geq 99.0\%$	Duksan (Korea)
1-propanol	C_3H_8O	99.0%	Samchun (Korea)

In this study, salicylic acid and N,N'-diacetylpiperazine was mentioned even though they were not used as a raw material. Both of them are derived from reaction between aspirin and piperazine.

Acetylsalicylic acid was chosen as the main model drug in this study. Acetylsalicylic acid is one of the most widely used analgesic, antipyretic, and anti-inflammatory drugs. It also has an antiplatelet effect and is used long-term, at low doses, to help prevent heart attacks, strokes, and blood clot formation in men at high risk for developing this condition [Gla01, Ouv04, Bon07, Mit67, Aju09]. However, Aspirin has a poor solubility in water and its rapid

4. Materials and methods

hydrolysed in the plasma to salicylic acid. Acetic acid has a limited intravenous use. In contrast, all coformers used in this study are common coformer in crystallization and have a high solubility and permeability. Especially, 4,4'-bipyridine, which is the main model drug is the most often found in cocrystal structures in the CDS database [Fáb09] because it is a rigid molecule and a good hydrogen bond acceptor, making it ideal for cocrystal studies.

Unfortunately, the Aspirin used as raw material transforms into multicomponent crystal forms of salicylic acid during co-crystallization as to be seen to this study. Salicylic acid also has antiseptic, preservative, analgesic, and anti-inflammatory properties, covering a broad spectrum of applications, including skin care products [Fon10, Mac00]. It is used for treatment of acne and psoriasis due to its anti-fungal properties to eliminate fungus involved in infection [Van90]. However, salicylic acid has low solubility in water, which influences its bioavailability.

Up to date several cocrystals of salicylic acid have been reported with several coformers [Chi07, Ber08, Sin74, Tak08, Lim97, Gos06, Buč09, Lu08, Chi09, Hua10, Elb10, Elb10, Hat10, Sko09, Wal03 Che10] such as meloxicam [Che10], temozolomide, carbamazepine [Chi09, Hua10], theophylline [Chi07], caffeine [Buč09, Lu08], creatinine [Gos06] and 4,4'-bipyridine [Wal03]. Cocrystals of salicylic acid (SAA) with 4,4'-bipyridine (4,4'-bipy), nicotinamide (NCT), isonicotinamide (INCT), piperazine (PPZ) and N,N'-diacetylpiperazine (N,N'-DPPZ) were selected as model systems in this study. The crystallographic and physicochemical properties of these cocrystals are described in chapter 4.

The molecular structure of salicylic acid (Figure 4.1) shows two functional groups, a carboxylic acid (-COOH) and an alcohol (-OH) that has one hydrogen bond and two acceptors. The Figure 4.2 indicates the molecular structure of coformers used in this study.

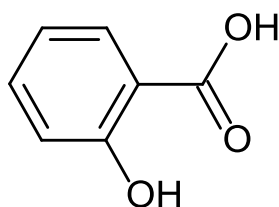


Figure 4.1: *Molecular structure of salicylic acid.*

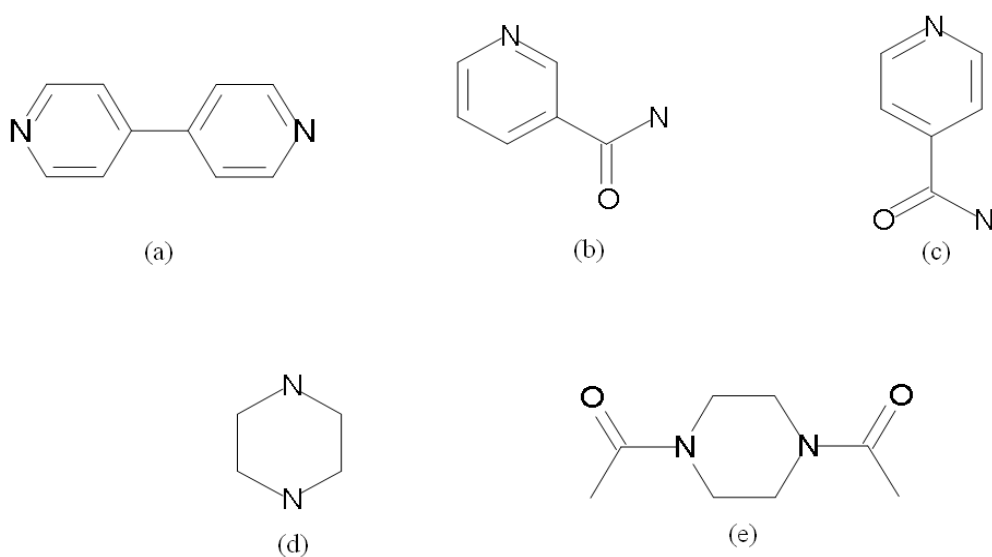


Figure 4.2: Molecular structure of the coformers (a) 4,4'-bipyridine, (b) nicotinamide, (c) isonicotinamide, (d) piperazine, and (e) N,N'-diacetylpiperazine.

4.3 Methods

Preparation of SAA cocrystals: Formation of cocrystal experiments were based on cooling/evaporation crystallization of mixed solutions which are appropriate in stoichiometric molar ratio of aspirin with coformers. The solutions were prepared by dissolving appropriate amounts of starting materials in 1:1, 1:2, 1:3, and 2:1 stoichiometric ratios in an appropriated solvent. The solutions were cooled down and slowly evaporated under magnetically stirred condition at desired temperatures for 24 hours. Suspensions were filtered together under vacuum and dried at 40°C overnight in the oven. The specific experiment to get a suitable crystal for single crystal X-ray diffraction was conducted similarly to those explained above. The crystals of suitable size and quality were obtained by seeding with small quantities of material from previous experiments.

In-situ monitoring crystallization: In-situ monitoring of formation of SAA cocrystals was carried out using a Raman spectrometer. The experimental set-up used in cocrystal formation is shown in Figure 4.3. It consists of a crystallizer, a Raman spectrometer measurement system and a temperature control system. These experiments were conducted as batch crystallization. During the operation, Raman spectra, PXRD pattern and temperature were measured with the elapsing time.

4. Materials and methods

The crystallizer was a 100mL-jacketed cylindrical glass vessel equipped with a U-type impeller (agitation rate: 400rpm, impeller diameter: 4cm, vessel diameter: 5cm) and the Raman MR probe. After the mixture of aspirin and its coformer were dissolved in a solvent at a higher temperature than its saturation temperature, the solution was maintained at 50°C under agitation until equilibrium is reached. Then the batch temperature is cooled down at a cooling rate of 0.5K/min. The crystals were sampled at regular intervals using a solid-liquid separator with a glass vacuum filter. Raman spectra of solution and suspension were measured using a Kaiser Raman RXN2 immersion sensor with respect to time.

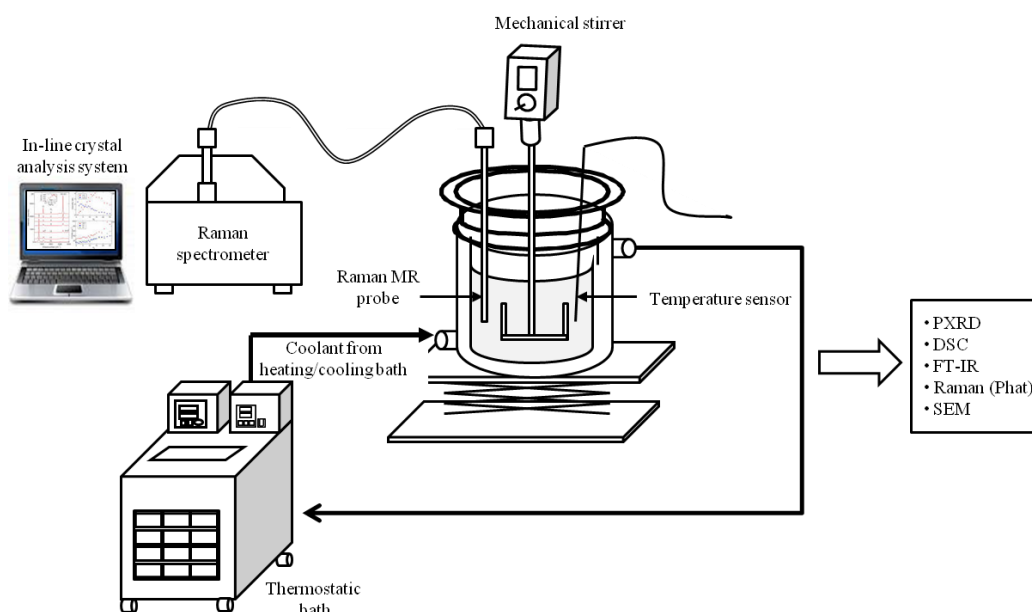


Figure 4.3: Experimental batch crystallization set-up, equipped with a Raman spectroscopy probe.

4.4 Solid-state and analytical instrumentation

XRD, DSC, FTIR, Raman spectroscopy, SEM, and single crystal X-ray diffraction techniques have been applied to characterize the new cocrystals obtained by crystallization. The starting materials, salicylic acid, formed cocrystal such as: SAA-4,4'-bipy cocrystal, SAA-NCT cocrystal, SAA-INCT cocrystal, SAA-PPZ cocrystal, and SAA-NDAP cocrystal. The molecule structures of all of these cocrystals which are identified by single crystal X-ray diffraction were also presented in this work.

4. Materials and methods

4.4.1 Powder x-ray diffraction

PXRD pattern of various powder samples were collected using a SamrtLab X-ray diffractometer (Rigaku) with Cu K α radiation (1.54056 Å). The tube voltage of 45kV and amperage of 200mA were set. The sample was placed on a silicone plate at room temperature. Data were collected from 3° to 45° (2 θ) at a continuous scan rate of 5K/min.

4.4.2 Differential scanning calorimetry

DSC is a thermoanalytical technique in which the thermal effects of tested samples, such as the melting point and enthalpies of phase transitions, can be measured. In this study, DSC measurements were carried out using a Mettler Toledo DSC 1 instrument which was calibrated for temperature and cell constants using indium. Test samples (3-5mg) were analyzed in crimped aluminium pans with pinholes. Measurements were carried out in the DSC from 0 to 300°C at a heating rate of 10K/min under nitrogen purge at 50mL/min.

4.4.3 Scanning electron microscopy

Scanning electron microscopy is an electron microscope that provides images of a sample through scanning the sample with a focused beam of electrons. In this study, the surface and morphology characteristics of cocrystals were investigated by scanning electron microscopy (SEM: JSM-6300, JEOL, Japan). The test samples were sprinkled onto double-sided tapes that had been secured onto an aluminium stub and then have seen gold sputter-coated under an argon atmosphere. The specimens were scanned with an electron beam of voltage of 5-10kV.

4.4.4 Raman spectroscopy

Raman spectroscopy is a spectroscopic technique used to observe vibrational, rotational, and other low-frequency modes in a system [Ger89]. Raman spectra of solid phases were collected with a Kaiser Raman RXN2 (Kaiser Optical Systems, Ann Arbor MI, USA) equipped with a light-emitting diode laser (785nm, 450mW) as an excitation source. The spectra range of this system is from 100 to 1890 cm⁻¹, and the spectra acquired with 4 cm⁻¹ spectral width and 30 s exposure. The iCRaman software (Mettler-Toledo) was used in combination with this system. The measurements were carried out at room temperature.

4. Materials and methods

Solid phase transformations were monitored using the same Raman spectroscopy as used in Raman spectra characterization, with an immersion probe in-situ Raman spectroscopy method. The immersion probe was used to collect the spectra of the solid phase in aqueous suspensions. The spectra were collected between 100 and 1890 cm^{-1} with a resolution of 4 cm^{-1} . The experimental set up is shown in Figure 4.4. The Raman spectra during in-situ monitoring were automatically collected every 2 minutes for 5 hours controlled by the iCRaman software.

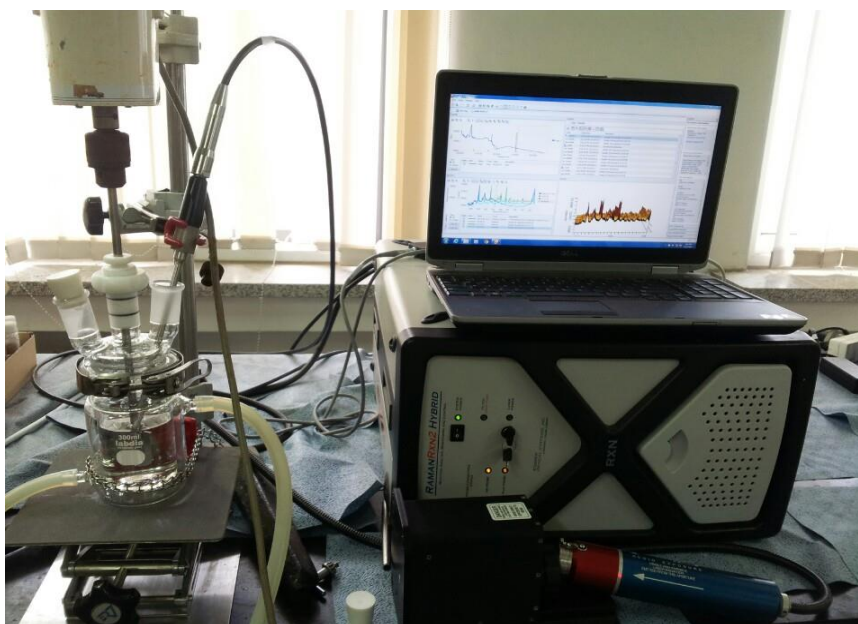


Figure 4.4: Raman spectrometer for in-situ monitoring.

4.4.5 FT-IR spectroscopy

The FTIR data were obtained using instrumentation and procedures similar to those described earlier [Don94, Car98]. The infrared spectra were collected on a Thermo Nicolet 6700 Fourier transform infrared spectrometer to identify functional groups by measuring the absorption at characteristic wavelengths of bonds that vibrate independently of one another. The sample was prepared using the KBr pellet technique. A small amount of sample was mixed thoroughly with relative more KBr in a mortar while grinding with the pestle to form a homogeneous powder, which was then compressed into a solid pellet. Measurement settings for the Thermo Nicolet 3700 FTIR are: A total of 256 scans, a resolution of 4 cm^{-1} and a data range of 4000-400 cm^{-1} .

4.4.6 Single crystal diffraction

Single crystal X-ray diffraction studies were performed on a Bruker SMART APEX II CCD diffractometer with graphite monochromated Mo K α radiation ($\lambda=0.71073$ Å). The structure solution, refinement and data output were fully solved by direct methods refined by full-matrix least squares against F^2 all reflections using SHELXTL. Mercury 3.1 was used for the creation of figures and analysis of hydrogen bonding interactions in the crystal lattice.

5. Results and discussion

5.1 N-H...O, O-H...O hydrogen bonded supramolecular formation in the cocrystal of salicylic acid with N-containing bases

All resulting cocrystals, salicylic acid/4,4'dipyridyl (2:1), salicylic acid/nicotinamide (1:1), salicylic acid/isonicotinamide (1:1), salicylic acid/piperazine (1:0.5) and salicylic acid/ N,N'-diacetylpiperazine (2:1) (derived from reaction between aspirin and piperazine) are obtained from solution cooling/evaporation experiments (these are referred to as guest molecules below: see Table 5.1). The structural analysis has shown that the well-known COOH...N heterosynthon was considered the key element in the cocrystals design strategy. The carboxylic acid...pyridine hydrogen bond is an often used supramolecular synthon. The crystal structures of all cocrystals were determined by single-crystal X-ray¹.

It has been attempted to introduce a N-containing base molecule into the center of the hydrogen bonded dimers of salicylic acid. Even though aspirin is chosen as raw material in the preparation of the cocrystals, unexpectedly the ketene functional group on the aspirin has dropped off in the formation of the cocrystal (Fig. 5.1). A similar kind of geometric change has been reported in the structure of salicylic acid and piperazine [Sko09].

In the salicylic acid molecule, the carboxylic acid is acting as the hydrogen-bond donor. When salicylic acid interacts with cofomers including the N atoms, the molecules form N...H-O and N-H...O hydrogen bonds as shown in Fig. 5.2. In the salicylic acid molecule, there is the carboxylic acid acting as the hydrogen-bond donor. The structure of pure salicylic acid exhibits interactions between *o*-H atoms and hydroxyl groups [Sko09].

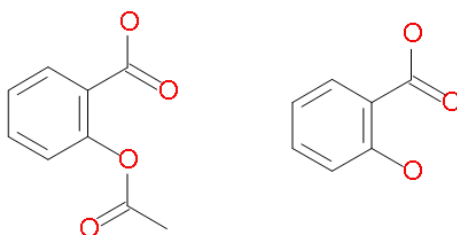
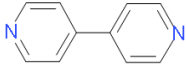
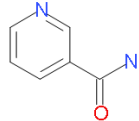
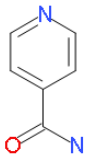
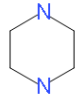
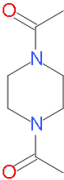


Figure 5.1: Structural formula of aspirin (Acetylsalicylic acid), salicylic acid (derived from reaction between aspirin and cofomers).

¹ CCDC 1043461, 1043489, 1043490, 1043492 and 1043493 contains the supplementary crystallographic data for this paper. Crystallographic data for all structures have been deposited to the Cambridge Crystallographic Data Centre and is available free of charge from <http://www.ccdc.cam.ac.uk>.

5. Results and discussion

Table 5.1: Guest molecules structure and melting point data for starting material and new cocrystals.

Cocrystal	Cocrystal former	Molar ratio	Cocrystal former mp [°C]	Cocrystal mp [°C]	
1		4,4'dipyridyl	2:1	112.16	156.10
2		Nicotinamide	1:1	129.51	138.19
3		Isonicotinamide	1:1	128.11	131.72
4		Piperazine	1:0.5	112.68	221.50
5		N,N'-diacetylpiperazine	2:1	-	112.27

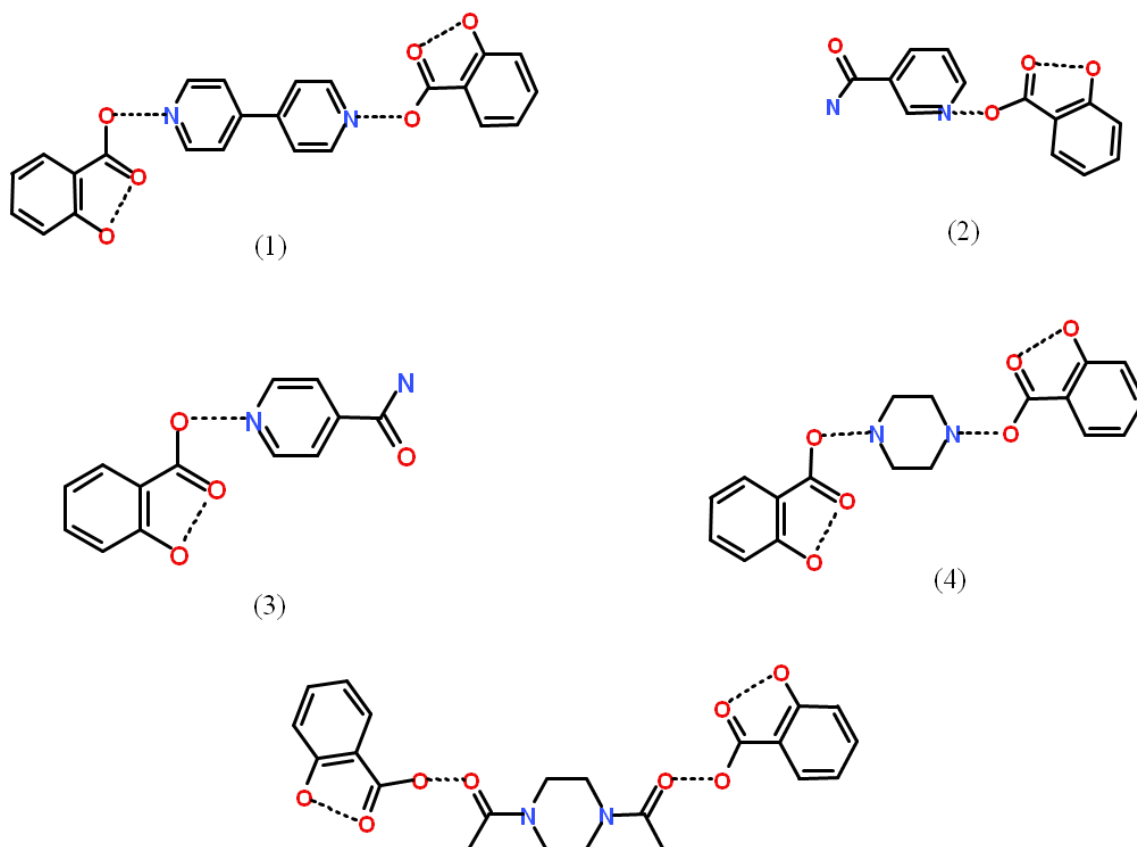


Figure 5.2: Hydrogen bond interactions between salicylic acid and coformers. (1) formed between salicylic acid and 4,4'-dipyridyl, (2) formed between salicylic acid and nicotinamide, (3) formed between salicylic acid and isonicotinamide, (4) formed between salicylic acid and piperazine, and (5) formed between salicylic acid and N,N'-diacetylpiperazine.

5.1.1 Preparation of cocrystals

(1) Salicylic acid/ 4,4'-dipyridyl (2:1)

Separate saturated solutions of aspirin (0.3602g, 2.0mmol) and 4,4'-dipyridyl (0.1560g, 1.0mmol) in ethanol at 50°C were combined under stirring for 30min. The vial containing a clear solution was then cooled rapidly to 35°C producing crystals. Afterwards, the colorless crystals were isolated on a 3µm filter paper (Whatman) using a vacuum filtration and were stored at 40°C overnight to dry. The specific experiment suitable to generate crystals for single crystal X-ray diffraction was conducted similarly by dissolving aspirin (3.603g, 0.02mol) and 4,4'-dipyridyl (1.561g, 0.01mol) in 15mL ethanol at 50°C. The clear solution was allowed to cool very slowly to 35°C and crystals of suitable size and quality were obtained by seeding with small quantities resulting from previous experiments. The obtained crystals

5. Results and discussion

were determined to be from aspirin that had been hydrolyzed to 2-hydroxybenzoic acid and co-crystallized with 4,4'-dipyridyl in a 2:1 stoichiometry.

(2) Salicylic acid/ nicotinamide (1:1)

Separate saturated solutions of aspirin (0.1801g, 1.0mmol) and nicotinamide (0.1222g, 1.0mmol) in ethanol at 50°C were combined under stirring for 30min. The vial containing a clear solution was then cooled rapidly to 30°C producing single crystals. Afterwards, the colorless crystals were isolated on a 3µm filter paper (Whatman) using a vacuum filtration and were stored at 40°C overnight to dry. There was no further specific experiment carried out to obtain suitable crystals for single crystal X-ray diffraction since the crystal size and quality from the screening experiments was already good enough. The obtained crystals showed that aspirin had been hydrolyzed to 2-hydroxybenzoic acid and the co-crystallized with nicotinamide in an 1:1 stoichiometry.

(3) Salicylic acid/ isonicotinamide (1:1)

The mixture of aspirin (0.1802g, 1.0mmol) and isonicotinamide (0.1222g, 1.0mmol) in ethanol of 1mL at 60°C was dissolved and combined under stirring for 30min. The vial containing a clear solution was then cooled rapidly to 45°C producing crystals. Afterwards, the colorless crystal were isolated on a 3µm filter paper (Whatman) using vacuum a filtration and were stored at 40°C overnight to dry. There was no need for further specific experiments to obtain suitable crystals for single crystal X-ray diffraction since the crystal size and quality from screening experiments produced already good enough crystals. The obtained crystals showed that aspirin had been hydrolyzed to 2-hydroxybenzoic acid and co-crystallized with isonicotinamide in an 1:1 stoichiometry.

(4) Salicylic acid/ piperazine (1:0.5)

Separate saturated solutions of aspirin (0.1804g, 1.0mmol) and piperazine (0.1737g, 2.0mmol) in 1-propanol at 60°C were combined under stirring for 30min. The vial containing a clear solution was then cooled rapidly to 50°C producing single crystals. Afterwards, the colorless crystals were isolated on a 3µm filter paper (Whatman) using a vacuum filtration and were stored at 40°C overnight to dry. The specific experiments of suitable crystals for single crystal X-ray diffraction were conducted similarly by dissolving aspirin (1.8017g, 0.01mol) and piperazine (1.728g, 0.02mol) in 15mL of 1-propanol at 50°C. The clear solution was allowed to cool with a cooling rate of 0.1K/min to 10°C and crystals of suitable size and

5. Results and discussion

quality were obtained by seeding with small quantities from previous experiments. The obtained crystals showed that aspirin had been hydrolyzed to 2-hydroxybenzoic acid and had co-crystallized with piperazine in an 1:0.5 stoichiometry.

(5) Salicylic acid/ N,N'-diacetylpiperazine (2:1)

Separate saturated solutions of aspirin (0.7206g, 4.0mmol) and piperazine (0.1723g, 2.0mmol) in 1-propanol at 60°C were combined under stirring for 30min. The vial containing a clear solution was then cooled rapidly to 50°C producing single crystals. Afterwards, the colorless crystals were isolated on a 3µm filter paper (Whatman) using a vacuum filtration and were stored at 40°C overnight to dry. A specific experiment suitable to produce crystals for single crystal X-ray diffraction was conducted similarly by dissolving aspirin (3.60g, 0.02mol) and piperazine (0.8614g, 0.01mol) in 30mL of ethanol at 50°C. The clear solution was allowed to cool with a cooling rate of 0.1K/min to 10°C and crystals of suitable size and quality were obtained by seeding with small quantities from previous experiments. The obtained crystals showed that aspirin had been hydrolyzed to 2-hydroxybenzoic acid and had co-crystallized with N,N'-diacetylpiperazine which is derived from piperazine in a 2:1 stoichiometry.

5.1.2 Results and discussion

Each solid phase which was obtained via an experiment was first characterized using DSC, PXRD, Raman and SEM. The molecule structure of the coformers, molar ratio and melting point of the starting materials and the cocrystals is to be found in Table 5.1.

Of the available pharmaceutically acceptable guest candidates, is the nitro group having the ability to form hydrogen bonds with the carboxyl group. Therefore, it is the strategy of crystal design to use the N atom as hydrogen donor in the multicomponent cocrystals which is assembled in the carboxyl-pyridyl group. The functional group including the N atom is considered to be a good supramolecular substrate since they represent one of the most ubiquitous functional groups in crystal engineering and it can readily form hydrogen bondings [Wey09]. Commonly it forms heterosynthons with the carboxylic OH groups [Rem03, Tra05, Aak05, Aak06]. The expected carboxylic acid bond to the nitrogen hydrogen is present in all structures but # 5.

The asymmetric unit of 1-5 consists of salicylic acid and is one of the coformer molecules used in this study (Fig. 5.2). In all cocrystals, strong intramolecular hydrogen bonds of O-H...O type are formed within the salicylic acid molecules, with a carbonyl O atom of the

5. Results and discussion

carboxylic acid group as acceptor and OH group at the ortho position as donor. Hence, the carboxylic acid OH group remains available as donor for another hydrogen bond formation with guest molecules. The details of the hydrogen bond geometry are listed in Table 5.2.

Table 5.2: *Hydrogen bond geometry for cocrystals.*

Cocrystal	D-H...A	d(D-H)	d(H...A)	d(D...A)	<(DHA)
1	O(9)-H(9)...N(11)	1.02(2)	1.60(2)	2.6237(12)	174.8(15)
	O(10)-H(10)...O(8)	1.06(2)	1.58(2)	2.5625(13)	152.7(17)
	O(9)-H(9)---N(11)	1.07(2)	1.53(2)	2.5999(17)	177.7(16)
2	O(10)-H(10)---O(8)	1.01(2)	1.62(2)	2.5460(16)	151.0(2)
	N(19)-H(19A)---O(10)#1	0.899(18)	2.095(19)	2.989(2)	172.0(15)
	N(19)-H(19B)---O(18)#2	0.89(2)	1.96(2)	2.851(2)	171.1(17)
3	O(1)-H(1)...O(2)#1	0.84	1.91	2.633(2)	144.2
	O(3)-H(3A)...N(1)#2	0.84	1.81	2.647(2)	171.5
	N(1)-H(1)...O(1)#3	0.88	2.49	3.035(3)	120.7
	N(1)-H(1)...O(2)#4	0.88	2.51	2.742(3)	96.1
4	N(1)-H(1)...O(3)#5	0.88	2.26	2.700(3)	110.9
	O(1)-H(1A)...O(3)#1	0.84	1.80	2.538(3)	145.8
	C(8)-H(8B)...O(2)#6	0.99	2.43	3.356(4)	155.6
5	O(1)-H(1)...O(2)#1	0.84	1.87	2.6023(17)	145.2
	O(3)-H(3A)...O(4)#3	0.84	1.73	2.5333(16)	159.8

5.1.2.1 Thermal analysis of cocrystals

The DSC, thermo analysis gives the thermal behavior and comparable results for the starting materials and the synthesized cocrystals as shown in Fig. 5.3. The DSC data of the cocrystals revealed single sharp endotherms at 156.1, 138.79, 131.72, 221.50 and 112.27°C for the product 1 to 5, respectively. These endothermic peaks occurred at significantly different temperatures as those of 4,4'-dipyridyl (112.16°C), nicotinamide (129.51 °C),

5. Results and discussion

isonicotinamide (128.11 °C) and piperazine (112.68 °C), indicating the formation of cocrystals and not the physical mixtures. Melting points of the cocrystals 1 to 3 and 5 are between those of the starting materials (salicylic acid and co-former guest), whereas the melting point of cocrystal 4 is higher than that of either components. Endothermic melting peaks in the DSC curves showing the thermal behavior of cocrystals are narrow and no signals at higher temperatures indicating the presence of pure components as can be seen.

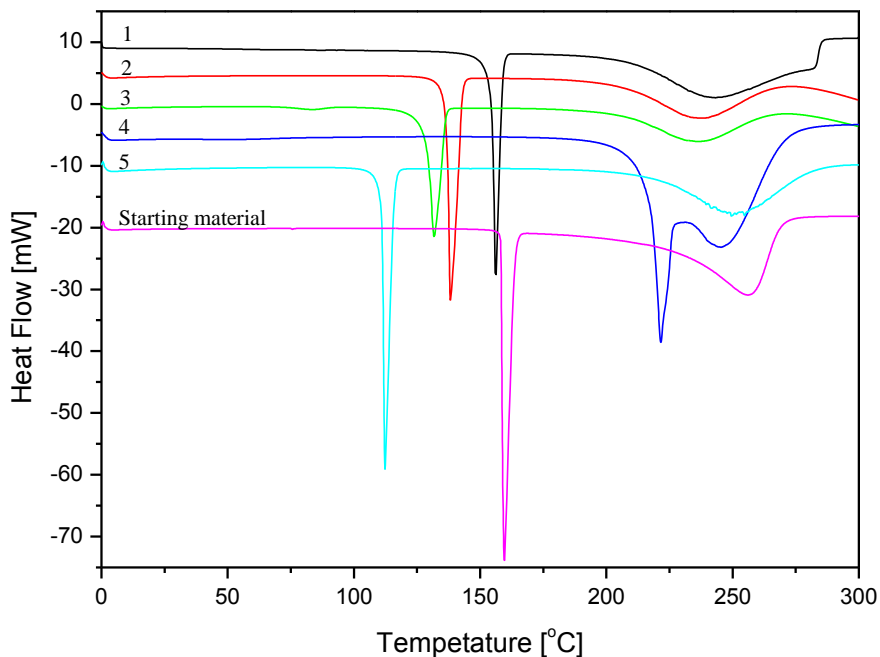


Figure 5.3: DSC curves for cocrystals 1 to 5 and the starting material.

5.1.2.2 X-ray powder diffraction

X-ray powder diffraction measurements were conducted for the synthesized cocrystals. Each cocrystal exhibits a unique PXRD pattern in comparison to salicylic acid and the co-formers, as shown in Fig. 5.4. It reveals the information about the crystal structure, chemical composition, and physical properties of the material and also helps in structural characterization. The experimental PXRD pattern for cocrystals confirmed that salicylic acid formed new solid phases with all five coformers. For the combination with all coformers completely new pattern were obtained indicating the formation of new solid forms. An experimental PXRD pattern as well as pattern calculated from single crystal data is obtained for each cocrystal. The X-ray powder pattern calculated from single crystal data for cocrystals exhibited good agreement with the experimental pattern obtained for the sample (Fig. 5.5). The pattern show that the main diffraction peaks of the starting material and the

5. Results and discussion

coformers disappeared, and are replaced by a series of new peaks. PXRD analysis supports the formation of cocrystals of salicylic acid and five diverse cofomers by showing different pattern in the diffractogram with that of the starting material.

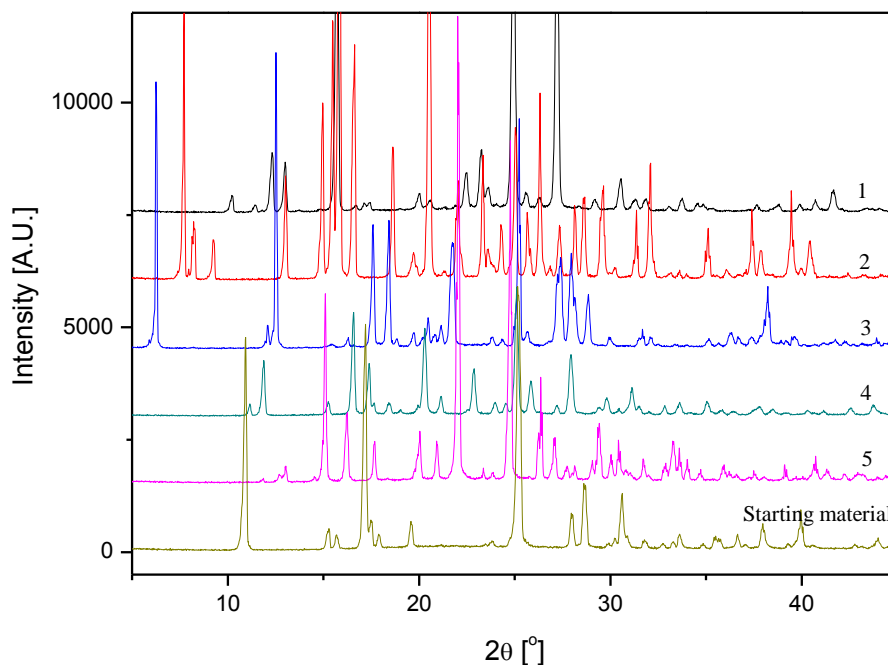


Figure 5.4: Comparison of experimental PXRD pattern for the cocrystals 1 to 5 and starting material. 1: salicylic acid/4,4'dipyridyl (2:1), 2: salicylic acid/nicotinamide (1:1), 3: salicylic acid/isonicotinamide (1:1), 4: salicylic acid/piperazine (1:0.5), and 5: salicylic acid/ N,N'-diacetyl/piperazine (2:1).

5. Results and discussion

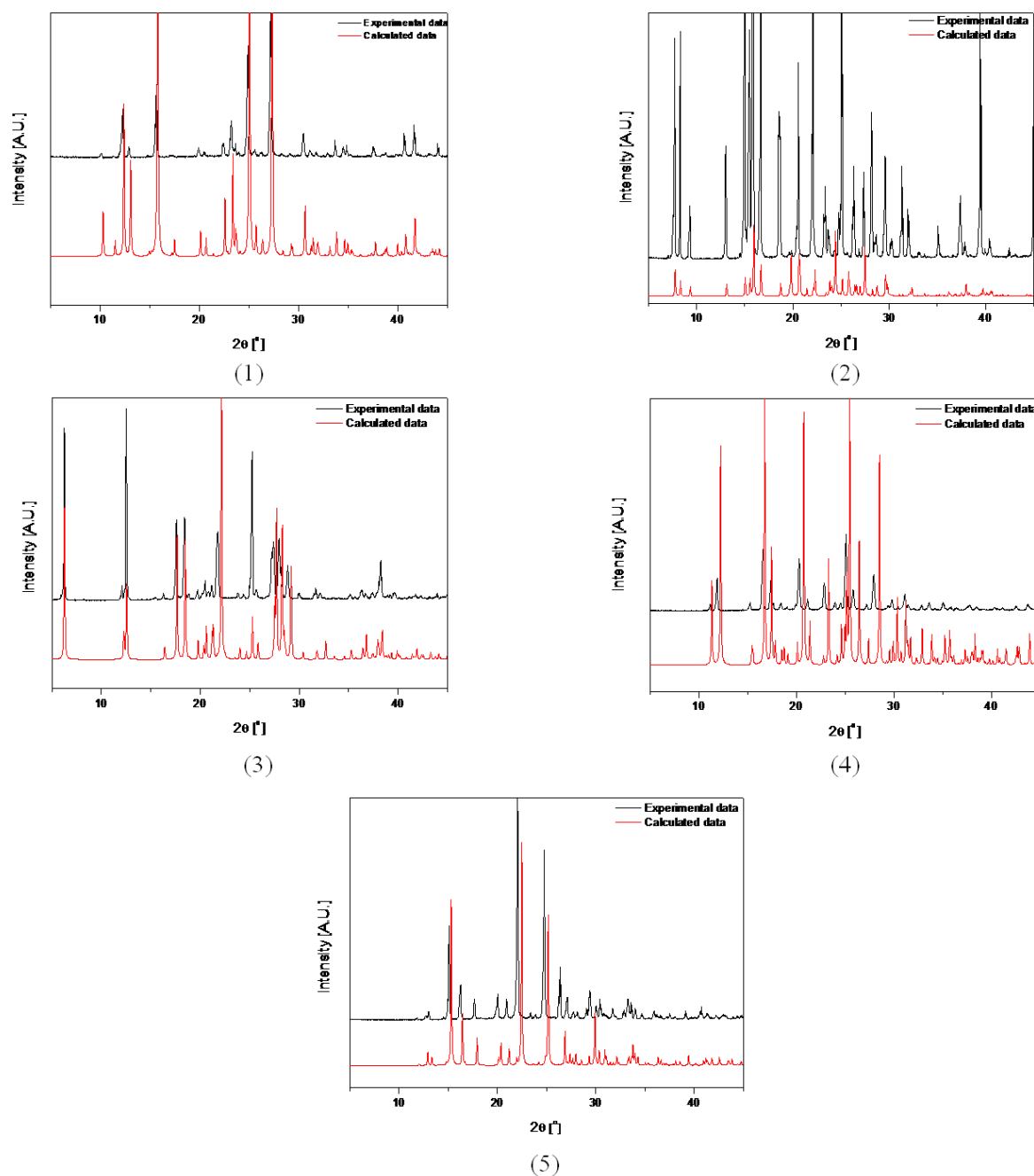


Figure 5.5: Comparison of experimental PXRD pattern and calculated PXRD pattern from single crystal data for the cocrystals 1 to 5 .1: salicylic acid/4,4'dipyridyl (2:1), 2: salicylic acid/nicotinamide (1:1), 3: salicylic acid/isonicotinamide (1:1), 4: salicylic acid/piperazine (1:0.5), and 5: salicylic acid/ N,N'-diacetylpiperazine (2:1).

5.1.2.3 SEM analysis

Single crystals of SAA-4DP, SAA-NCT, SAA-INCT, SAA-PRZ, and SAA-N,N'-

5. Results and discussion

diacetylpiperazine have characteristic morphologies, which allow to distinguish them from SAA under a SEM (Fig. 5.6).

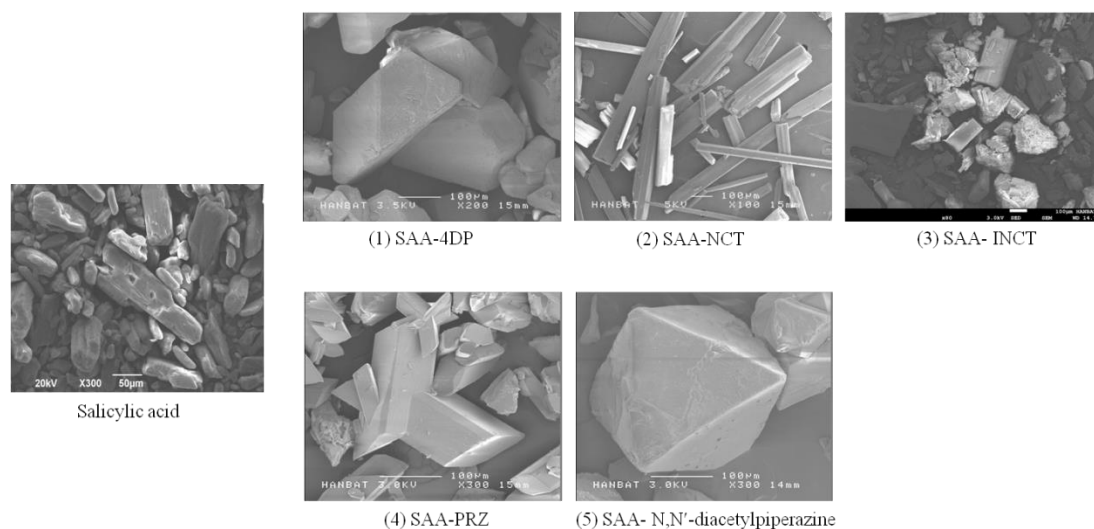


Figure 5.6: SEM microphoto crystal habit of salicylic acid (SAA) and the corresponding cocrystal with 4DP, NCT, INCT, PRZ, and N,N'diacetylpiperazine can be distinguished by their different shapes.

5.1.2.4 Crystal structures

To explore the molecular arrangement and hydrogen bonding in cocrystals, single crystals were analyzed, and their structures were determined. The unit cell parameters and hydrogen bond distances are summarized in Tables 5.2 and 5.3. That compounds 1 to 5 are indeed cocrystals rather than salts which is supported by the analysis of the crystallographic parameters (Table 5.3).

(1) Salicylic acid/4,4'dipyridyl (2:1)

Cocrystal 1 is crystallized in 2:1 stoichiometric ratio by a cooling process in ethanol. 4,4'dipyridyl is a double hydrogen bond acceptor. Therefore it is a suitable compound to form hydrogen bonded cocrystals with salicylic acid. In the crystal structure of 1, the SAA dimer remains intact and the pyridine moieties act as acceptor to the anti-oriented NH's of the SAA dimer. The hydrogen-bonding interaction in 1 results in a triclinic space group P-1 via the association of one 4,4'dipyridyl and two salicylic acid molecules (Fig. 5.7). As expected, strong intramolecular hydrogen bonds of O-H...O are formed within salicylic acid. The asymmetric unit contains two salicylic acid and one 4,4'dipyridyl molecule held together through an acid-pyridine heterosynthon with O-H...O and O-H...N hydrogen bond distances

5. Results and discussion

of 2.6237 and 2.5625Å, respectively. Additionally, the salicylic acid and 4,4'-dipyridyl are linked through an intermolecular O-H...N hydrogen bond within the carboxylic acid OH group and pyridine N11 of an adjacent 4,4'-dipyridyl moiety.

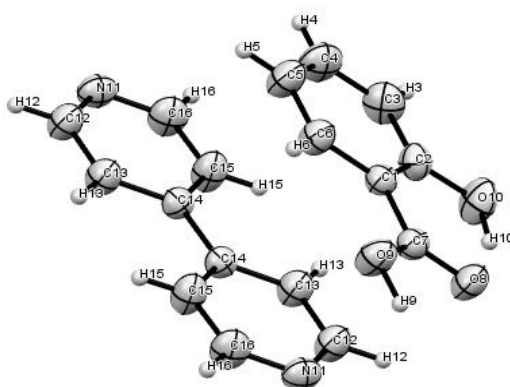


Figure 5.7: An ORTEP view of the asymmetric unit of the cocystal 1 with the atomic numbering scheme (elloids shown at the 40% probability level).

(2) Salicylic acid/nicotinamide (1:1)

The hydrogen-bonding interaction in 2 result in a monoclinic space group P_21/n . The crystal structure determination of 2 displays 1:1 assemblies of salicylic acid and nicotinamide in the asymmetric unit. Salicylic acid and nicotinamide form a chain by connecting the carboxylic acid OH group with the nitrogen of the pyridine ring via O-H...N hydrogen bonding (Fig. 5.8). The components are held together through an acid-pyridine heterosynthon with O-H...O (O8-O10) and O-H...N (O9-N11) the distances are 2.5999 and 2.5460Å, respectively.

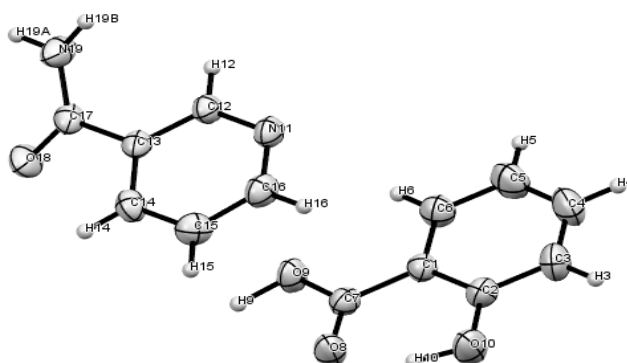


Figure 5.8: An ORTEP view of the asymmetric unit of the cocystal 2 with the atomic numbering scheme (elloids shown at the 40% probability level).

(3) Salicylic acid/isonicotinamide (1:1)

Isonicotinamide is one of the most effectively used cocrystallizing compounds, as the pyridine N atom of the isonicotinamide molecule readily acts as a hydrogen bond acceptor when faced with good hydrogen bond donors such as carboxylic acids and alcohols [Vis03, Sar08]. The hydrogen-bonding interaction in 3 result in a monoclinic space group P2 (1)/c. The asymmetric unit consists of one molecule of a salicylic acid and isonicotinamide dimers in 3 are linked through an intermolecular O-H...N hydrogen bonding, involving carboxylic acid groups of the salicylic acid and the aromatic nitrogen of isonicotinamide an adjacent salicylic acid motif. Such dimers are connected through isonicotinamide molecules located at the inversion center into infinite chains via hydrogen bonds of O4-H2A...N2 and O4-H2B...N4 interactions (Fig. 5.9). Also, cocrystal 3 exhibits the primary amide functionalities of two isonicotinamide molecules form an amide-amide supramolecular homosynthon. The amide-amide supramolecular homosynthon in 3 exhibits N-O distances of 3.035 and 2.742Å, respectively.

Although cocrystals 2 and 3 are isostructural, the intermolecular hydrogen bondings are quite differnt. This structural variation result in a change of physical properties such as melting point and dissolution rate.

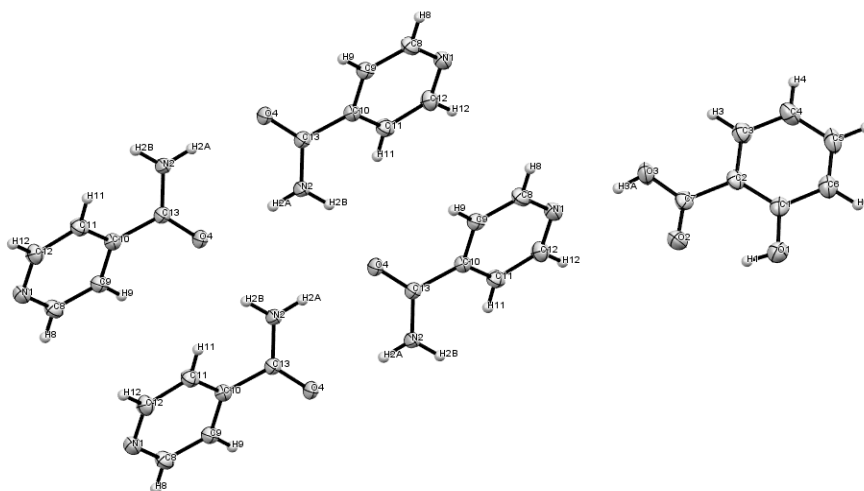


Figure 5.9: An ORTEP view of the asymmetric unit of cocrystal 3 with the atomic numbering scheme (elloids shown at the 40% probability level).

(4) Salicylic acid/piperazine (1:0.5)

The assignment of 4 as a cocrystal is based on location of the relevant H atom using the X-ray data. The hydrogen-bonding interaction in 4 result in a monoclinic space group P2(1)/c via the association of one molecule of a salicylic acid and one-half of a piperazine molecule.

5. Results and discussion

The asymmetric unit consists of one molecule of a salicylic acid and piperazine in 4 are linked through trifurcated hydrogen bonds involving pyridine NH and CO groups of neighboring molecules forming arrangement, such as N1-H1...O1, N1-H1...O2 and N1-H1...O3 (Fig. 5.10).

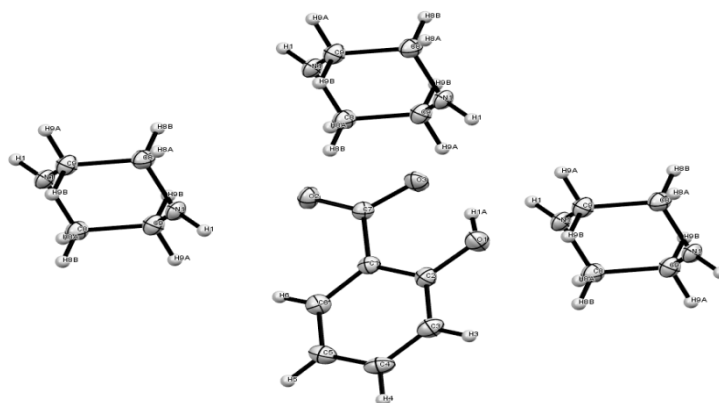


Figure 5.10: An ORTEP view of the asymmetric unit of cocrystal 4 with the atomic numbering scheme (elloids shown at the 40% probability level).

(5) Salicylic acid/*N,N'*-diacetylpiperazine (2:1)

Cocrystal 5 also exhibits 2:1 stoichiometry and contains acid-CO group supramolecular heterosynthon. The cocrystal of 5 with *N,N'*-diacetylpiperazine crystallizes in orthorhombic space group *Pbca*. Its asymmetric unit contains two salicylic acid and one *N,N'*-diacetylpiperazine molecules. In cocrystal 5, the carboxylic acid OH group is connected oxygen atom of CO group via hydrogen bonds of O3-H3A...O4. In the cocrystal of 5 with *N,N'*-diacetylpiperazine, there are no N-H...O hydrogen bonds although the N atom is retained. Thus, the 5 are stabilized by two strong O-H...O hydrogen bonds as shown in Fig. 5.11.

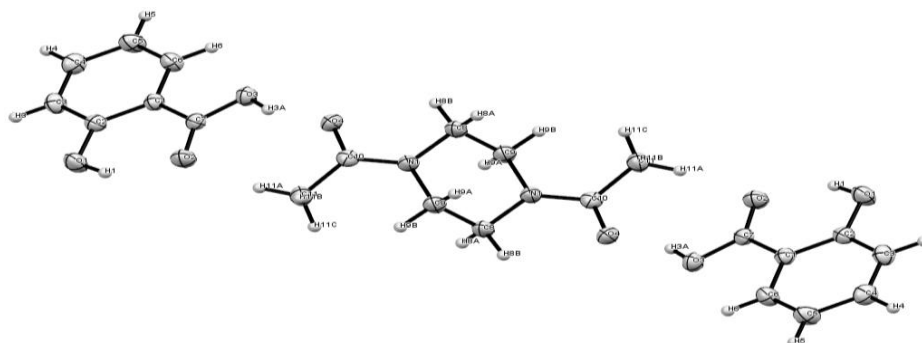


Figure 5.11: An ORTEP view of the asymmetric unit of cocrystal 5 with the atomic numbering scheme (elloids shown at the 40% probability level).

5. Results and discussion

Table 5.3: Crystallographic data for cocrystals 1 to 5.

	1	2	3	4	5
Empirical formula	C ₂₄ H ₂₀ N ₂ O ₆	C ₁₃ H ₁₂ N ₂ O ₄	C ₁₃ H ₁₂ N ₂ O ₄	C ₉ H ₁₀ NO ₃	C ₂₂ H ₂₆ N ₂ O ₈
Formula weight	432.42	260.25	260.25	180.18	446.45
T [K]	296(2)	296(2)	200(2)	175(2)	177(2)
Crystal system	Triclinic	Monoclinic	Monoclinic	Monoclinic,	Orthorhombic
Space group	P-1	P 2 ₁ /n	P2(1)/c	P2(1)/c	Pbca
a [Å]	7.871(1)	11.234(2)	8.3765(8)	6.2465(6)	11.5548(11)
b [Å]	8.385(2)	4.9368(9)	5.1018(5)	14.4442(14)	13.2597(12)
c [Å]	8.668(2)	23.003(4)	28.169(3)	9.2703(9)	13.6959(13)
α, [°]	88.632(1)	90	90	90	90
β, [°]	81.859(2)	98.333(3)	90.238(2)	92.542(2)	90
γ, [°]	66.234(3)	90	90	90	90
V, [Å ³]	517.97(2) ³	1262.2(4)	1203.8(2)	835.60(14)	2098.4(3)
Z	2	4	4	4	4
ρ _{calc} , [Mg/m ³]	1.386	1.369	1.436	1.432	1.413
μ, [mm ⁻¹]	0.101	0.103	0.108	0.109	0.108
Goodness-of-fit on F ²	1.081	0.854	1.117	1.165	1.026
R indices (all data)	0.2551	0.0894	0.0959,	0.1045	0.0808
wR2 (all data)	0.1326	0.1099	0.1665	0.2250	0.1321
R indices [I>2σ(I)]	0.0447	0.0437	0.0490,	0.0611	0.0473
wR2 [I>2σ(I)]	0.1536	0.0952	0.1107	=0.1621	0.1096

5.1.2.5 Raman spectroscopy

As already shown in the own report for SAA-4,4'-bipy, a comparison of the solid phase Raman spectra of SAA, the co-former, and the corresponding cocrystal allow to establish whether a new solid form has been generated [Lee14]. This is illustrated for the starting material and the cocrystals 1 to 5 in Fig. 5.12, showing that each cocrystal exhibits a unique Raman spectrum in comparison to salicylic acid and the co-formers. Among the most important evidence for cocrystal formation is the observation that all spectra show different characteristic peaks, which are typical for crystal structures. For example, in the spectra range of 1200-1000cm⁻¹, the starting material (SAA) has three characteristic peaks at 1155,

5. Results and discussion

1095, and 1031 cm^{-1} , while each cocrystal has different peaks in this region. This difference suggests the formation of a cocrystal of SAA and the co-formers.

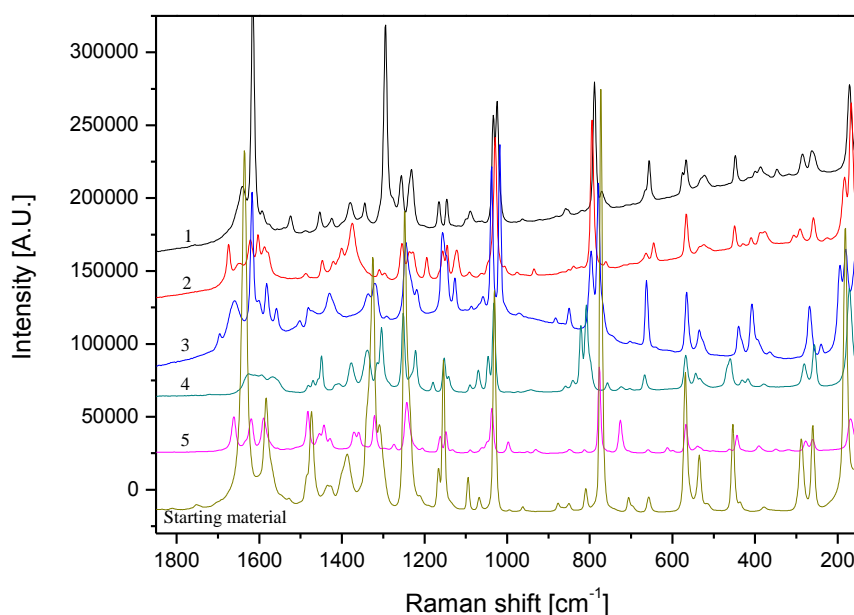


Figure 5.12: Raman spectra of the cocrystals 1 to 5.

5.1.3 Monitoring cocrystal formation by Raman spectroscopy

In-situ Raman spectroscopy has been used as a screening tool for cocrystal formation. Raman spectroscopy as a PAT (process analytical technology) tool provides an effective in line method to monitor and quantify the cocrystal formation or transformation [Jay09, Rod06]. The reaction monitoring has as main advantages, the decrease in process time and less quantity of residuals. With the monitoring, it is possible to design the experiments more efficiently and understand the reaction mechanism involved by following changes in characteristic peaks such as growth, diminishment, and shifting corresponding to solid phase changes to obtain a qualitative assessment of the induction time and the rate of formation.

Cocrystal screening of salicylic acid was conducted using a Raman spectroscopy with 5 cocrystal formers such as 4,4'-dipyridyl, nicotinamide, isonicotinamide, piperazine and N,N'-diacetylpiperazine. In own work [Lee14], the in-situ monitoring of salicylic acid/4,4'-dipyridyl cocrystal forming by using Raman spectroscopy is described. Here is described an in-situ monitoring of the formation of salicylic acid-nicotinamide cocrystals. Fig. 5.13 shows variations in Raman spectra with elapsed time of aspirin/ nicotinamide solution and the transformation of salicylic acid/ nicotinamide cocrystals in solution were identified by

5. Results and discussion

using Raman spectroscopy. An overlay of Raman spectra across the 730-810 cm^{-1} region is shown in Fig. 5.13. The arrows indicate unique peaks for the starting material, ASA/NCT solution and SAA/NCT cocrystals. The blue arrow presents a characteristic peak (788 cm^{-1}) for cocrystals that are not present in the spectra of ASA/NCT and ASA solutions. At 810-730 cm^{-1} , the formation of cocrystal from ASA and NCT were characterized by peak shifts from 750 to 788 cm^{-1} . The shifts results from a change in the hydrogen bond interactions. At the beginning of the process, only the ASA spectrum, with the characteristic peaks at 750, and 780 cm^{-1} were observed. A peak at 761 cm^{-1} starts to appear after adding NCT solution into the ASA solution. The characteristic peak of SAA/ NCT cocrystals appears at 788 cm^{-1} and increases in its peak intensity with elapsing time. Using the cocrystal peak at 788 cm^{-1} , it is possible to measure the formation of cocrystals.

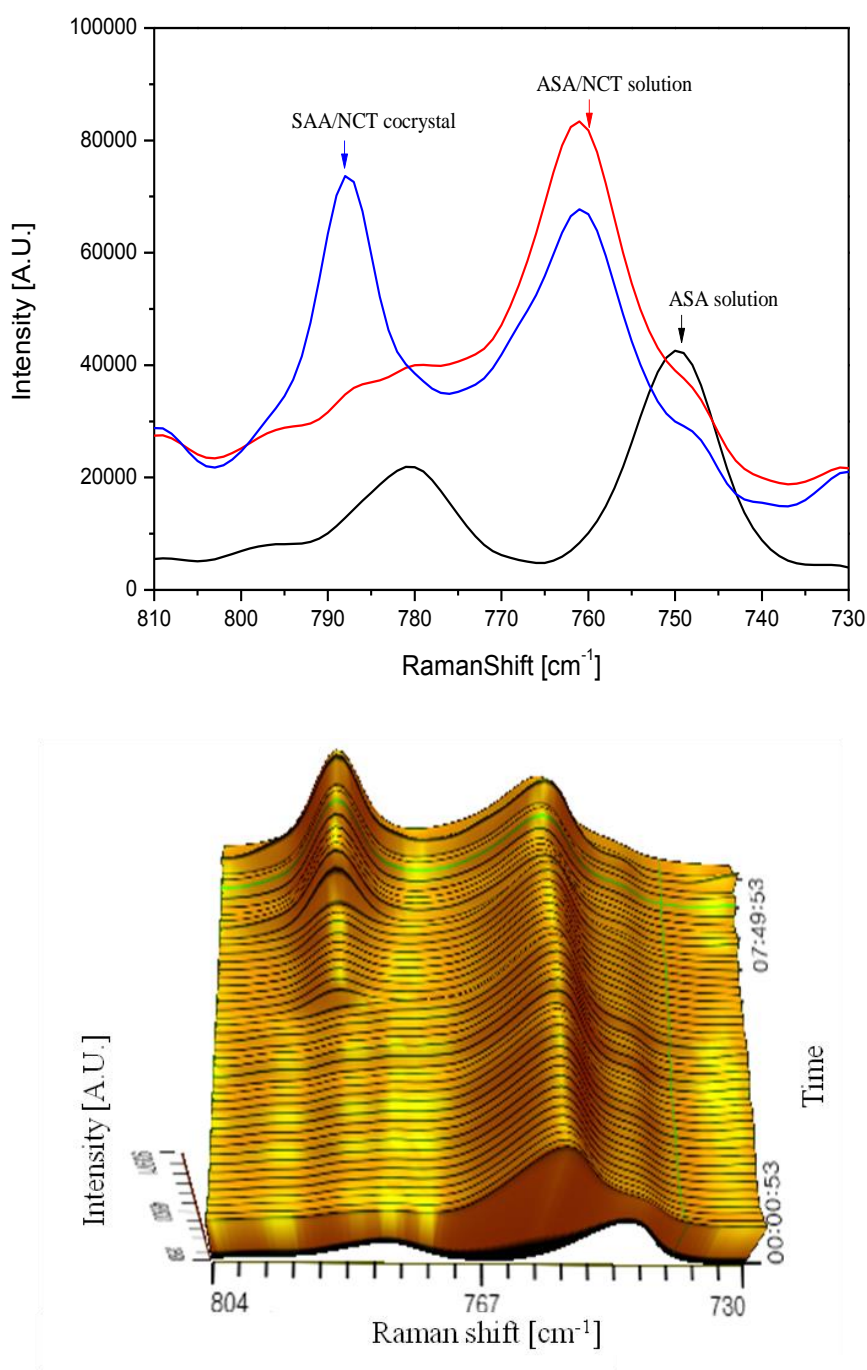


Figure 5.13: Change of Raman spectra in the range of 810-730cm⁻¹ (top), 3D waterfall spectra (bottom).

5.1.4 Property of cocystal

The novel cocystals were evaluated concerning their physical stability with respect to solubility. Cocystal phase stability experiments have been conducted in water at different

5. Results and discussion

temperatures, and changes have been examined in the intrinsic solubility, in order to reveal to what extent the structural variations within the cocrystals of SAA influence the biopharmaceutical properties of this API. Fig. 5.14 shows that cocrystals have a higher solubility than a single component at various temperatures. In short, salicylic acid is known as poorly soluble material in water, approximately 2.36g/L at 30°C [Nor06]. The solubility of the cocrystals is increased because the cocrystals have more stability in water (SAA-4DP: 47.4g/L, SAA-NCT: 38.6g/L, SAA-INCT: 16.7g/L, SAA-PRZ: 5.03g/L and SAA-NDAT: 14.0g/L). The higher stability of new salicylic acid cocrystals can lead to improved solubility and dissolution rates, and therefore theoretically lead to an increased bioavailability. This improved solubility is considered sufficient for formulations of cocrystal. Thus, it is good evidence that 5 new salicylic acid cocrystals were successfully obtained by solution crystallization.

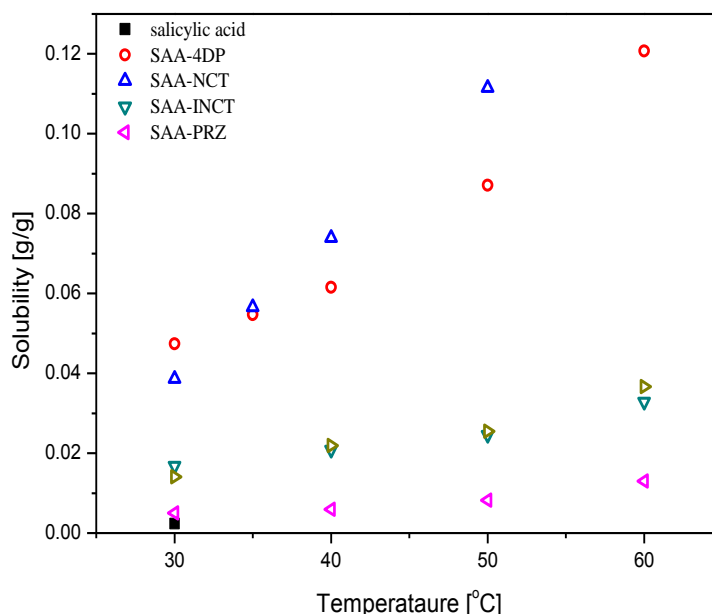


Figure 5.14: Solubility of new salicylic acid cocrystals at various temperatures.

5.1.5 Conclusions

Five novel cocrystals of salicylic acid with 4,4'dipyridyl, nicotinamide, isonicotinamide, piperazine and N,N'-diacetylpiperazine which contain N atoms have been prepared with cooling/evaporation crystallization and have been characterized by single crystal X-ray diffraction. It brings out clearly the primary intermolecular interactions in forming interesting hydrogen bond pattern between the carboxylic acid OH group and nitrogen atom of salicylic

5. Results and discussion

acid. The strong hydrogen bond donor hydroxyl is introduced to interact with the nitrogen atoms of the pyridyl group that are underutilized as hydrogen bond acceptors. This approach will help selection of API-guest screening and synthesis that have a potential of forming structurally interaction. The solubility experiments conducted on salicylic acid and cocrystals to demonstrate that these have different solubilities. This result shows the possibility that of the physical properties of the API can be altered through the application of cocrystals.

5.2 In-situ monitoring of the formation of a salicylic acid-4,4'-dipyridyl cocrystal using Raman spectroscopy

The in-situ process analysis technology Raman spectroscopy was used to observe and control a cocrystallization process. Raman spectroscopy is a well-established technique for both in-situ and fast quantitative measurements of the solid-state. In addition, Raman spectroscopy provided additional information on the crystal structure of the salicylic acid-4,4'-bipy cocrystals.

The control and optimization of the cocrystal formation in batch crystallization processes requires an in-situ measurement technique. Raman spectroscopy can be used to measure solution concentrations directly monitoring crystal morphology as the cocrystals are being formed. Especially, Raman spectroscopy takes a center stage in the past recent years as 'one of the fastest, most reliable and most suitable techniques to identify crystal forms in drug products and can be easily exploited routinely for monitoring phase changes in drug products and quality control assays' [Aue03]. It has several advantages; i) special sample preparation is not required [Tay00], ii) it is well suited to monitor the solid phase in slurries including aqueous media [Wan00], iii) the technique is a non-contact measurement [Sko03], iv) a remote detection through fiber-optic coupling of sampling probes is possible [Hu05].

Raman spectroscopy has been used for a qualitative monitoring of chemical reactions in solutions, and chemometrics has been used to follow the progress of reaction [Sve99, Fai03]. A wide range of applications of Raman spectroscopy to analyze and monitor processes were published such as the determination of the concentration of active principles [Ver02, War05], polymorphic transformation [Aue03, Ném05, Pra02], hydrate, anhydrate composition [Air03, De98] in solid dosage forms. In addition, in-situ monitoring during the processing of a solid API has been studied including polymorphic transformation [O'Br04, Sta02], measurement of supersaturation during crystallization of lysozyme [Sch99], formation of cocrystals [Rod06, Qia13].

5.2.1 Identification of ASA-4,4'-bipy cocrystals

5.2.1.1 Single-crystal x-ray crystallography

All data for molecular structure determination was measured on a SMART APEX II CCD diffractometer. XRD single crystal diffraction identifies the crystals as 2:1 SAA- 4,4'-bipy

5. Results and discussion

cocrystals. It crystallizes in a triclinic system with a space group P-1 and cell parameters $a=7.8712(10)\text{\AA}$, $b=8.3851(2)\text{\AA}$ and $c=8.6683(3)\text{\AA}$. The crystal data for SAA-4,4'-bipy cocrystals are presented in Table 5.4. Salicylic acid contains a carboxylic acid group and a hydroxyl group, while 4,4'-bipyridyl contains pyridine groups. Fig. 5.15 shows the hydrogen-bonding interaction between the carboxylic acid and pyridine, and such intermolecular forces also make contributions to stability of crystal structure [Jet03]. Table 5.5 indicates the detailed hydrogen bonds in the crystal. Salicylic acid and 4,4'-bipyridyl are connected by N---H hydrogen bonds between the N atom of 4,4'-bipyridyl and H atom of salicylic acid. Moreover, the O---H hydrogen bonds of salicylic acid molecules are also connected. To be more specific, the intermolecular hydrogen bonding of O(9)-H(9)---N(11) and O(10)-H(10)---O(8) are observed.

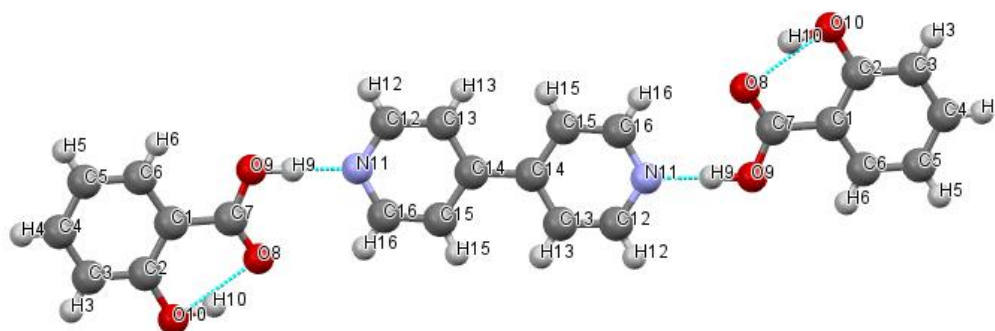


Figure 5.15: The molecules of SAA-4,4'-bipy cocrystals, showing the atom labeling scheme and the intermolecular hydrogen bonds (dashed line).

Table 5.4: Crystal data and structure refinement of SAA-4,4'-bipy cocrystal.

Empirical formula	$C_{24} H_{20} N_2 O_6$
Formula weight	432.42
Temperature	296(2) K
Wavelength	0.71073 \AA
Crystal system, space group	Triclinic, P -1

5. Results and discussion

	$a = 7.87120(10) \text{ \AA}$	$\alpha = 88.6320(10)^\circ$
	$b = 8.3851(2) \text{ \AA}$	$\beta = 81.859(2)^\circ$
Unit cell dimensions	$c = 8.6683(2) \text{ \AA}$	$\gamma = 66.234(3)^\circ$
Volume	517.97(2) \AA^3	
Z, Calculated density	1, 1.386 Mg/m^3	
Absorption coefficient	0.101 mm^{-1}	
F(000)	226	
Crystal size	0.32 x 0.26 x 0.24 mm	
Theta range for data collection	2.375 to 28.327 deg.	
Limiting indices	$-10 \leq h \leq 10, -11 \leq k \leq 11, -11 \leq l \leq 11$	
Reflections collected / unique	14177 / 2585 [R(int) = 0.0475]	
Completeness to theta = 25.242	100.0 %	
Absorption correction	None	
Refinement method	Full-matrix least-squares on F^2	
Data / restraints / parameters	2585 / 0 / 154	
Goodness-of-fit on F^2	1.081	
Final R indices [$I > 2\sigma(I)$]	R1 = 0.0447, wR2 = 0.1243	
R indices (all data)	R1 = 0.0543, wR2 = 0.1326	
Extinction coefficient	0.065(11)	
Largest diff. peak and hole	0.183 and -0.220 e.\AA^{-3}	

5. Results and discussion

Table 5.5: *Hydrogen bonds for SAA- 4,4'-bipy cocrystal [A and deg.].*

D-H...A	d(D-H)	d(H...A)	d(D...A)	<(DHA)
O(9)-H(9)...N(11)	1.02(2)	1.60(2)	2.6237(12)	174.8(15)
O(10)-H(10)...O(8)	1.06(2)	1.58(2)	2.5625(13)	152.7(17)

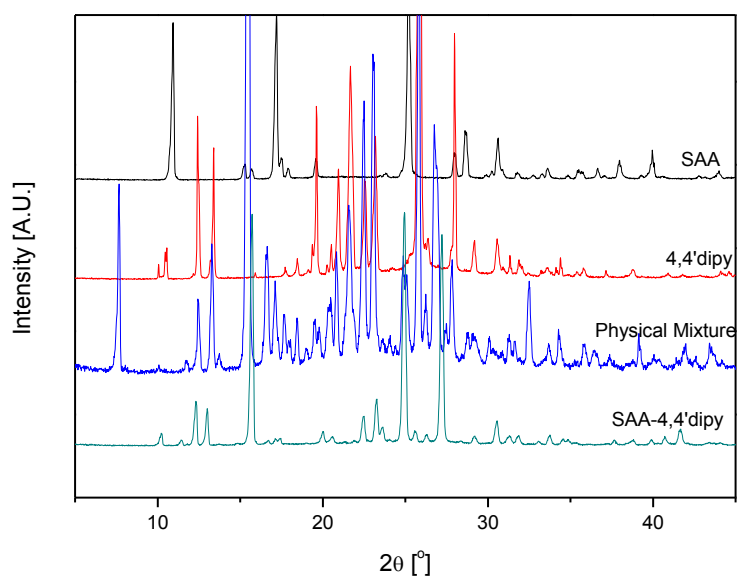
Symmetry transformations used to generate equivalent atoms:

#1 -x,-y+1,-z+2

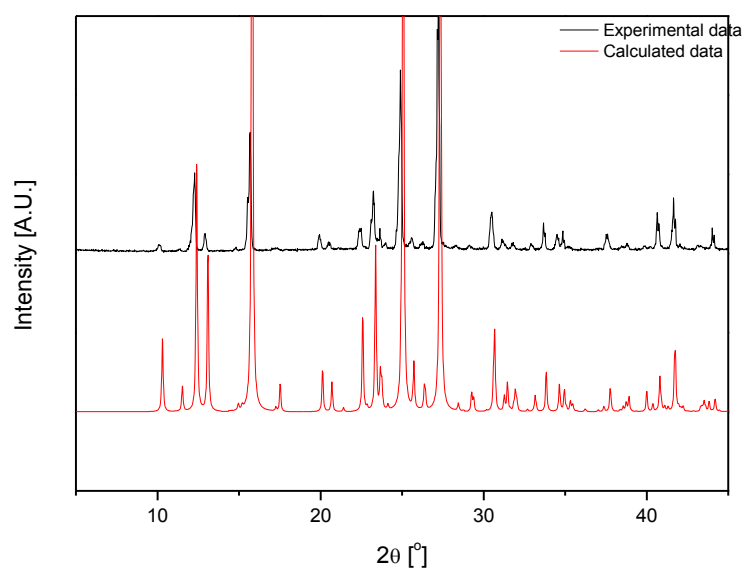
5.2.1.2 XRD analysis

The experimental X-ray diffraction pattern of the 2:1 salicylic acid: 4, 4'dipyridyl shows that a new material has been formed in Fig. 5.16. The diffraction pattern of the product of crystallization from ethanol indicates the formation of a new material which obviously differs compared to starting materials and the physical mixture.

Investigations with a range of other solvents including methanol, 1-propanol, isopropanol, n-butanol, 2-butanol and acetone with various stoichiometric molar ratios have been carried out. The SAA-4,4'-bipy cocrystal formed in all of these solvents except acetone at a molar ratio 2:1. Details of these experiments are summarized in Table 5.6:



(1)



(2)

Figure 5.16: (1) Powder X-ray diffraction pattern of the product of the crystallization in ethanol compared to the starting materials and the physical mixtures, and (2) comparison between calculated data from single crystal diffractometer and experimental data from this study.

5. Results and discussion

Table 5.6: Details of the experiment conducted using aspirin: 4, 4'dipyridyl by crystallization.

Co-former	Ratio (API:Co-former)	Solvents						
		EtOH	MeOH	1-butanol	1-propanol	IPA	2-butanol	Acetone
4,4'dipyridyl	2:1	Form3	Form3	Form3	Form3	Form3	Form3	Mix
	1:1	Form3	Form3	Form3	Form3	Amorphous	Form3	Mix
	0.5:1	Mix	Mix	Form3	Form3	-	Form3 Mix	-
	3:1	Form3	Form3	Form2	Form3	Form2 Mix	-	-
	0.25:1	Mix	Mix	Mix	Mix	Mix	-	-
	1.5:1	Form3	Form3	Form3	Form3	Form2	-	-
	5:1	Form3	Form3	Form3 Mix	Form3 Mix	Form3 Mix	Form3 Mix	-

* Form 3 indicates SAA-4,4'-bipy cocystal mentioned in this paper.

* Form 2 indicates SAA-4,4'-bipy cocystal different XPD pattern and DSC curve with form 3.

* Mix indicates Mixture of ASA and 4,4'-bipy.

5.2.1.3 DSC analysis

The DSC traces and thermal behavior for SAA, 4,4'-bipyridyl, ASA-4,4'-bipy physical mixture and SAA-4,4'-bipy cocystals are shown to confirm the formation of SAA-4,4'-bipy cocystals, in Fig. 5.17 and Table 5.7. The DSC thermograms of SAA, 4,4'-bipyridyl, ASA-4,4'-bipy mixture and SAA-4,4'-bipy cocystal show melting points of 159.58, 112.16, 59.87 and 155.52 °C, respectively. The thermal behavior of the new crystals is significantly different from salicylic acid and 4,4'-bipyridyl, providing therefore further support for a new crystal.

5. Results and discussion

This different melting phenomenon of the cocrystals revealed the changes in crystal packings and lattice energies.

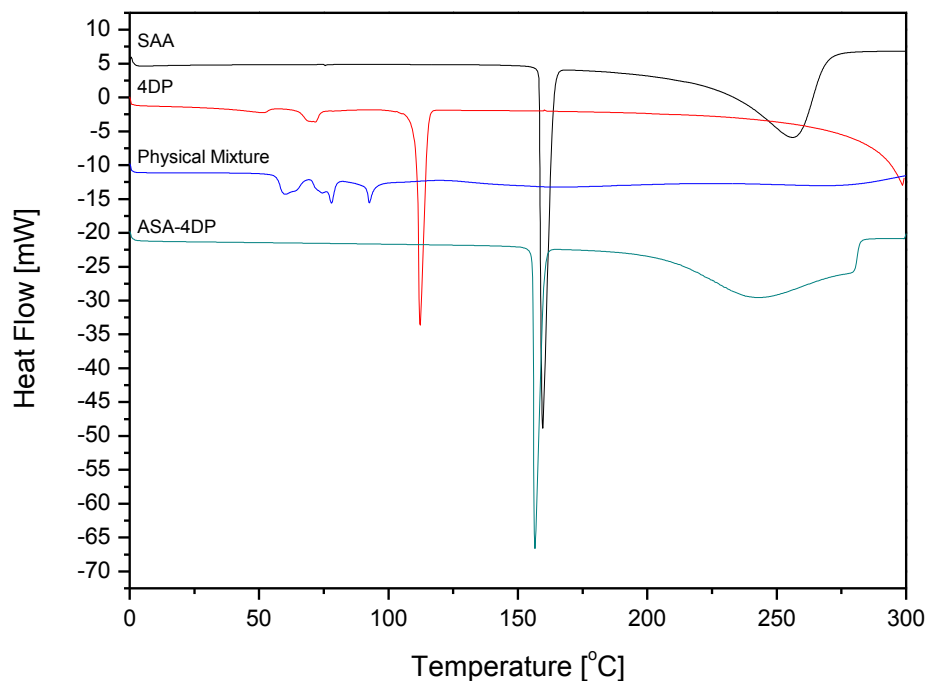


Figure 5.17: 2:1 Salicylic acid/4,4'dipyridyl DSC thermograms.

Table 5.7: The DSC thermograms of starting materials and cocrystal.

Sample	Peak 1		Peak 2	
	T, [°C]	ΔH , [J/g]	T, [°C]	ΔH , [J/g]
SAA	159.58	-179.91	256.23	-410.03
4,4' dipyridyl	112.16	-103.39	298.52	-383.66
ASA-4,4'-bipy Mixture	59.87	-18.35	77.98	-17.38
SAA-4,4'-bipy cocrystal	155.52	-140.15	246.07	-557.88

5. Results and discussion

5.1.2.4 SEM analysis

The surface and morphology of the cocrystals were assessed by SEM. As shown in Fig. 5.18, the single SAA-4,4'-bipy cocrystals exhibit a prism-like habit. Compared to the raw material aspirin which shows thin plate crystals, a possible epitaxial relationship between these solid forms was presupposed [Sim81].

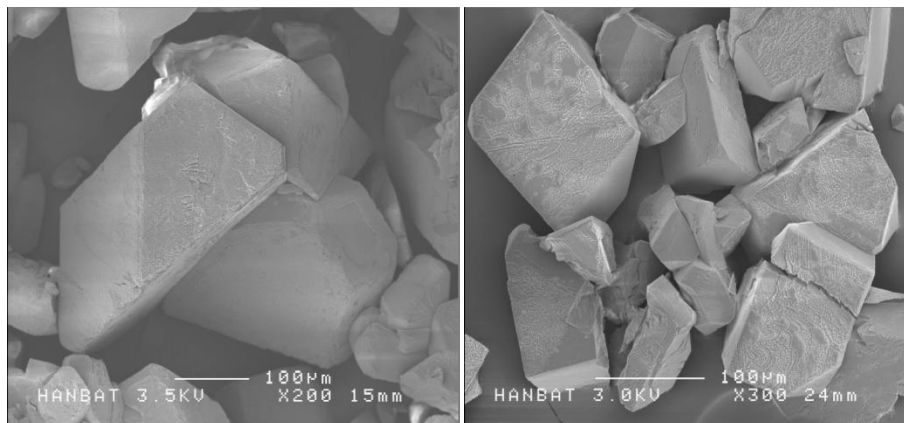


Figure 5.18: SEM images of a crystalline product in ethanol.

5.2.1.5 Raman spectroscopy analysis

The Raman spectra of raw materials, physical mixtures and SAA-4,4'-bipy cocrystals, is shown in Fig. 5.19. It exhibits several differences between the physical mixture and the cocrystals. For example, in the spectra range of 1100-1000 cm^{-1} , the mixture has three characteristic peaks at 1043, 1022, and 1002 cm^{-1} , whereas cocrystals have two different characteristic peaks at 1033 and 1025 cm^{-1} . This difference suggests the formation of a cocrystal of SAA-4,4'-bipy and not a physical mixture of two components.

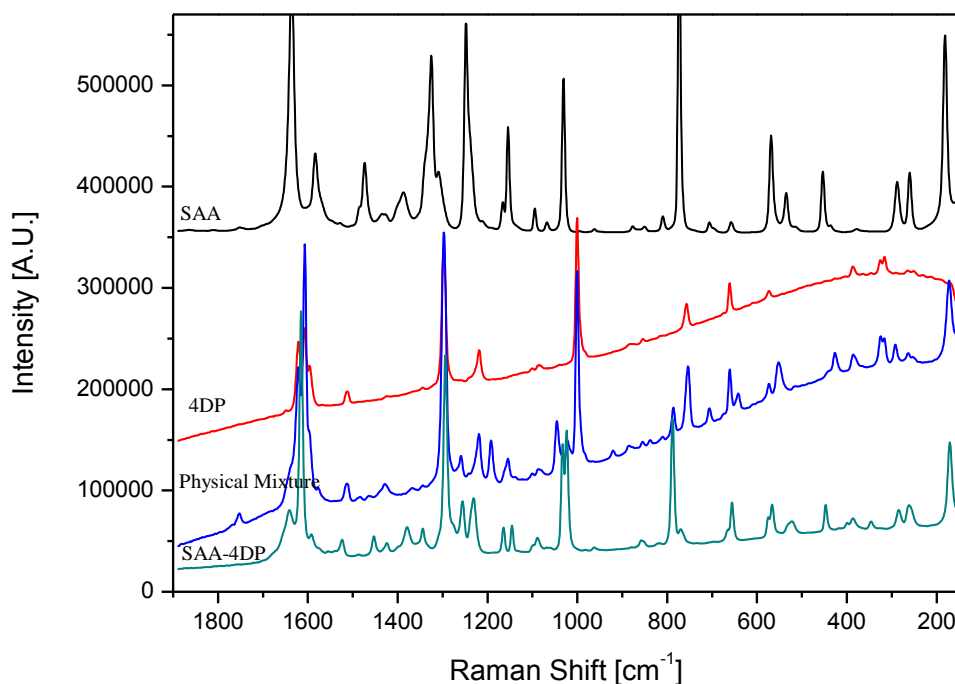


Figure 5.19: Raman spectra of the starting materials, mixtures and SAA-4,4'-bipy cocrystals.

5.2.1.6 FTIR spectroscopy analysis

IR spectroscopy has been widely employed to identify the supramolecular synthon [Des95] and different pattern in crystal structures [Muk13]. IR has been used to monitor cocrystal formation and single synthon detection. SAA-4,4'-bipy cocrystals are formed through hydrogen bonds in which the carboxylic acid groups from SAA and 4,4'-bipy provide a pyridine group. The analysis of SAA-4,4'-bipy cocrystal by FTIR (Fig. 5.20) reveals a change of the vibrational bands for N-H...O and O-H...N hydrogen bonds in the range of 2600-1800cm⁻¹ region which is characteristic of an acid-pyridine synthon [Muk13]. It is a characteristic property of cocrystal formation. The IR spectra of the three forms of the SAA, 4,4'-bipy, and SAA-4,4'-bipy cocrystals shows clear differences that both molecules are present in a new phase. The N-H and O-H stretches of SAA are found at 3234cm⁻¹, while the C-H vibrational bands of 4,4'-bipy are found at 3025cm⁻¹ and 3081cm⁻¹. The characteristic spectra of SAA-4,4'-bipy cocrystal are found at 1929cm⁻¹ and 2411cm⁻¹. The IR spectra of each compounds and cocrystal are presented in Fig. 5.20 and peak identities are shown in Table 5.8.

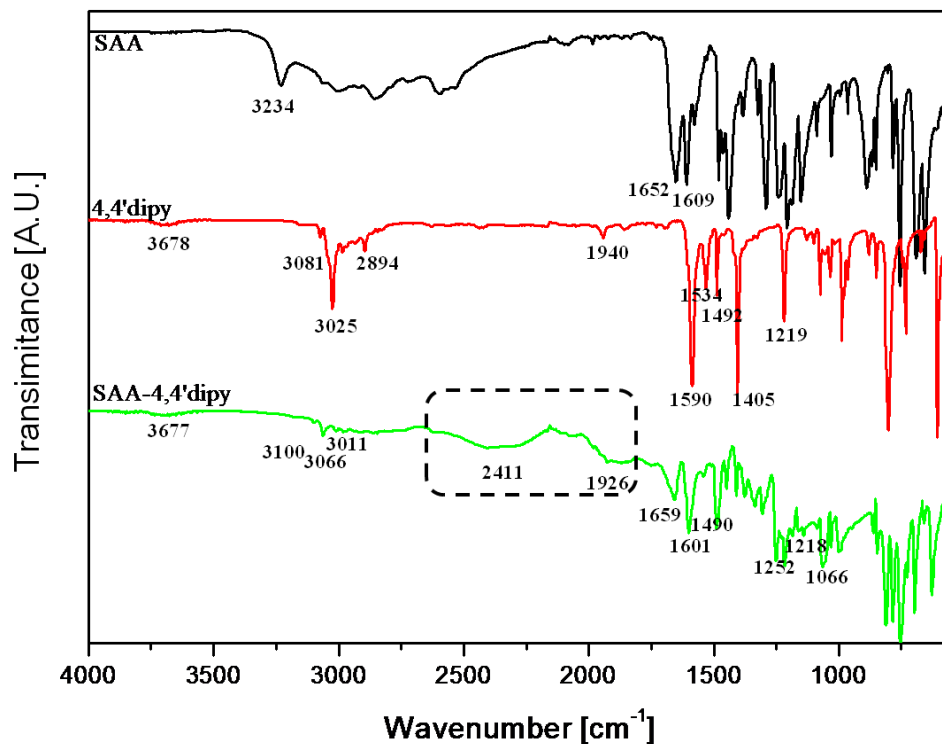


Figure 5.20: FTIR spectra of SAA, 4,4'-bipy and SAA-4,4'-bipy cocrystal.

Table 5.8: Stretching band position of the SAA, 4,4'-bipy and SAA-4,4'-bipy cocrystals.

Compound	Wavenumber [cm ⁻¹]								
	V _{OH,NH}	V _{C=O}	V _{benzene ring}	V _{C-H}	V _{C-C}	V _{C-N}	V _{C-O}	V _{O-H...O}	V _{O-H...N}
SAA	3234	1652	1605	-	-	-	-	-	-
4,4'-bipy	-	-	-	3025/3081	1590	1492	-	-	-
cocrystal	3677/3066	1659	1601	3100		1490	1252/1218	3200-1600	1926/2411

5.2.2 In-situ monitoring during formation of cocrystals using Raman spectroscopy

In-situ monitoring of solution mediated phase mixtures of aspirin and 4,4'-dipyridyl used as cofomers were analyzed by Raman spectroscopy for 5h. Raman spectra of mixtures of ASA and 4,4'-bipy in a stoichiometric molar ratio of 2:1 in ethanol suggested that binary mixtures form a new crystalline form. The Raman spectra at various selected time points were illustrated in Fig. 5.21. It can be ascertained more clearly that the progressive cocrystal formation of SAA-4,4'-bipy by cooling crystallization from the changes in Raman spectra since spectra obtained provided both physical information and chemical information on cocrystals [Koj06]. The great interests of Raman peak changes illustrate the corresponding Raman spectra in the range of 1600-1620, 1000-1045 and 750-790 cm^{-1} in Fig. 5.21.

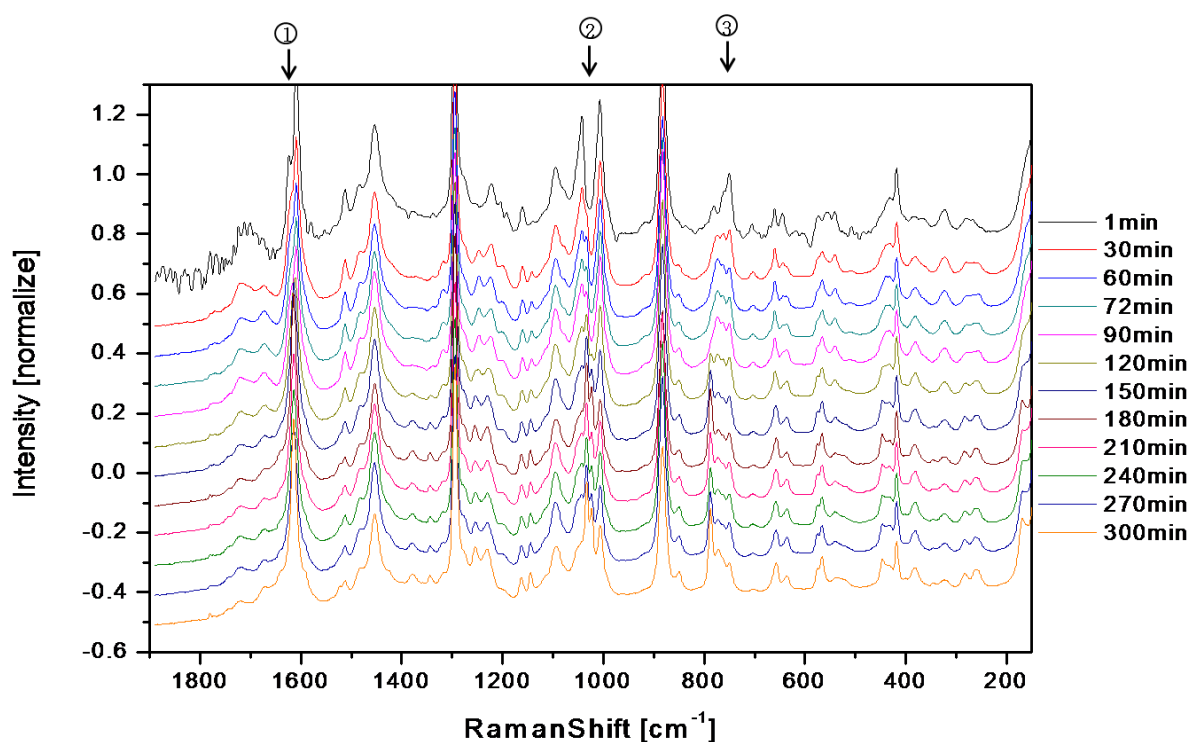
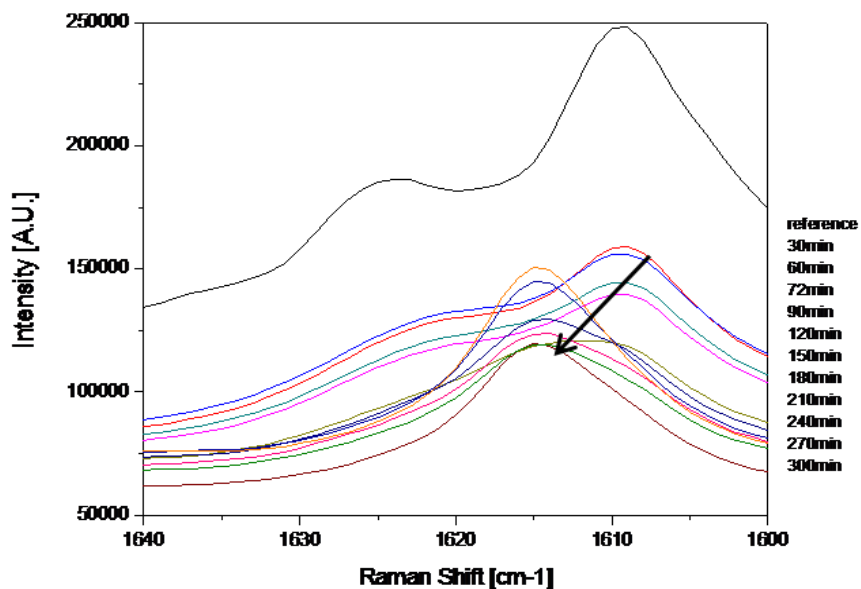


Figure 5.21: Raman spectra of ASA-4,4'-bipy in ethanol with respect to elapsed time.

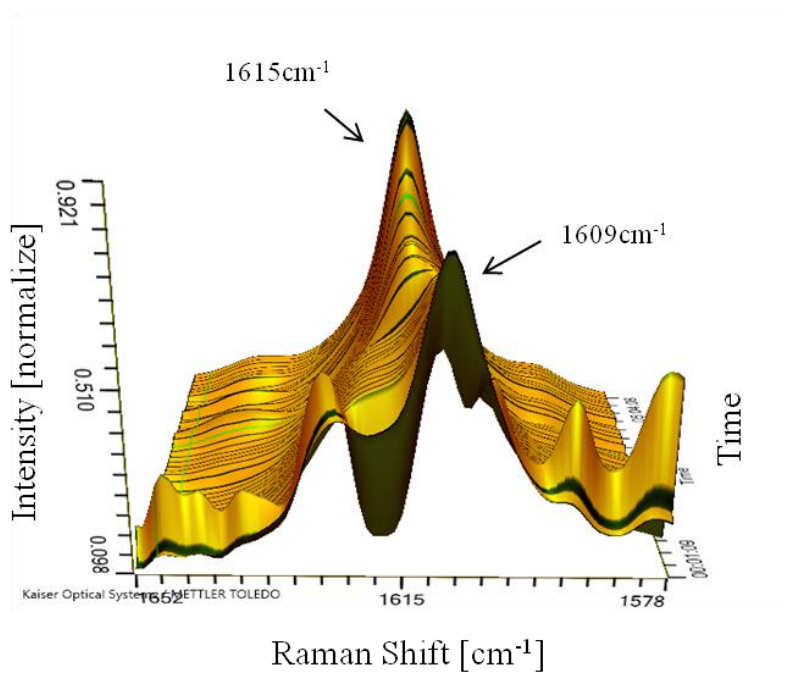
The first region, at 1600-1620 cm^{-1} is easily explained. The formation of cocrystals from ASA and 4,4'-bipy was characterized by the peak shifts C-C stretch from 1609 to 1615 cm^{-1} , which is caused by a change in the hydrogen bond interaction. From Fig. 5.22 (1) (2), it can be seen that the Raman spectra changed in the 1600-1620 cm^{-1} range between 110min to 150min, suggesting that the ASA and 4,4'-bipy starting materials start to co-crystallize of SAA-4,4'-bipy at this point. It is more clear to see the, Raman peak position is time-

5. Results and discussion

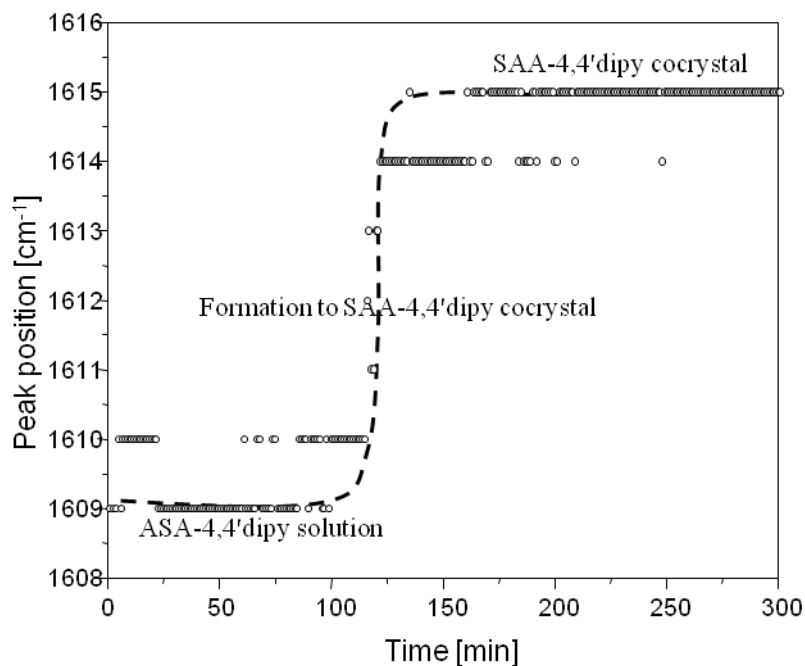
dependent as illustrated in Fig. 5.22 (3). Characteristic peaks of ASA-4,4'-bipy solution gradually disappear at 1609cm^{-1} , while that of the cocystal of SAA-4,4'-bipy at 1615cm^{-1} presents and increases in peak intensity with respect to time.



(1)



(2)

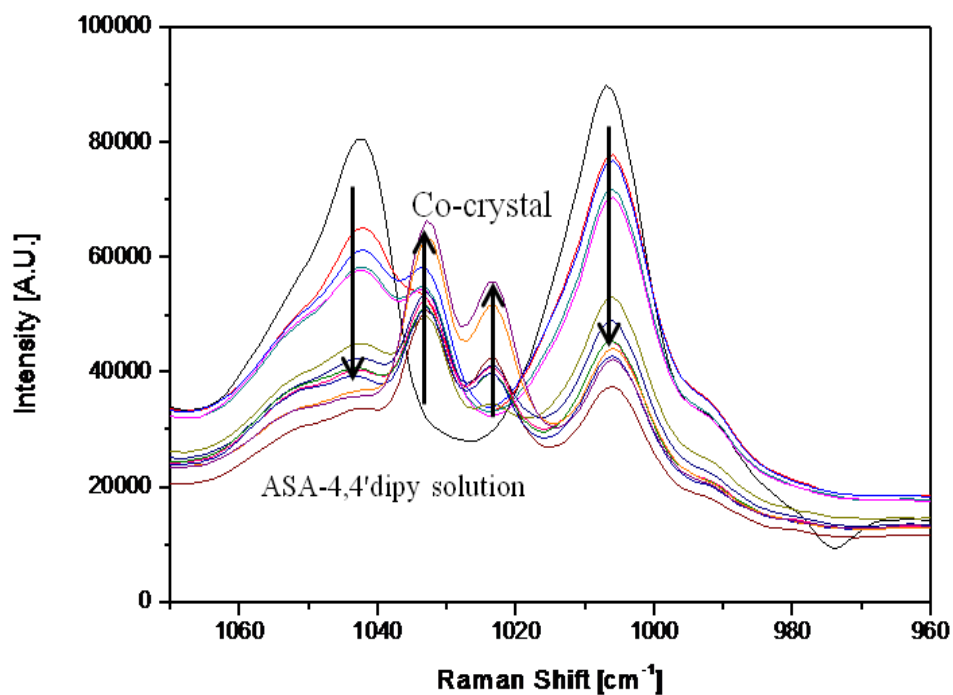


(3)

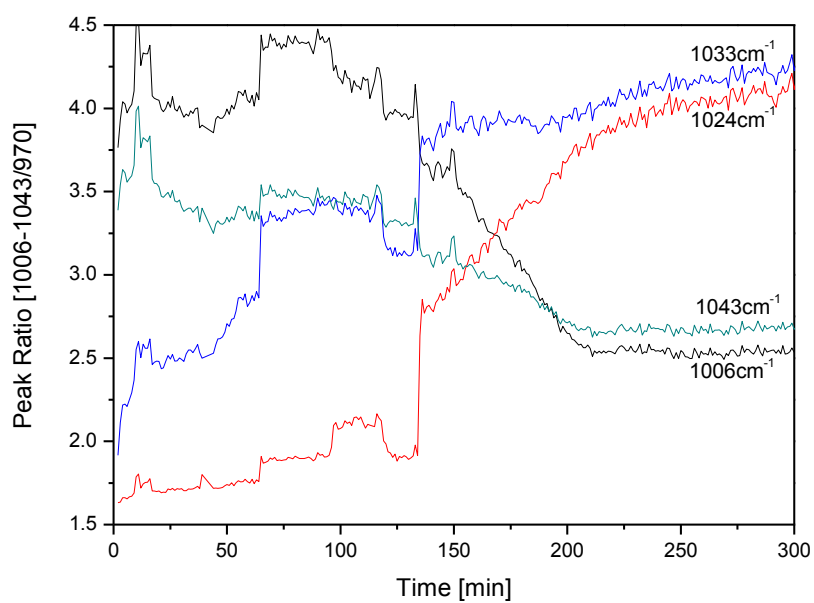
Figure 5.22: (1) A shift in the Raman spectra in the range of $1600\text{-}1620\text{cm}^{-1}$ in the formation of cocrystals, (2) 3D waterfall spectra, and (3) Raman peak position with respect to relative time showing transformation ASA-4,4'-bipy solution to cocrystals of SAA-4,4'-bipy.

The Raman peak intensity relies on the concentration of the materials. To quantify the solid-state change during formation of cocrystals, the ratios of selected peak intensities are presented in Fig. 5.23. The decrease of the peaks 1043 and 1006cm^{-1} are characteristic for the ASA-4,4'-bipy solution. The appearance of the peaks 1024 and 1033cm^{-1} are characteristic of SAA-4,4'-bipy cocrystals and observed with relative operating time during crystallization process. The peak intensity selected was normalized using the consistent peak at 970cm^{-1} . Surely, the peak intensity ratio of $1043\text{cm}^{-1}/970\text{cm}^{-1}$ and $1006\text{cm}^{-1}/970\text{cm}^{-1}$ were declined with the increase of relative time from 3.38 to 2.53 and from 3.76 to 2.67, respectively, but the peak intensity ratio of $1033\text{cm}^{-1}/970\text{cm}^{-1}$ and $1024\text{cm}^{-1}/970\text{cm}^{-1}$ increased from 1.91 to 4.22 and from 1.63 to 4.11, respectively. This phenomenon revealed the cocrystal formation of SAA-4,4'-bipy was induced by cooling crystallization.

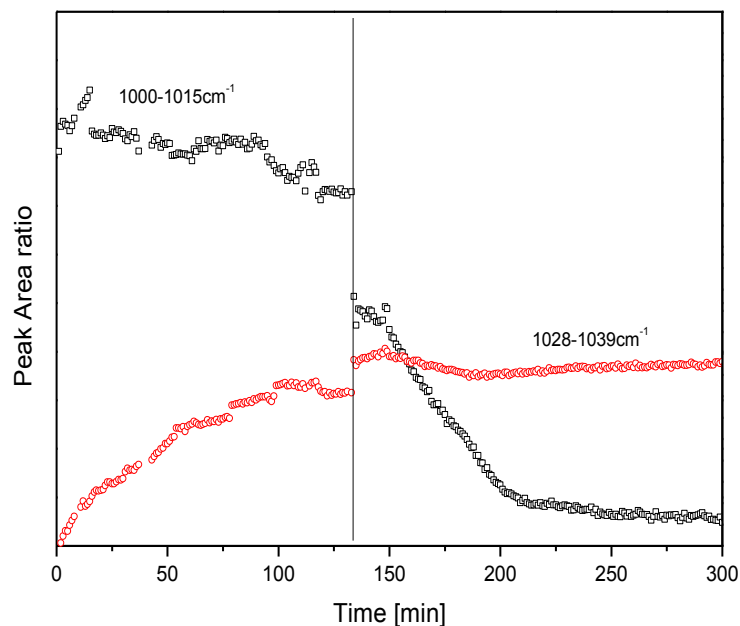
5. Results and discussion



(1)



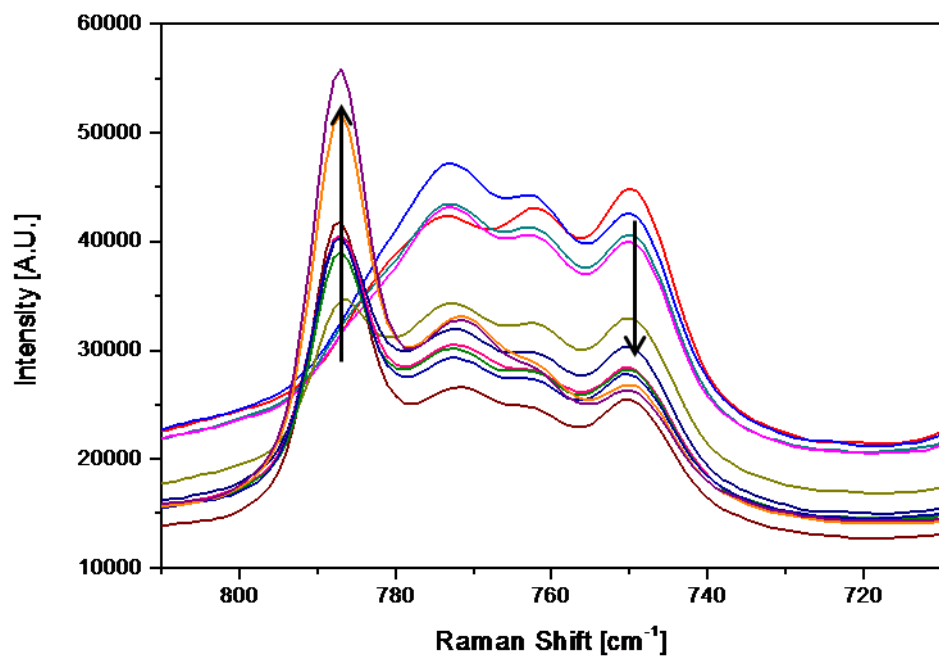
(2)



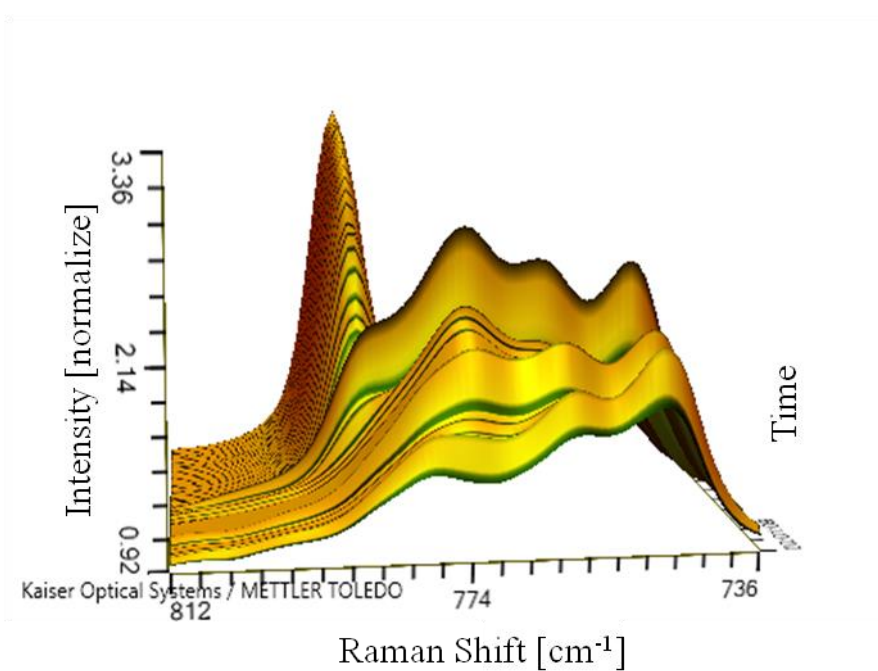
(3)

Figure 5.23: (1) Raman spectra showing cocrystal formation and ASA-4,4'-bipy solution decline, (2) a changes in Raman peak intensity ratio in the formation of cocrystals with relative time, and (3) peak area change between $1000-1015\text{cm}^{-1}$ and $1028-1039\text{cm}^{-1}$ as the crystallization process is changing.

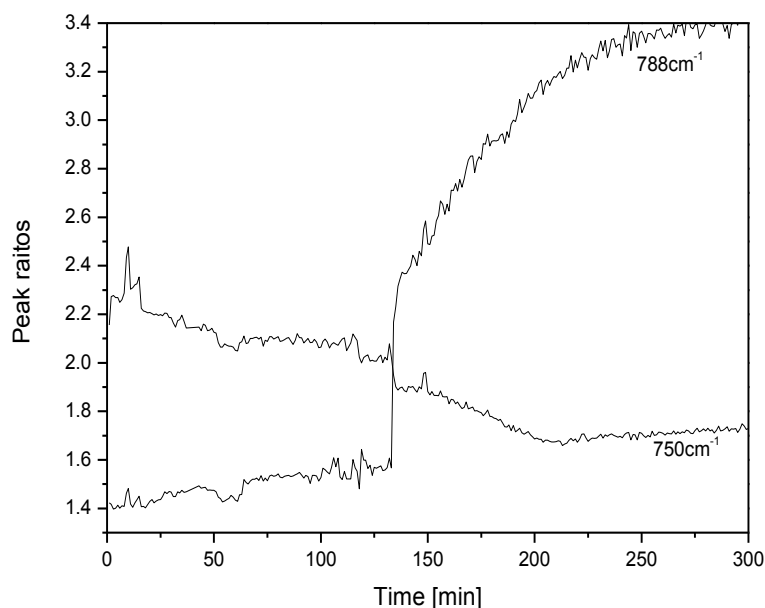
Fig. 5.24 shows spectra between 750 and 790cm^{-1} , which are one of the significant changes. At the beginning of the process, only the aspirin-4,4'-dipyridyl solution spectrum, can be observed at the characteristic peaks at 750 , 762 and 778cm^{-1} . It starts to appear a peak at 788cm^{-1} after 120min as well as an increase in the peak intensity with respect to the operating time. Using the cocrystals, which have their peak at 788cm^{-1} . It is possible to measure the formation of cocrystal. Fig. 5.24(3) presents the peak ratios of $788/720\text{cm}^{-1}$ and $750/720\text{cm}^{-1}$ to evaluate the relative intensities. The peak intensities at selected spots were normalized using the consistent peak at 720cm^{-1} . Surely, the peak intensity ratio of $750\text{cm}^{-1}/720\text{cm}^{-1}$ was declined with the increase of relative times from 2.15 to 1.73 , but the peak intensity ratio of $788\text{cm}^{-1}/720\text{cm}^{-1}$ increased from 1.42 to 3.45 .



(1)



(2)



(3)

Figure 5.24: (1) Change in the Raman spectra in the range of $750\text{-}790\text{cm}^{-1}$, (2) 3D waterfall spectra, and (3) operating time affecting the changes in Raman peak intensity ratio of ASA-4,4'-bipy system.

5.2.3 Conclusion

The formation of cocrystals of SAA-4,4'-bipy during a crystallization was monitored by using an in-situ measurement by Raman spectroscopy. Raman spectroscopy is a useful tool for in-situ monitoring to measure transformation of cocrystals as a function of time in a batch crystallization operation. The cocrystals formed were identified with single-crystal X-ray crystallography, PXRD, off-line Raman spectroscopy, DSC and SEM. From the in-situ measurements of the Raman spectroscopy, the shift of the Raman spectra peak, which is the criterion of cocrystal formation, the transformation from ASA-4,4'-bipy solution to SAA-4,4'-bipy cocrystal can be measured in-line processing. As a result, formation of new cocrystals using aspirin and 4,4'dipyridyl as cofomer was successfully monitored by Raman spectroscopy.

5.3 Supramolecular reaggregation of aspirin-4,4'dipyridyl cocrystals from cocrystals of salicylic acid-4,4'dipyridyl

To screen the change of salicylic acid (SAA)-4,4'dipyridyl (4,4'dipy) cocrystals to aspirin (ASA)-4,4'dipyridyl (4,4'dipy) cocrystals is the aim here. Transformation of SAA-4,4'dipy cocrystals into ASA-4,4'dipy cocrystals was observed. Cocrystals of SAA-4,4'dipy are concomitantly formed in aspirin/4,4'dipyridyl/ethanol solutions, resulting from aspirin decomposition. Eventually cocrystals of ASA-4,4'dipy are obtained from a sequence of the in-situ reaction by controlling the operating condition. Both cocrystals have the same hydrogen bonding interaction between the drug molecules in which carboxylic acid-pyridine except crystal packing arrangements. The ketene functional group decomposes in salicylic acid cocrystal formations reaggregates during solution mediated cocrystallization that led to the formation aspirin cocrystals.

Aspirin has a poor solubility in water and it is rapidly hydrolysed in the plasma to salicylic acid and acetic acid has limited its intravenous use [Aju09, Mit67, Taw68]. For this reason, several multicomponent crystal forms of salicylic acid have been reported with several cofomers such as carbamazepine [Aro11], piperazine [Sko09], as well as 4,4'-dipyridyl [Lee14]. When aspirin was used as raw material those chemicals caused the chemical decomposition of aspirin. However, this was the first observation of the transformation of change from salicylic acid cocrystals to aspirin cocrystals. Cocrystal screening of salicylic acid-4,4'dipyridyl from acetylsalicylic acid-4,4'dipyridyl solution caused by aspirin's in-situ decomposition has been reported previously [Lee14]. Herein Walsh et al., [Wal02] can be used as reference (CCDC 188916) to identify with ASA-4,4'dipy cocrystals since crystals obtained in this study are not large enough and opaque to analyze the single crystal structure. Here, it has induced supramolecular reaggregation of SAA-4,4'dipy cocrystals into ASA-4,4'dipy cocrystals when doing a control the thermodynamic parameters such as cooling temperature, cooling rate, and supersaturation. Fig 5.25 indicates the molecular structure of starting materials and structure of cocrystals treated here.

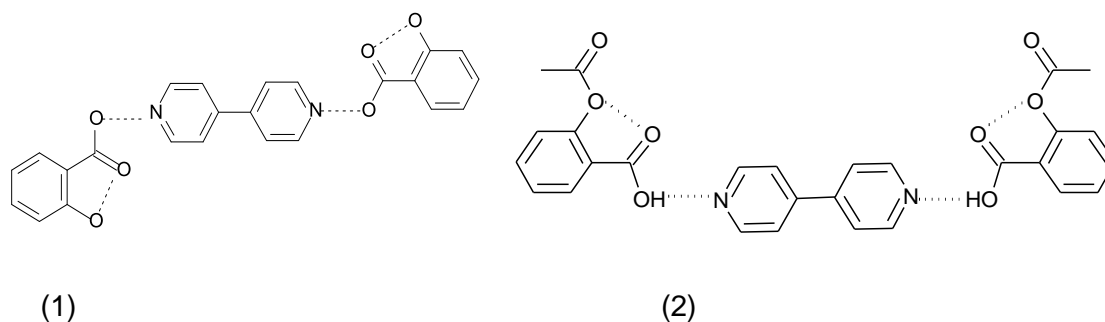


Figure 5.25: Molecular structures of SAA-4,4'dipy cocrystal(1), and ASA-4,4'dipy cocrystal (2) [Wal02].

5.3.1 Cocrystal preparation

SAA-4,4'dipy cocrystals were prepared via the following method: Supersaturation was created by cooling a solution of 2:1 mixture of ASA(0.3602g, 2.0mmol) and 4,4'dipy (0.1560g, 1.0mmol) in ethanol from 50 °C to 35°C. 0.3602g of ASA (2.0mmol) and 0.1560g of 4,4'-dipy (1.0mmol) were added into the solvent. All the solid phase was dissolved by keeping it in the solution under agitation until the equilibrium is reached in a bath at 50°C. Then the bath was cooled very rapidly until 35°C. The suspension was filtered and solid products were isolated on a 3µm filter paper (Whatman) using a vacuum filtration and were held at 40°C overnight to dry. The solid phases were confirmed to be SAA-4,4'dipy cocrystals by powder x-ray diffraction, Raman spectroscopy, and differential scanning calorimetry.

ASA-4,4'dipy cocrystals were obtained via the following method: All conditions are the same as above see the SAA-4,4'dipy cocrystal preparation except the cooling temperature. The cooling temperature for the preparation of the ASA-4,4'dipy cocrystal was 50°C to 10°C.

The transformation was carried out under temperature and cooling rate conditions; transformation from SAA-4,4'dipy cocrystals to ASA-4,4'dipy cocrystals was performed below 15°C with a high cooling rate. High cooling rates favor the formation of cocrystals of ASA-4,4'dipy cocrystals even at higher cooling temperatures.

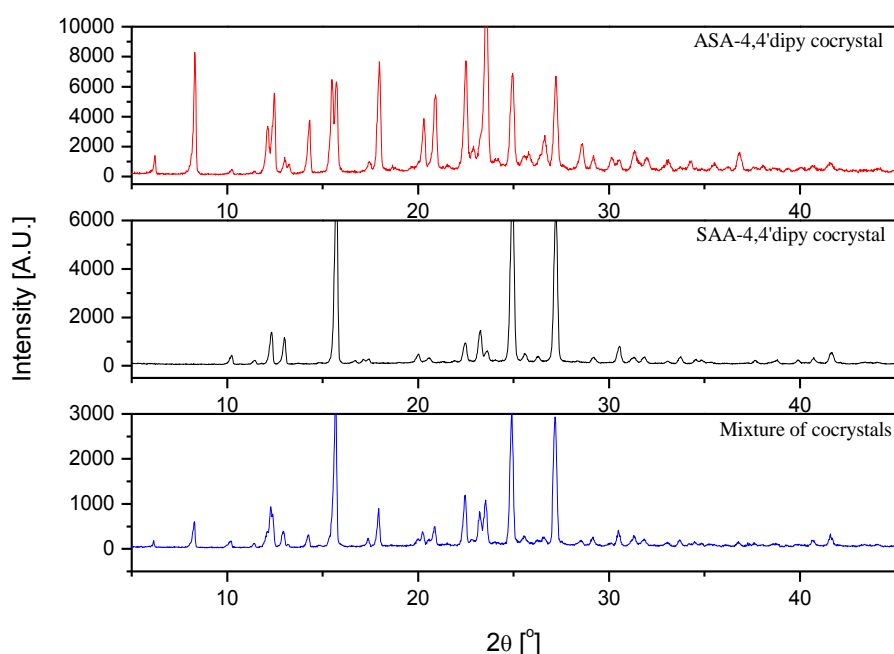
In the own work [Lee14], it has been reported that crystalline samples of SAA-4,4'dipy cocrystals can be prepared by cocrystallization of 2:1 ASA and 4,4'dipy in ethanol at 30°C.

5.3.2 Identification of cocrystals

In the own work [Lee14], it has been reported that crystalline samples of SAA-4,4'dipy cocrystals can be prepared by cocrystallization of 2:1 ASA and 4,4'dipy in ethanol at 30°C.

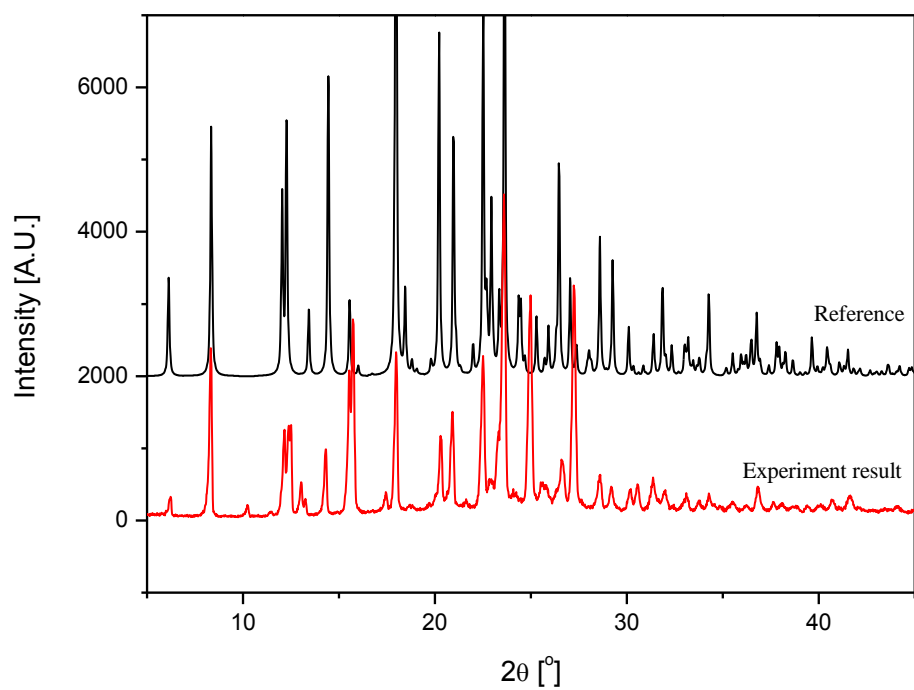
5. Results and discussion

Fig. 5.26 shows the solid-state identity of SAA-4,4'dipy cocrystals, ASA-4,4'dipy cocrystals and mixtures of between cocrystals using XRD, DSC and Raman spectroscopic analyses. The characteristic XRD peaks of SAA-4,4'dipy cocrystals were observed at 10.1° , 12.3° , 12.8° , 14.8° , 15.5° , 15.6° , 17.2° , 19.8° , 20.5° , 22.4° , 23.0° , 23.2° , 23.6° , 23.9° , 24.8° , 25.6° , 26.2° , 27.0° , 27.1° , 27.2° , 28.3° , 29.1° , 30.4° , 31.1° , 31.7° , 32.9° , 33.6° , 34.4° , 34.8° , and $37.5^\circ(2\theta)$, while those of ASA-4,4'dipy cocrystals were observed at 6.2° , 8.3° , 10.2° , 12.1° , 12.4° , 12.9° , 13.2° , 14.3° , 15.5° , 15.7° , 17.4° , 17.9° , 18.6° , 20.3° , 20.9° , 22.5° , 22.8° , 23.5° , 24.9° , 25.5° , 25.7° , 26.6° , 27.2° , 28.5° , 29.1° , 30.1° , 30.5° , 31.2° , 32.0° , 33.1° , and $34.2^\circ(2\theta)$ in Fig. 5.26-(1). In order to make sure that the crystals obtained in this study were ASA-4,4'dipy cocrystals, the XRD values were compared with literature [Wal03]. This is in good agreement with the XRD pattern report in literature (Fig. 5.26-(2)). Fig. 5.26-(3) displays the DSC curves of cocrystals. One endothermic peak at 156.10°C with 140.15J/g (SAA-4,4'dipy cocrystals) and another peak at 89.35°C with 69.91J/g (ASA-4,4'dipy cocrystals) were found in the DSC curves. The representative Raman spectra of SAA-4,4'dipy cocrystals, ASA-4,4'dipy cocrystals and mixtures of between cocrystals are also shown in Fig. 5.26-(4). Three most significant peaks between SAA-4,4'dipy cocrystals and ASA-4,4'dipy cocrystals were observed at 1760 , 1206 , and 755cm^{-1} .

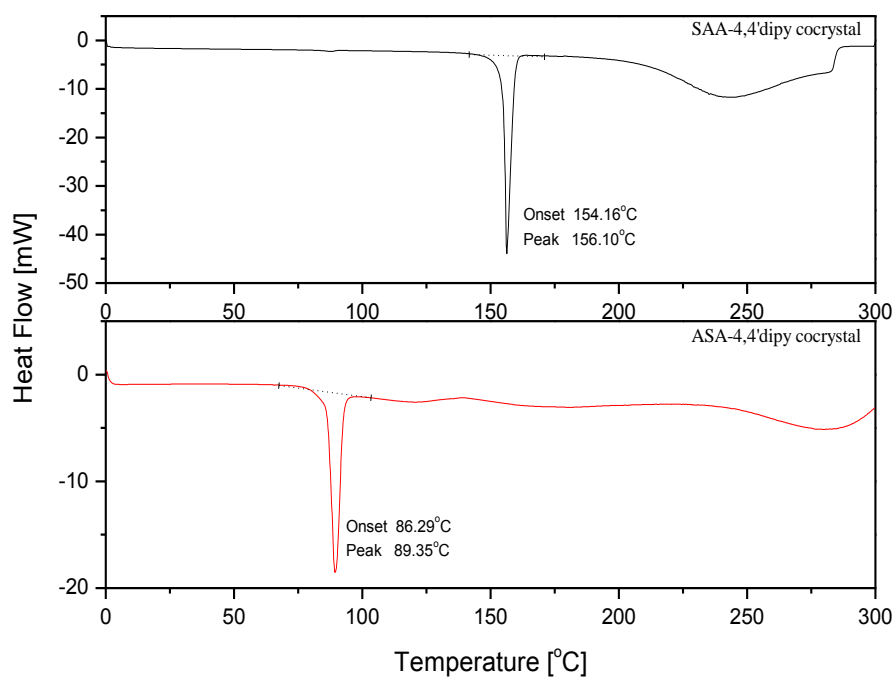


(1)

5. Results and discussion



(2)



(3)

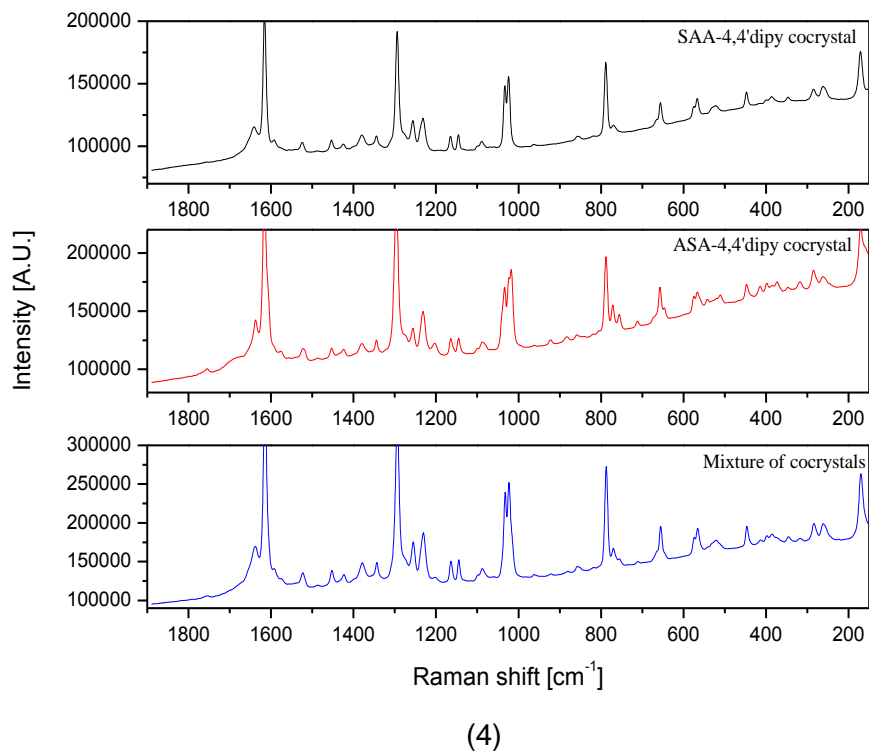


Figure 5.26: XRD pattern (1), XRD comparison between experiment result and literature (2), DSC curves (3), and Raman spectra (4) of SAA-4,4'dipy cocrystals, ASA-4,4'dipy cocrystals, and mixture of cocrystals.

5.3.3 In-situ measurement in cooling crystallization (solid-state)

Cooling crystallization was carried out for the transformation from SAA-4,4'dipy cocrystals to ASA-4,4'dipy cocrystals using Raman spectroscopy. The experiments were carried out at overall concentrations of SAA-4,4'dipy cocrystals in ethanol $C_{\text{SAA-4,4'dipy cocrystal}} = 0.04052\text{g/mL}$. The weighed SAA-4,4'dipy cocrystals were added to ethanol at 30°C and the vial was closed and gently shaken for a short time. The suspension was cooled down to 0°C at a cooling rate of 0.5K/min for 2h. Raman spectroscopy was employed to monitor the change of liquid phase as well as the solid phase. The solution was sampled at regular intervals using a solid-liquid separator with a glass filter to identify solid-state properties using PXRD, DSC, and Raman spectroscopy (Phat probe). After the transformation was complete, the suspension was filtered. The obtained product was dried and analyzed using the above mentioned instruments.

5.3.3.1 Optical microscope

Fig. 5.27 shows images captured during the transformation from SAA-4,4'dipy cocrystals to

5. Results and discussion

ASA-4,4'dipy cocrystals with time. The first image shows the SAA-4,4'dipy cocrystals (prism-like crystals) immediately after nucleation. In time, these prism-like SAA-4,4'dipy cocrystal crystals grow until another form, the ASA-4,4'dipy cocrystals, appear at 4512s. This are rounded plate-like shaped, and eventually fully displaced (at 5233s), prism-like SAA-4,4'dipy cocrystals. As a result, SAA-4,4'dipy cocrystals are initially formed and then transformation occurs from SAA-4,4'dipy cocrystals to ASA-4,4'dipy cocrystals.

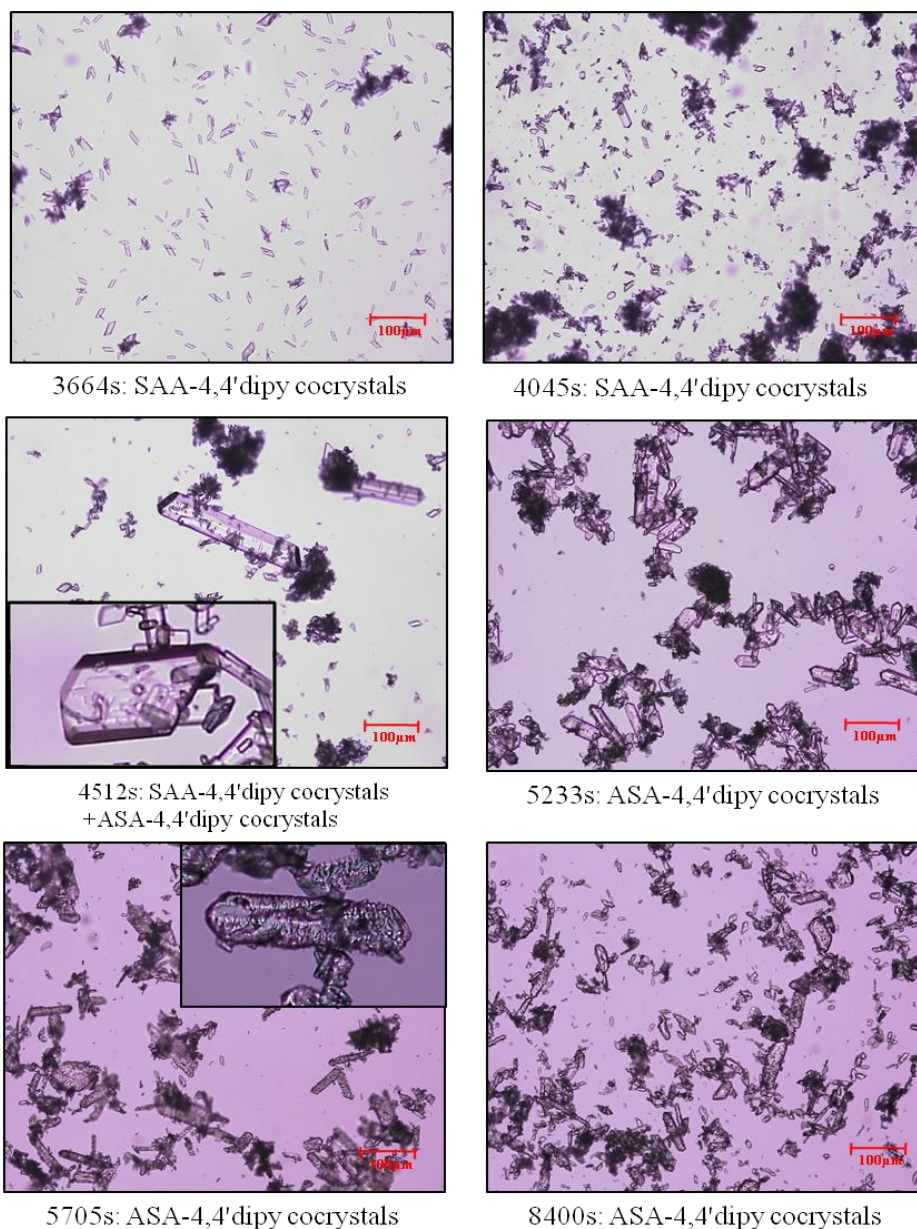


Figure 5.27: Microscopic photos of the crystals obtained from the solvent-mediated phase transformation from SAA-4,4'dipy cocrystals to ASA-4,4'dipy cocrystals in ethanol with elapsing time.

5.3.3.2 Powder x-ray diffraction

SAA-4,4'dipy cococrystals and ASA-4,4'dipy cococrystals show different XRD pattern during the cococrystallization experiments. The progressive transformation of SAA-4,4'dipy cococrystals with cooling was more clearly revealed from the changes in XRD (Fig. 5.28). SAA-4,4'dipy cococrystals have previously been characterized by single crystal x-ray diffraction which is matched to its simulated XRD pattern. In case of ASA-4,4'dipy cococrystals, peaks were observed 6.226, 18.313, 12.128, 14.324, and 17.979 with the elapsing time.

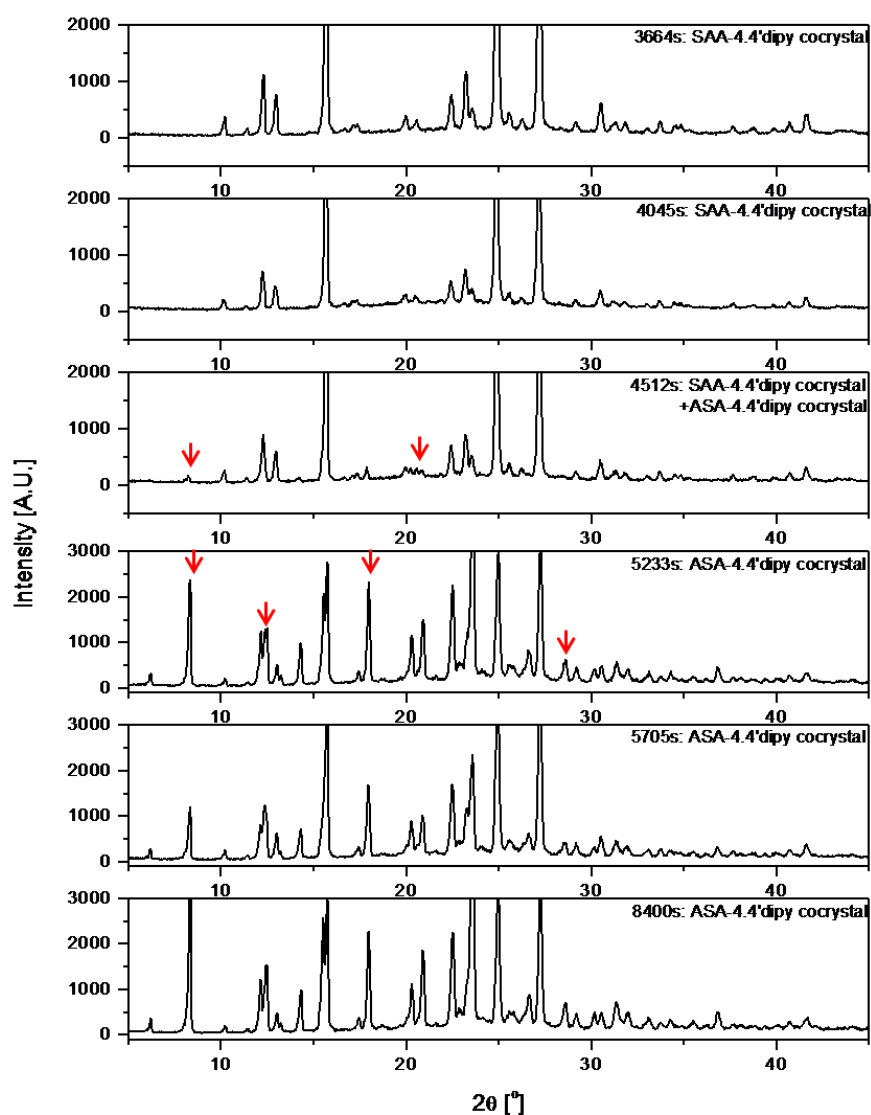


Figure 5.28: Comparison of PXRD pattern of transformation from SAA-4,4'dipy cococrystals to ASA-4,4'dipy cococrystals during cococrystallization experiment.

5.3.3.3 Raman spectroscopy

Raman spectroscopy reveals that SAA-4,4'dipy cocrystals convert to ASA-4,4'dipy cocrystals in the temperature range 50 to 10°C. The ongoing cocrystal transformation of SAA-4,4'dipy cocrystals to ASA-4,4'dipy cocrystals was more clearly proclaimed from changes in Raman spectra (Fig. 5.29). There are several characteristic peaks available to compare and identify the cocrystals. SAA-4,4'dipy cocrystals have characteristic peaks in spectra range of 1000 to 1300 cm^{-1} (1295, 1256, 1233, 1166, 1147, 1033, and 1025 cm^{-1}) which are reported in a own work [Lee14], while the appearance of 1208 and 1047 cm^{-1} band, which shows characteristic peaks of ASA-4,4'dipy cocrystals were observed in the same spectra range during a cocrystallization experiment.

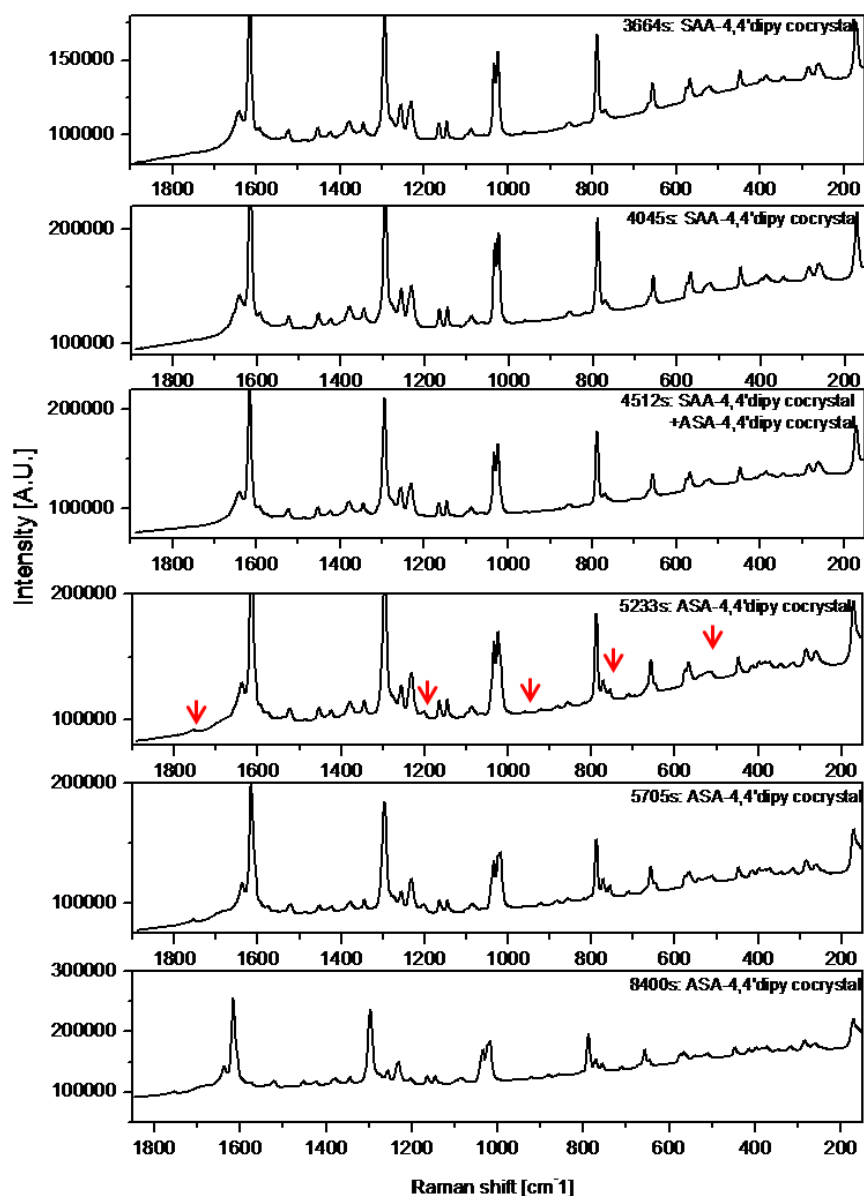


Figure 5.29: Raman spectra at different transformation times.

5.3.3.4 Thermal analysis (DSC)

Thermal analysis, DSC, provides valuable information that is characteristic of the two cocrystals, i.e. the change of cocrystals was confirmed by DSC. The phase transformations can be easily identified by the DSC. The DSC traces for all of the cocrystals are shown in Fig. 5.30. In the DSC experiments, both cocrystals were heated from 0 to 300°C. DSC thermograms show only one major endotherm for all of the cocrystals which corresponds to

5. Results and discussion

the melting process. SAA-4,4'dipy cocrystals have a sharp melting point at 156.10°C. ASA-4,4'dipy cocrystals showed a single endothermic peak at 89.35°C which was ascribed to the melting point. As shown in Fig. 5.30, a small endothermic peak appeared at 89.35°C, followed by a major endothermic peak at 156.10°C at 4045s. The small endothermic peak gradually increases with the elapsed of time, while the major endothermic peak (156.10°C) decreases. Finally, the major peak has disappeared at 5233s, suggesting that the change of small endotherms in the DSC thermogram is due to a phase transition from SAA-4,4'dipy cocrystals to ASA-4,4'dipy cocrystals.

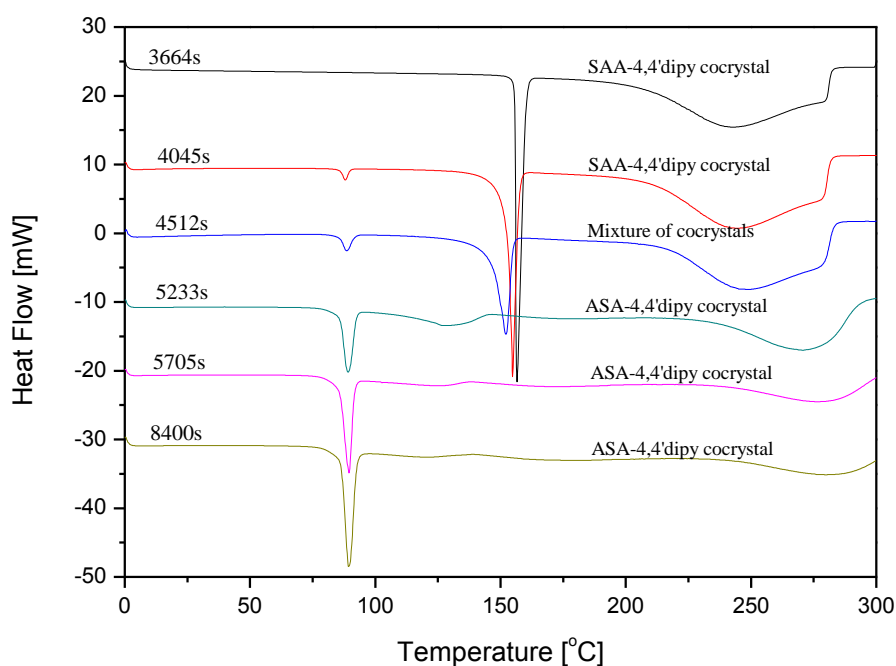


Figure 5.30: DSC traces of SAA-4,4'dipy cocrystals transformation with elapsed time.

5.3.4 In-situ monitoring the transformation of cocrystals using Raman spectroscopy (in solution)

The changes of SAA-4,4'dipy cocrystals to ASA-4,4'dipy cocrystals in ethanol was monitored and are analyzed and shown in Fig. 5.31. A representative time-resolved in-situ Raman spectral intensity change in the region of 1850-100 cm^{-1} over the course of the transformation are illustrated in Fig. 5.31. The Raman spectra of both cocrystals, shown in Fig. 5.32, displayed several differences which can be used to monitor the transformation of cocrystals. This differences can be seen clearly in the magnified spectra in Fig. 5.32. The great interests of Raman peak changes illustrate the corresponding Raman spectra in the

5. Results and discussion

range of 760-800, 980-1050, and 1570-1650 cm^{-1} .

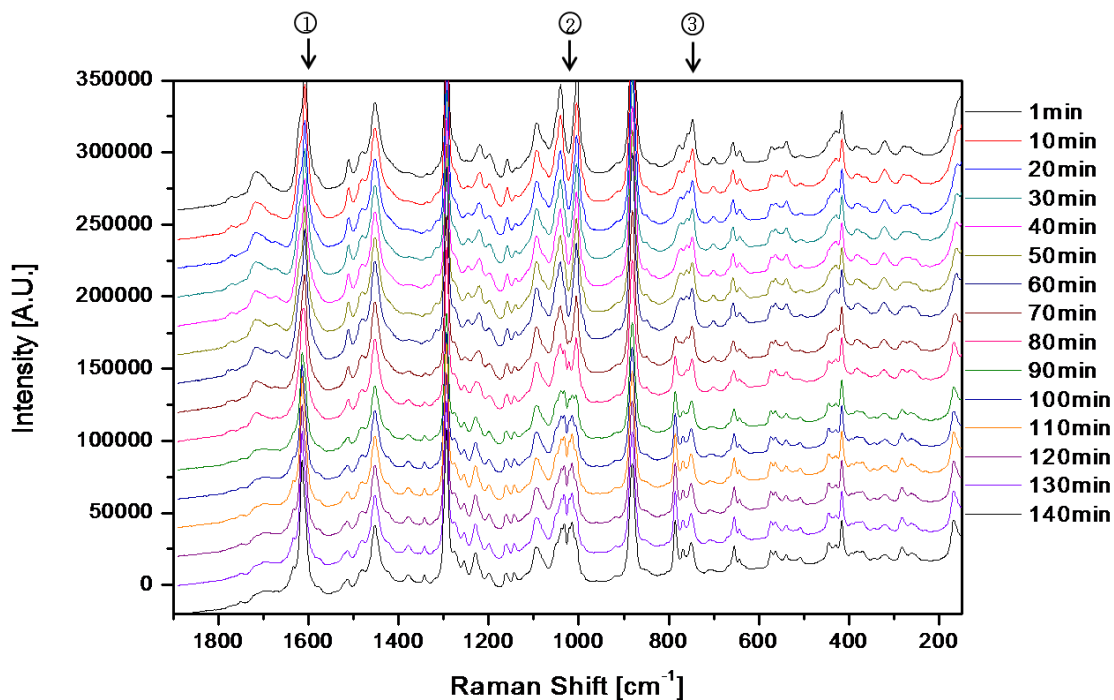
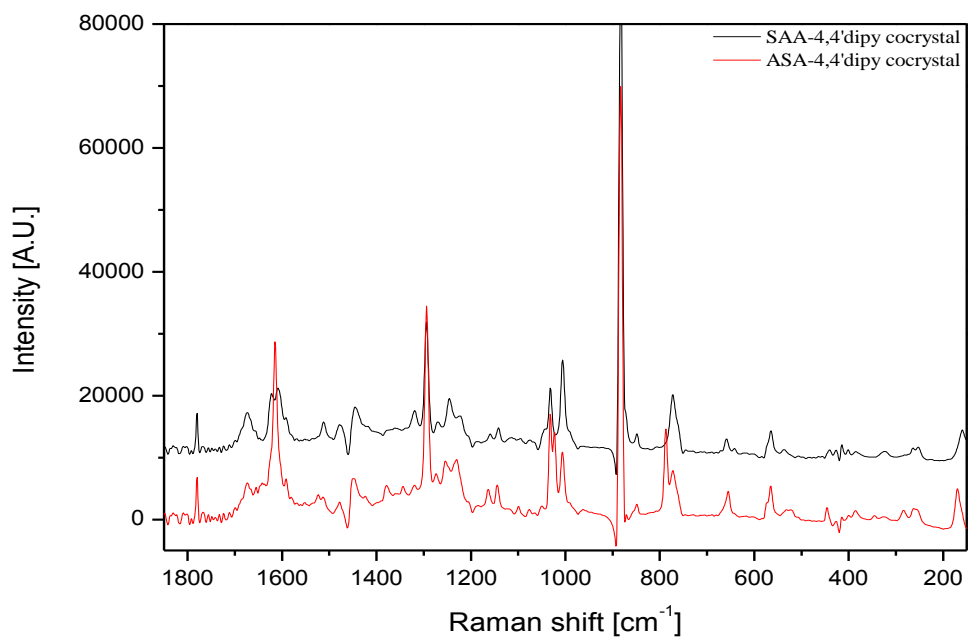


Figure 5.31: *In-situ Raman analysis of the transformation from the SAA-4,4'dipy cocrystal to ASA-4,4'dipy cocrystal with elapsed time.*



(1)

5. Results and discussion

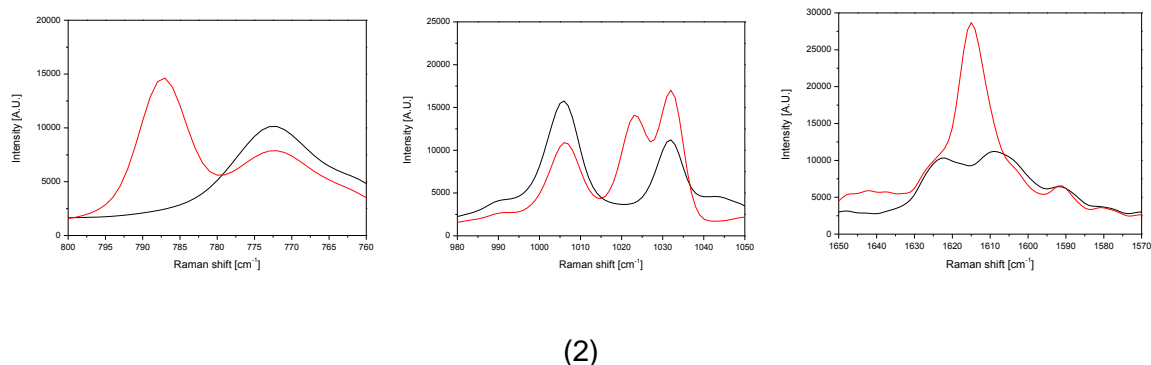
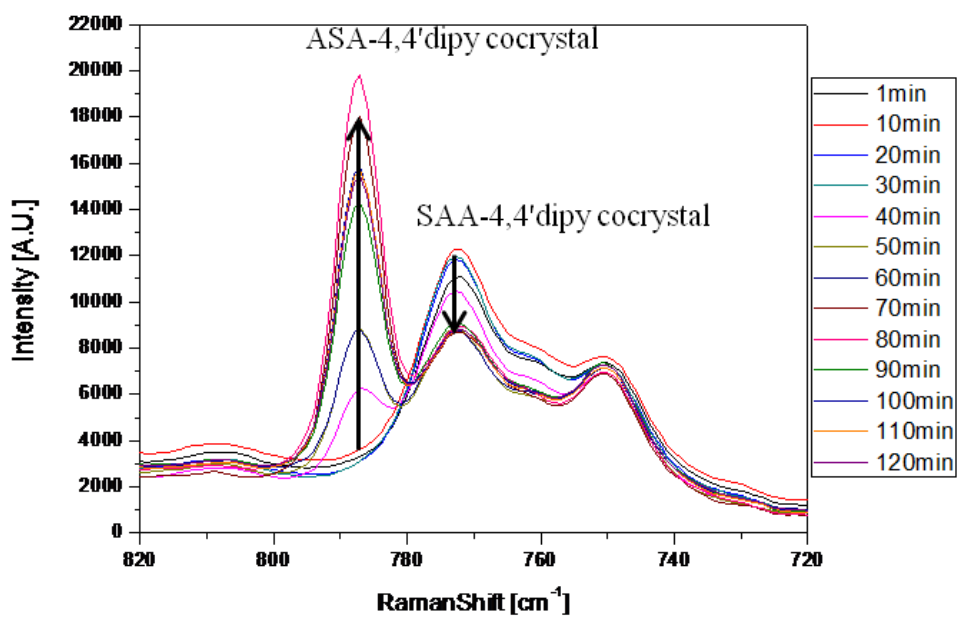


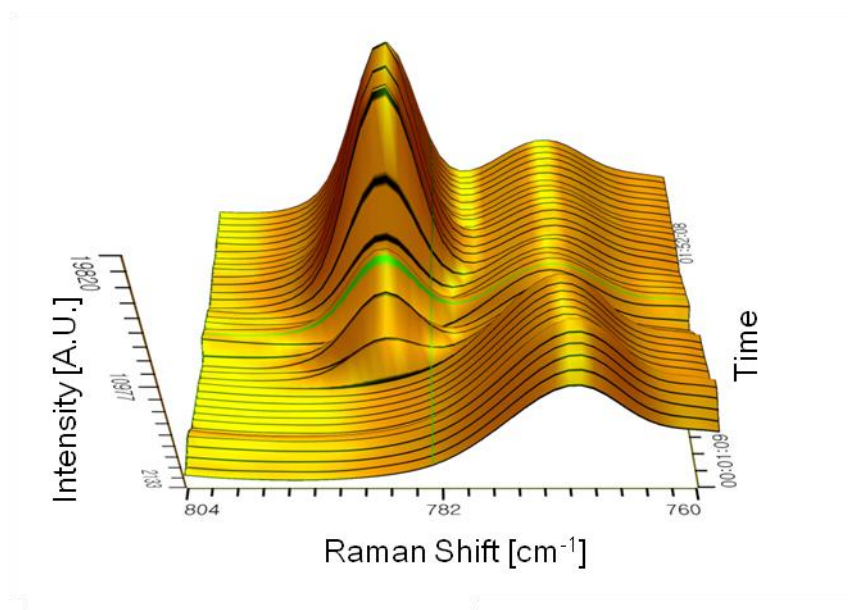
Figure 5.32: Raman spectra of SAA-4,4'dipy cococrystals and ASA-4,4'dipy cococrystals in ethanol (1). The enlarged view of Raman spectra in the spectra range of 760-800, 980-1050, and $1570-1650\text{cm}^{-1}$ (2).

To quantify the solid-state change during conversion of cococrystals, peak areas of selected peak are presented in Fig. 5.33. The decrease of the 773cm^{-1} peak, characteristic for the SAA-4,4'dipy cococrystals, and the appearance of the 788cm^{-1} peak, which is characteristic for the ASA-4,4'dipy cococrystals was observed with relative operating time during the crystallization process. The Raman spectra were normalized to a particular band of an internal standard. Typical Raman waterfall plots during the transition in the region of $760-800\text{cm}^{-1}$ are illustrated in Fig. 5.33-(2). It shows the time course of the transition from SAA-4,4'dipy cococrystals to ASA-4,4'dipy cococrystals at 30 to 10°C . It can be seen that the characteristic peak of the SAA-4,4'dipy cococrystals at 773cm^{-1} decreases in intensity, whereas that of the ASA-4,4'dipy cococrystals appears and increases in peak intensity at 788cm^{-1} , indicating that the SAA-4,4'dipy cococrystals were gradually transforming into ASA-4,4'dipy cococrystals. It is clear that turnover SAA-4,4'dipy cococrystals to ASA-4,4'dipy cococrystals was started after 40min and the transformation was completed in 80 to 85min. To have it more clear, the Raman peak area with the time-dependent transformation is illustrated Fig. 5.33-(3). The black and red curves represent the time profiles of the relative changes in the peak areas of SAA-4,4'dipy cococrystals and ASA-4,4'dipy cococrystals, respectively.

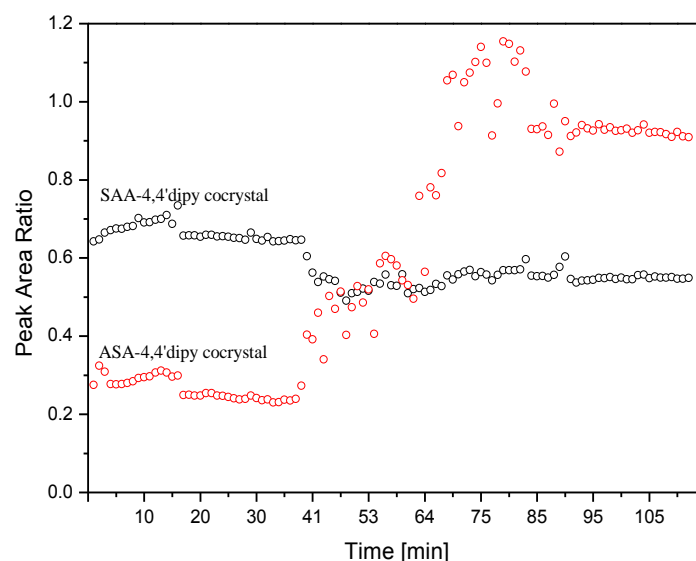
5. Results and discussion



(1)



(2)



(3)

Figure 5.33: Changes of Raman intensity at 773cm^{-1} and 788cm^{-1} during the transformation process. Selected spectra (1) real-time waterfall plots in the region of $760\text{-}800\text{cm}^{-1}$, (2) peak area change between $767\text{-}777\text{cm}^{-1}$ and $782\text{-}795\text{cm}^{-1}$, (3) during the crystallization process.

5.3.5 Formation and transformation of cocrystals

Fig. 5.34 shows the solubility of the SAA-4,4'dipy cocrystals and ASA-4,4'dipy cocrystals as a function of temperature 0 to 60°C as well as the cocrystals forming region. SAA-4,4'dipy cocrystals and ASA-4,4'dipy cocrystals are selectively formed by the operating parameters. It can be seen that both SAA-4,4'dipy cocrystals and ASA-4,4'dipy cocrystals were generated of fast cooling rates ($0.7\text{K}/\text{min}$) at operating temperature of 30°C in Fig. 5.34. When the cooling temperature cooled below 15°C the transformation occurs from the SAA-4,4'dipy cocrystals to ASA-4,4'dipy cocrystals at all condition even at slow cooling rates. Therefore, in transformation of cocrystals, cooling temperature and cooling rates are a major parameters to affect the transformation of the cocrystals. The solubility of ASA-4,4'dipy cocrystals is higher than those of SAA-4,4'dipy cocrystals, showing that SAA-4,4'dipy cocrystals are the thermodynamic stable form at higher temperature and providing the possibility to obtain the ASA-4,4'dipy cocrystals by rapid cooling.

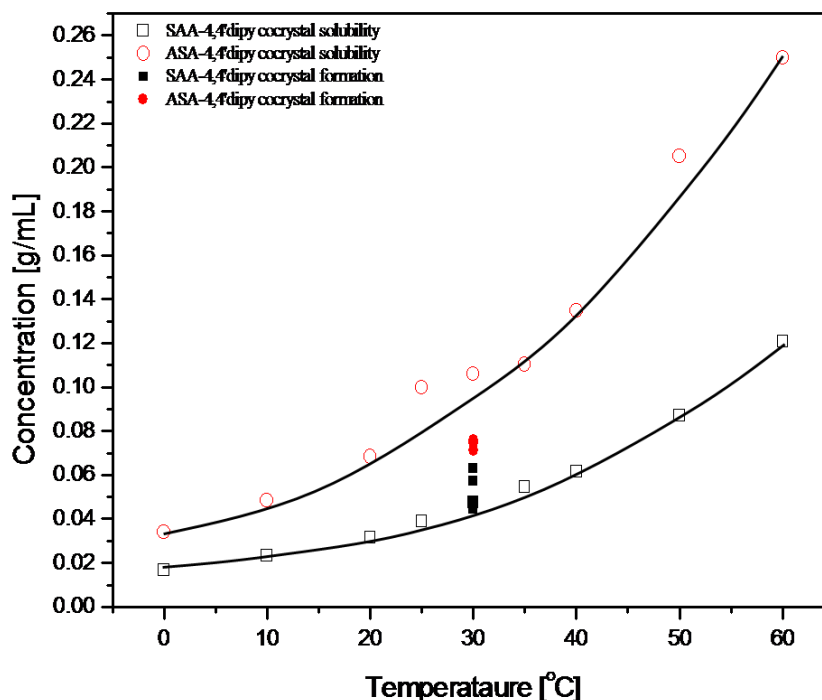


Figure 5.34: Solubility of SAA-4,4'dipy cocrystals and ASA-4,4'dipy cocrystals in ethanol, model solvent in temperature range 0 to 60°C and two different cocrystals forming area with cooling rate 0.7K/min.

5.3.6 Conclusions

The two different cocrystals (SAA-4,4'dipy cocrystals and ASA-4,4'dipy cocrystals) were characterized by PXRD, DSC, microscope, and Raman spectroscopy. The transformation from SAA-4,4'dipy cocrystals to ASA-4,4'dipy cocrystals have been probed using in-situ Raman spectroscopy to rapidly investigate a detailed insight into the mechanisms of transformation. It is possible to produce desired cocrystal forms by a controlled transformation process. The Raman spectroscopy permitted a real time monitoring of the disappearance and appearance of SAA-4,4'dipy cocrystals and ASA-4,4'dipy cocrystals, respectively. As a result, the transformation of cocrystals was successfully monitored by Raman spectroscopy. The supramolecular reaggregation of SAA-4,4'dipy cocrystals into ASA-4,4'dipy cocrystals was established by a solution crystallization method with ethanol as solvent.

5.4 Formation of salicylic acid/4,4'dipyridyl cocrystals based on the ternary phase diagram

The solubility behavior of salicylic acid (SAA)-4,4'dipyridyl (4,4'dipy) cocrystals is investigated in an ethanol solvent. The PSD of SAA-4,4'dipy cocrystals which are formed in a 2:1 stoichiometric ratio in ethanol are determined. The objective is to improve the understanding of the fundamentals of the formation mechanisms, solution behavior and solid-state properties of SAA-4,4'dipy cocrystals. It was found that the thermodynamic stability regions of the cocrystals and its components were defined by the phase solubility diagram. Besides, the kinetic also thermodynamic factor is important for the crystallization of cocrystals.

Until now, most studies on cocrystals have focused on the isolation of cocrystals for crystal structure determination, thermodynamic, synthesis, phase equilibrium, etc. [Lu09, Ain09, Sch09]. The variables that control the crystallization kinetics in the preparation of cocrystals have not been explicitly considered.

It will be described here how the measurement of TPD led to the discovery of a new solid form of a 2:1 cocrystal in ASA- 4,4'dipy-ethanol system. It will be focused on the effect of kinetic as well as on thermodynamic factors in the cocrystal formation in the cocrystal region in a phase diagram.

5.4.1 Experimental methods

5.4.1.1 Construction of the ternary phase diagram

The solubility of the invariant points of the pure substances were converted to mass fraction on a total mass basis (ASA+ 4,4'dipy + Ethanol), and plotted on a ternary axis in EtOH to generate the appropriate TPD using the ProSim Ternary Diagram software.

5.4.1.2 Determination of solubility

The solubility measurements of ASA and 4,4'dipy in ethanol were performed by the gravimetric method. An excess of solid phase is added to the desired solvent at 30°C and equilibrated with constant agitation for 24 hours. After the equilibrium has been reached, the agitation was stopped for 5 min to allow the remaining solid phase to settle. From the upper clear solution, three samples of 1mL each were filtered by a syringes into a pre-weighed

5. Results and discussion

glass vial (M_1). The weight of the vial with clear saturated solution is recorded right after filling with the solution (M_2). The solvent was allowed to evaporate in a fume hood (24hours) before transferring the glass vial to a vacuum oven which was held at 50°C. The weight of the vial is determined from time to time until there is no further weight change (M_3). The formula $(M_3-M_1)/(M_2-M_3)$ revealed the solubility, is expressed as g solid/g solvent.

To further examine the phase diagram of the system, the solid phase solubility was also measured at 30°C under nonstoichiometric conditions. The solubility of ASA and a 2:1 cocrystals as a function of 4,4'dipy concentration in ethanol was determined at 30°C by equilibrating the desired phase in solutions of known 4,4'dipy concentration. A small quantity of ASA (to saturated solution) was added into the 4,4'dipy solution in dribs and drabs. The ASA rapidly dissolved. When the amount of added ASA reached a certain point, cocrystals formed in the solution. 30 min later, the crystals were isolated and dried in a vacuum oven at 40°C overnight. The forming of cocrystals was verified using Raman spectroscopy. A gravimetric analysis was used to calculate the solubility. The eutectic point, also referred to as an invariant point, for the SAA-4,4'dipy cocrystal was determined by measuring the solubility of cocrystals + ASA and cocrystals + 4,4'dipy in ethanol. The mass ratio of cocrystals/ ASA and cocrystals/4,4'dipy was 1. The solubility of mixtures was measured by the gravimetric method described above. Then the relative amount of ASA, 4,4'dipy and cocrystal was calculated using a balance.

5.4.2 Solubility curves

The solubility curves ASA to 4,4'dipy in the ethanol, as shown in Fig. 5.35, were obtained by stirring solid drugs in a co-former solution at 30°C. Fig. 5.36 shows how the equilibrium concentration of ASA changes with various ratios of 4,4'dipy in ethanol. When the equivalent number of 4,4'dipy is zero, it means that there exists no 4,4'dipy in the solution. When the equivalent number of 4,4'dipy is unity, the molar ratio of ASA to 4,4'dipy in the slurry is 2:1 corresponding with the cocrystal composition. As shown in Fig. 5.35, the concentration of ASA decreases nonlinearly with the increasing 4,4'dipy concentration in ethanol. In Fig. 5.36, the solubility data of Fig. 5.35 are redrawn to illustrate the theory of solubility product. This behavior was explained by the solubility product equations [Neh05]. The line corresponds to the relation.

$$K = [ASA]^2[4,4'dipy] \quad (1)$$

The value of K was 0.0104molL⁻¹ of the solvent at 30°C.

5. Results and discussion

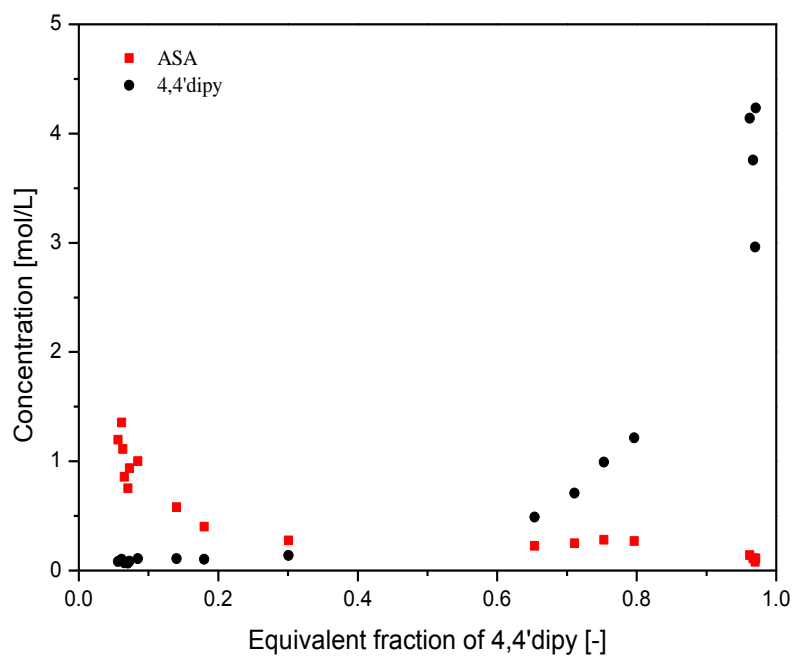


Figure 5.35: Solubility of ASA in ethanol with various concentrations of 4,4'dipy at 30°C.

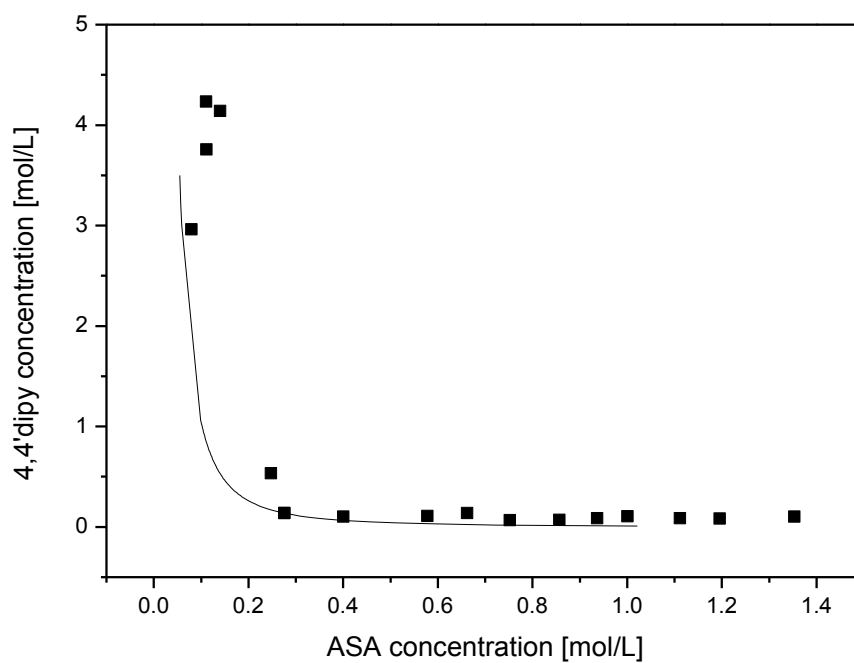


Figure 5.36: PSD for the 2:1 SAA-4,4'dipy cocrystals fitted to the solubility product rule.

5.4.3 The ternary phase diagram

In order to understand the formation of cocrystals, it is important to study the phase equilibrium between the API and the co-former. If the ternary phase of a system is known, crystallization experiments to acquire the cocrystals can be better designed and the outcome can be predicted. On the basis of the measurements of solubility and the PXRD results, it can be concluded that there is ASA/4,4'-bipy/ethanol phase diagram measured at 30°C in which there are six regions and two eutectic points. A schematic TPD is shown in Fig. 5.37. It is divided into six regions by the solubility curves of the cocrystal and single components. Region 1 is the undersaturated liquid domain in which all compositions are single phase liquids. In all other regions, solid phases exist in equilibrium with solutions. Zone 2/6 means the solution is in equilibrium with ASA/4,4'-bipy crystals and SAA/4,4'-bipy cocrystals. In zone 3 there is the solid compound ASA, the solid cocrystal and a liquid phase. In zone 4 there are SAA/4,4'-bipy cocrystals and a liquid phase. Zone 5 is like zone 3 the coformer with the solid compound 4,4'-bipy, the solid cocrystal and a liquid phase. The eutectic points C_1 and C_2 are the points where the solubility curves of ASA and 4,4'-bipy, meet up with the solubility curve of the cocrystals. The point A and B correspond to ASA and 4,4'-bipy solubility. The ASA and 4,4'-bipy ratio in the cocrystal is given by the point D. The zone of cocrystal formation is limited by concentration and the cocrystal exists with liquid in the region DC_1C_2 .

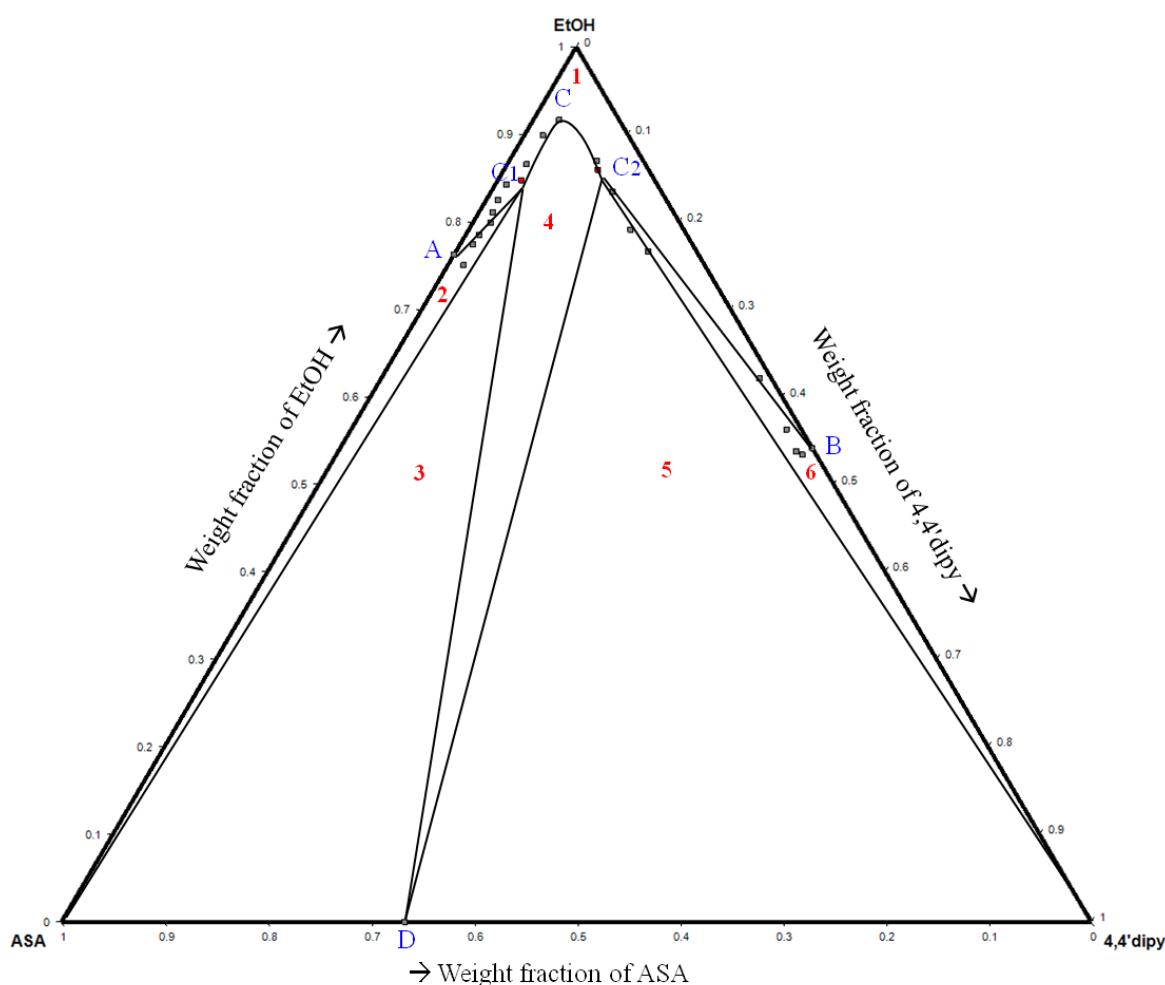


Figure 5.37: TPD of ASA/4,4'-bipy/ethanol at 30°C in mass %. Regions in the diagram are as follows: (1) solution phase, (2) ASA+ liquid (3) ASA+ cocrystals (4) cocrystal only (5) 4,4'-bipy+ cocrystals, and (6) 4,4'-bipy+ liquid.

5.4.4 Solid-state characterization

After the crystallization experiments, the crystalline residues were collected by filtration and dried, after which they were analyzed using PXRD, DSC, Raman and SEM.

Single crystal XRD verified the cocrystals as 2:1 SAA-4,4'dipy cocrystal, with space group P-1 and cell parameters $a=7.8712(10)\text{\AA}$, $b=8.3851(2)\text{\AA}$ and $c=8.6683(3)\text{\AA}$. Crystal images from cooling crystallization of ASA-4,4'dipy solution are shown in Fig. 5.38. The powder X-ray diffraction pattern of the 2:1 SAA: 4,4'dipy cocrystal is shown in Fig. 5.39. This revealed a characteristic diffraction pattern, which is differed from those of the two individual components and the physical mixture. It shows the agreement between the experimental

5. Results and discussion

powder XRD pattern of the 2:1 SAA-4,4'dipy cocrystals and that one calculated by the software Mercury from the single crystal structure data.

The DSC thermogram in Fig. 5.40 confirmed the presence of the cocrystals and indicated a sharp endothermic melting event with an onset temperature of around 155.52°C (with a heat of fusion, $\Delta H=140.15\text{J/g}$). On the contrary, ASA and 4,4'dipy showed melting onsets at around 141.59°C ($\Delta H=148.71\text{J/g}$) and 112.16°C ($\Delta H=103.39\text{J/g}$), respectively.

The Raman spectra of ASA, 4,4'dipy and the cocrystals are compared in Fig. 5.41. Raman spectra revealed evidence of significant intermolecular interactions based on two characteristic peaks. As shown in Fig. 5.41, particular differences between the spectra of the cocrystals and of pure materials are found in the spectra range of 1100-1000 cm^{-1} , the mixture has three characteristics peaks at 1043, 1022 and 1006 cm^{-1} , whereas cocrystals have two characteristics peaks at 1033 and 1024 cm^{-1} . This difference was used to identify cocrystals of SAA-4,4'dipy. The reason for these shifts of the Raman peaks was explained based on the single crystal X-ray diffraction data previously reported for the SAA-4,4'dipy cocrystals which showed that molecular association between ASA and 4,4'dipy occurs through hydrogen bonding [Lee14].

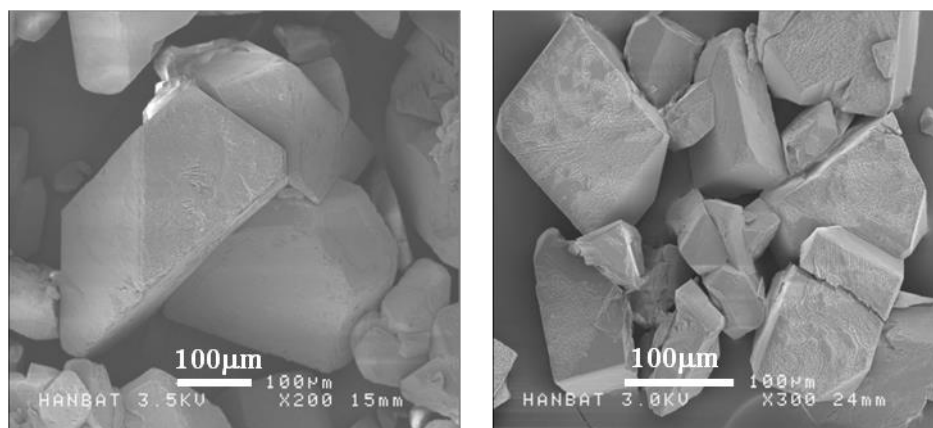


Figure 5.38: SEM images of a crystalline product in ethanol.

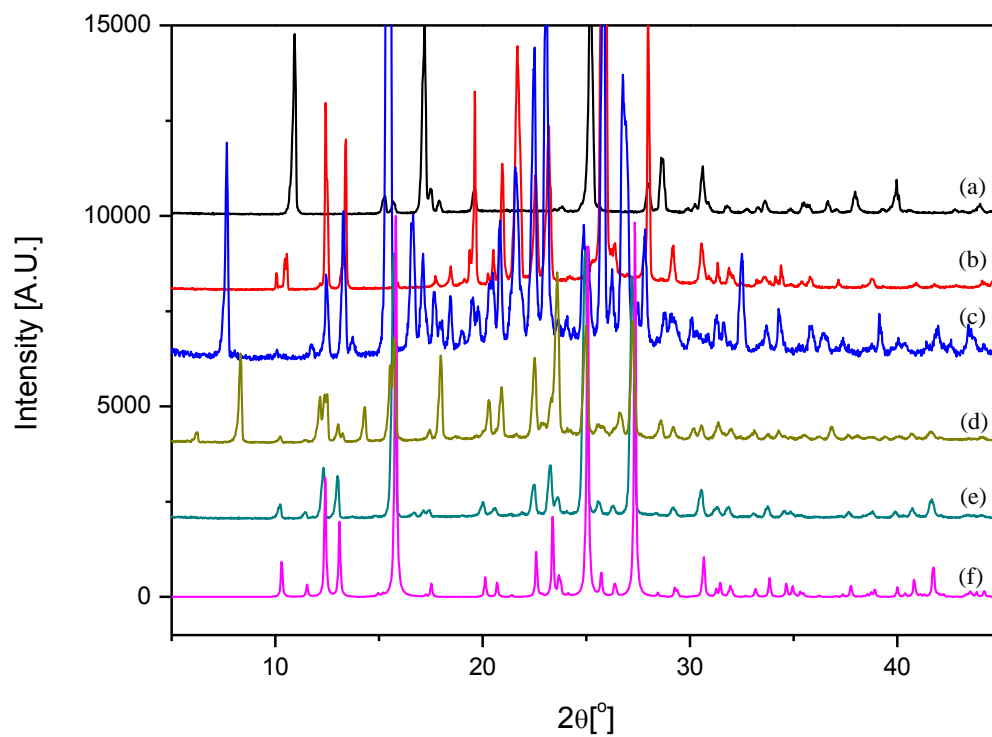


Figure 5.39: PXRD pattern of (a) pure ASA, (b) pure 4,4'-bipy, (c) physical mixture, (d) ASA/4,4'-bipy cocrystal, (e) SAA/4,4'-bipy cocrystal, and (f) SAA/4,4'-bipy cocrystal calculated based on single crystal data.

5. Results and discussion

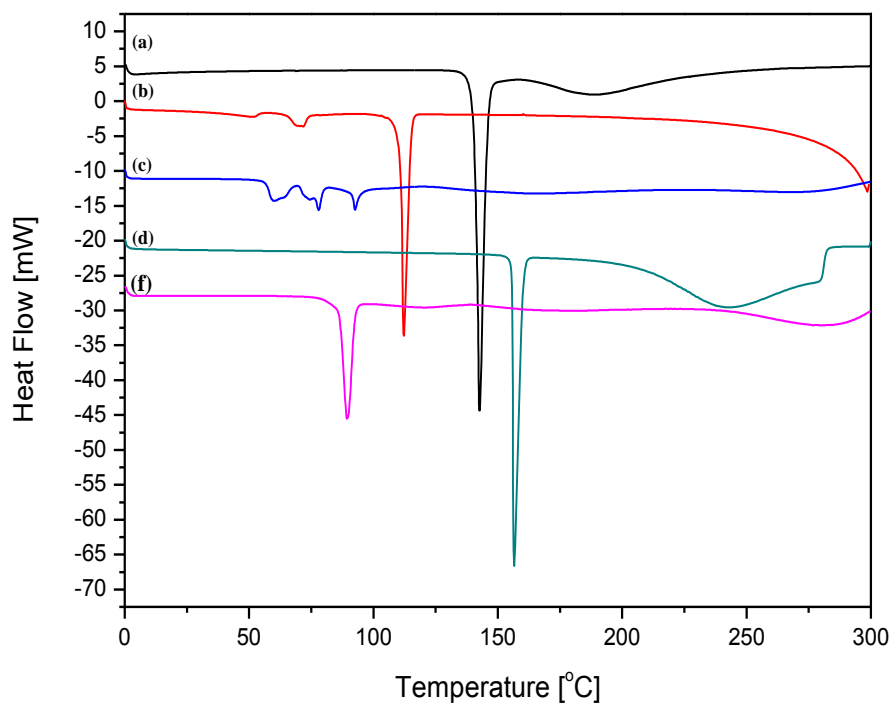


Figure 5.40: DSC thermograms of (a) pure ASA, (b) pure 4,4'-bipy, (c) physical mixture, (d) SAA/4,4'-bipy cocrystals, and (f) ASA/4,4'-bipy cocrystals.

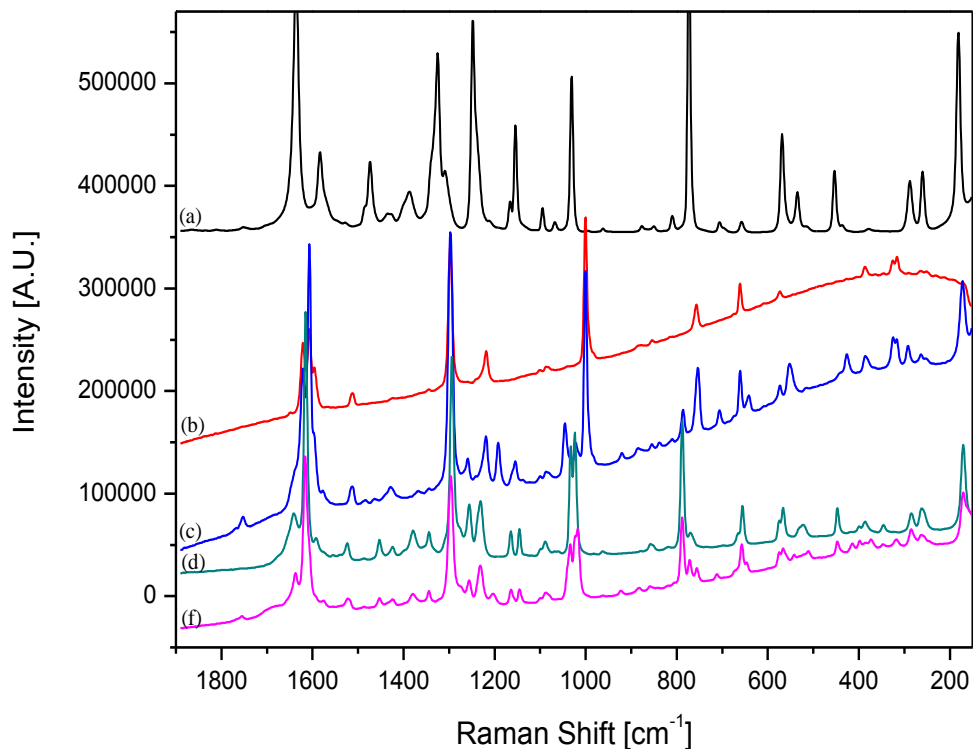


Figure 5.41: Raman spectra of (a) pure ASA, (b) pure 4,4'-bipy, (c) physical mixture, (d) SAA/ 4,4'-bipy cocrystals, and (f) ASA/ 4,4'-bipy cocrystals.

The solubility of ASA and SAA-4,4'dipy cocrystals were investigated in order to assess stability regions of SAA-4,4'dipy cocrystals in ethanol solutions. The solubility of pure substances, physical mixture and cocrystals in ethanol at various temperatures are shown in Fig. 5.42.

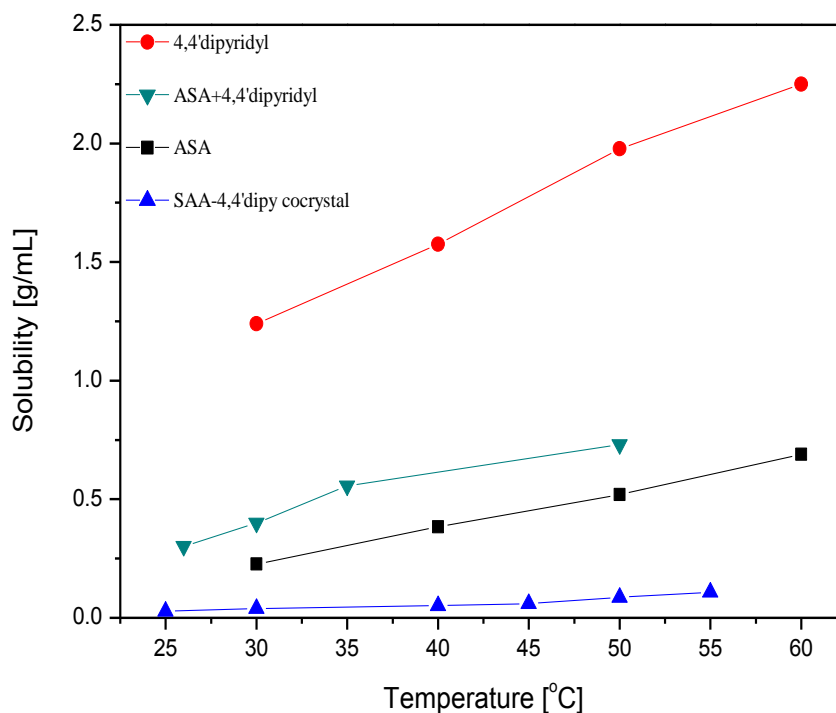


Figure 5.42: Solubility of the start materials and SAA-4,4'dipy cocrystals in ethanol.

5.4.5 The formation of cocrystals: the thermodynamic and the kinetic effect

Crystallization is a dynamic process in which, however, besides kinetic also thermodynamic factors determine the solid product form. With those factors most likely the formation of a metastable product will be achieved. As concerns kinetics, the different solid phases which might appear during the experiments were observed in the cocrystal region of TPD with kinetic factors. To elucidate how the TPD as shown in Fig. 5.37 can be used to design cocrystallization processes, two crystallization runs were performed; with different cooling rates and temperatures.

At first, the effect of the cooling rate was investigated. Experiments were performed by cooling from 50°C to 30°C with various cooling rates (0.2, 0.35, 0.7, 1 and 2K/min). In the experiments, 2:1 molar ratio of ASA and 4,4'dipy was introduced in ethanol at 50°C. After the suspension is completely dissolved, the solution cooled down at different cooling rates until it reaches 30°C at a constant agitation rate. After 30min from the start of nucleation, crystalline particles were filtered and dried at 40°C. The solid phase was systematically analyzed by PXRD measurements.

5. Results and discussion

As shown in Fig. 5.43, the effect of the cooling rate profile on the supersaturation is demonstrated through the analysis of the collected crystals at the end of each experiment. It can be seen that steep cooling profile produces ASA-4,4'dipy cococrystals, whereas low cooling profile generates SAA-4,4'dipy cococrystals even in higher supersaturation levels. This is to be explained by changing the nucleation rate by cooling rate. This fast cooling rate will cause a high nucleation rate that allows the formation of ASA-4,4'dipy cococrystals. The effect of the change in the cooling rate in the cococrystal forming region of TPD is presented in Fig. 5.44. As a result, the SAA-4,4'dipy cococrystals were produced in a cococrystal forming area at slow cooling rates (0.2K/min). However, it can be seen that both ASA-4,4'dipy cococrystals and SAA-4,4'dipy cococrystals were generated of fast cooling rates (0.7K/min) even in the cococrystal forming area. So, choosing an appropriate cooling rate will determine the type of final product.

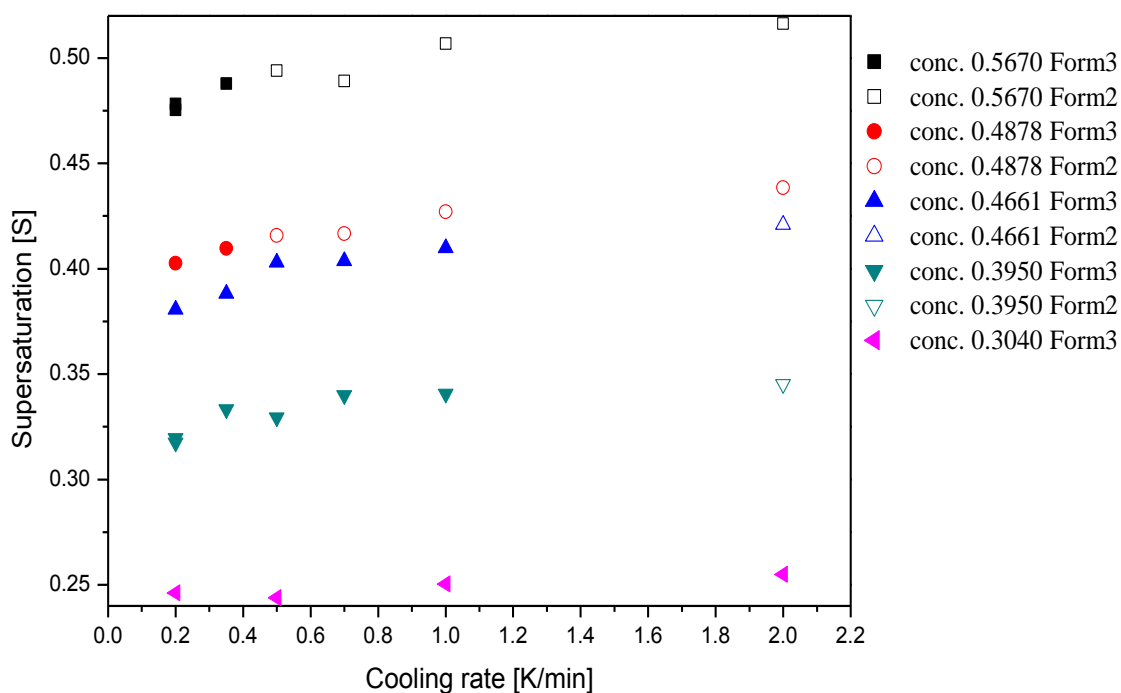
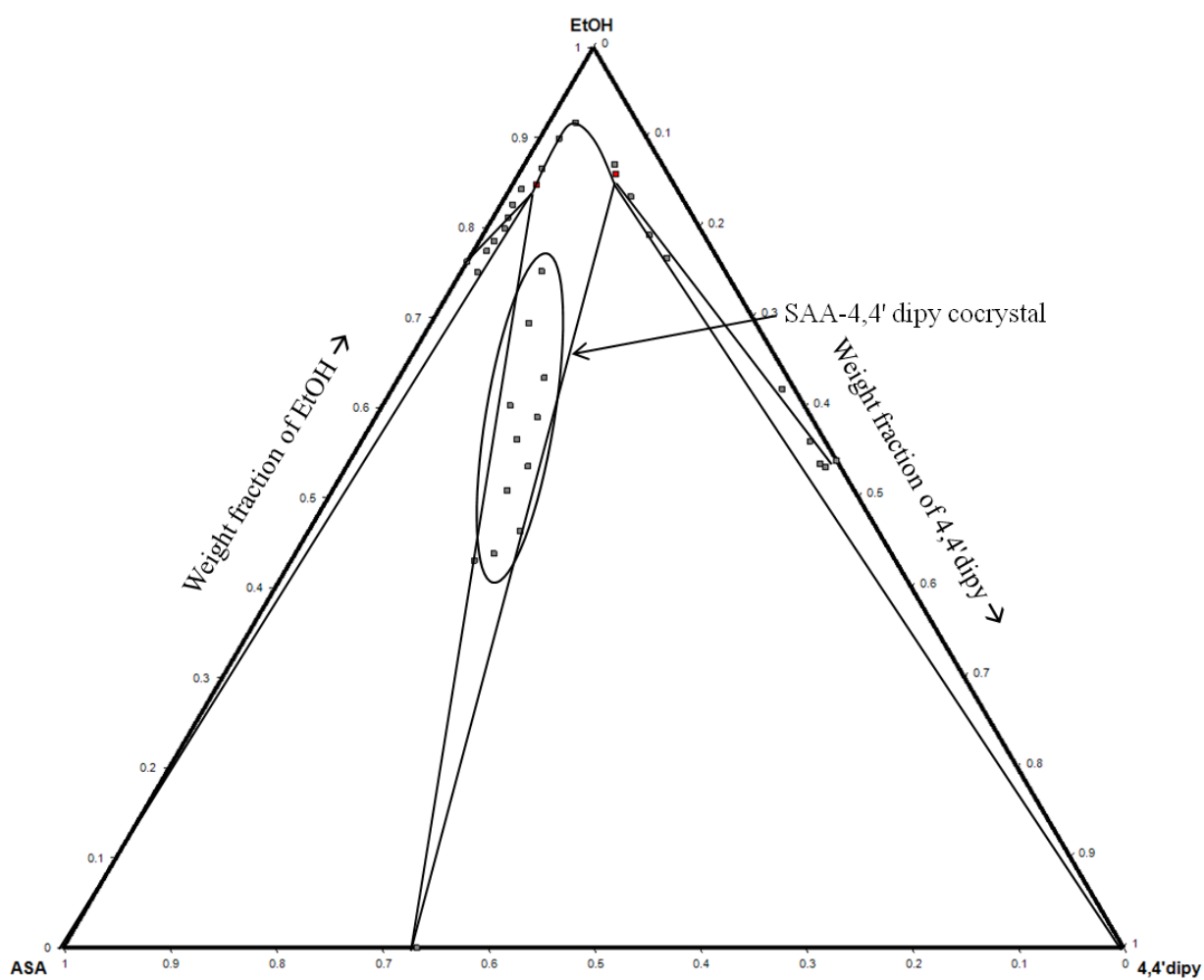


Figure 5.43: The effect of cooling rates with different concentrations (close: SAA-4,4'dipy cococrystal, open: ASA-4,4'dipy cococrystal).

5. Results and discussion



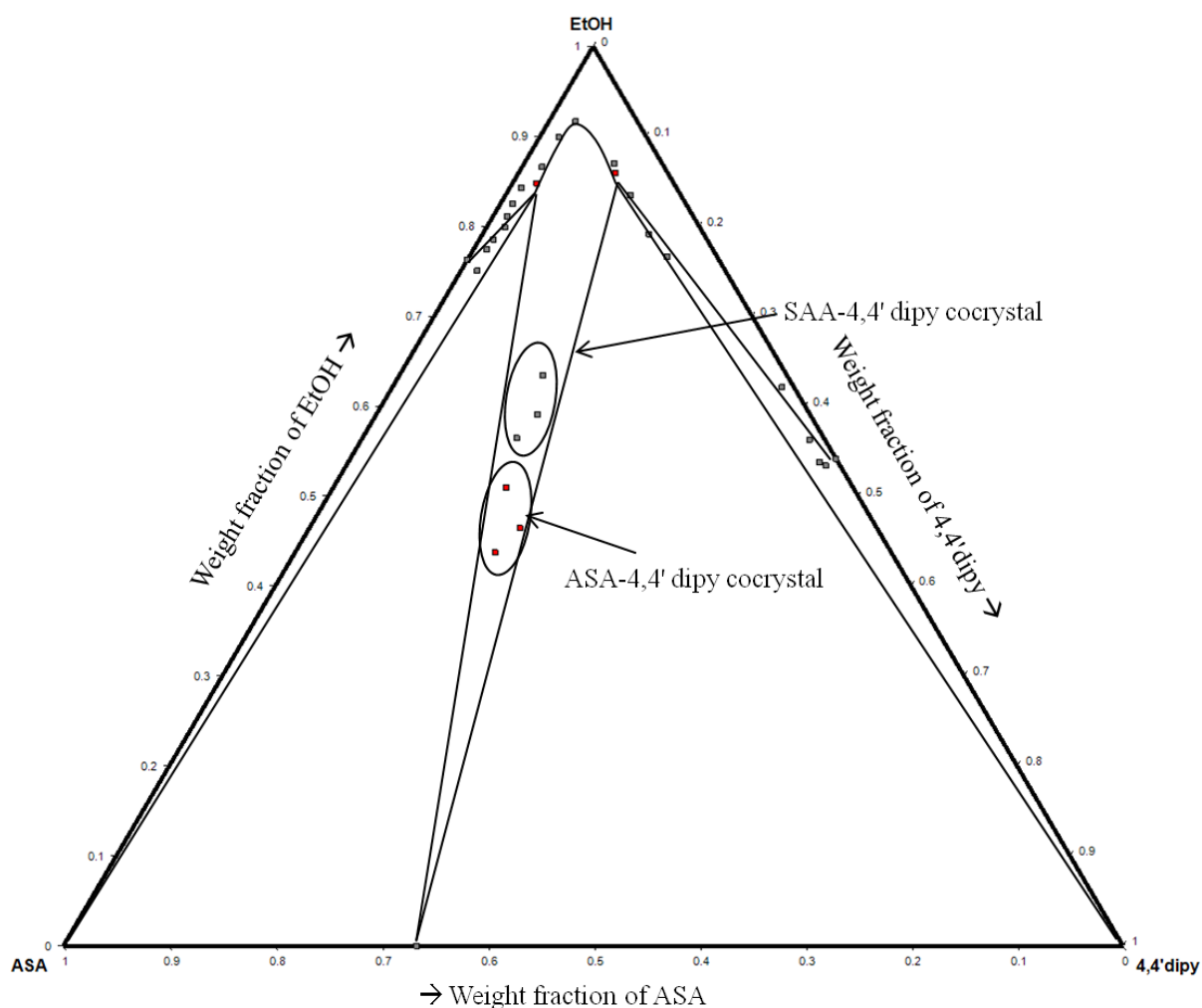


Figure 5.44: Operation point designed for the cocrystallization experiment with different cooling rates 0.2K/min (top), and 0.7K/min (bottom).

To demonstrate how the cooling temperature could affect the results obtained from cocrystallization processes, the experiments are carried out under the conditions of various cooling temperatures such as 15, 20, and 30°C. Fig. 5.45 shows the cocrystals change their form when the temperature change (15-50°C) at slow and fast cooling rates. In each case, slowly crystallized samples showed similar behavior to form of SAA-4,4'dipy cocrystals. On the other hand, high cooling rates favor the formation of ASA-4,4'dipy cocrystals even at higher cooling temperatures. The cooling rate is plotted against the supersaturation in Fig. 5.45. It can be seen that the SAA-4,4'dipy cocrystals are observed with slow cooling rates and low supersaturations at each temperature. Also, the cooling temperature gets lower and lower, the region of SAA-4,4'dipy cocrystals becomes narrower. The results from this work indicate that the cooling temperature can lead to different cocrystal types.

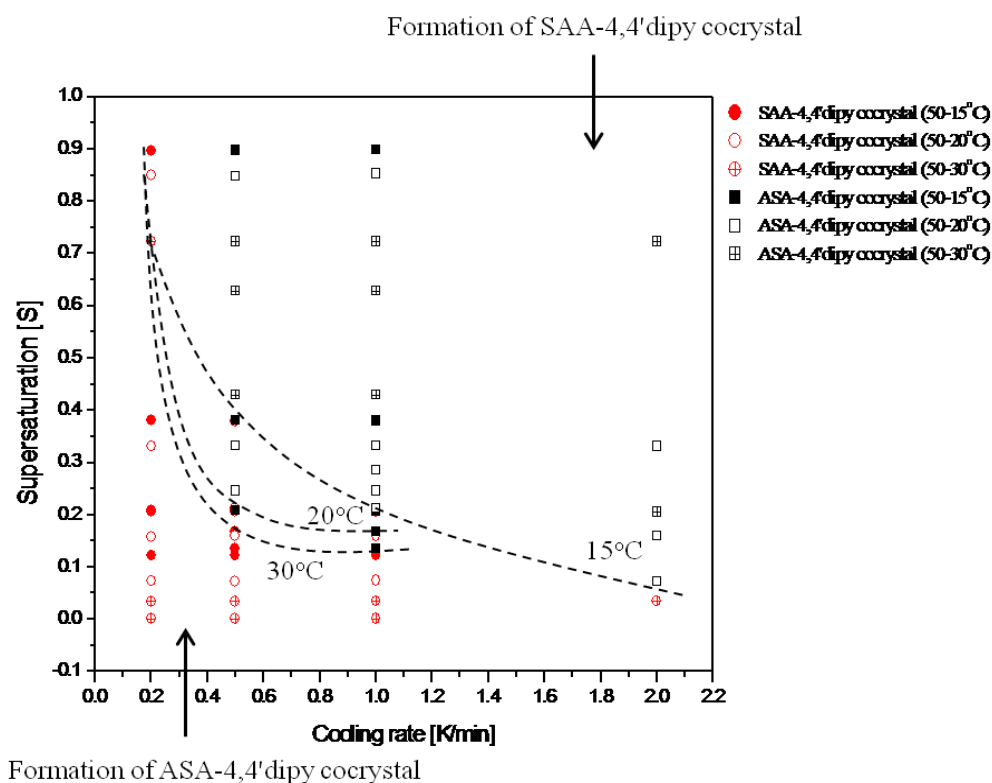


Figure 5.45: The effect of cooling temperature on cocystal formation with different cooling rates.

5.4.6 Conclusions

The ternary solid-liquid equilibrium diagrams of the system ASA/4,4'dipy/ethanol were measured at 30°C. The regions of saturated solution, cocystals, ASA+ cocystals, and 4,4'dipy+ cocystals were presented. It is clear that the range of compositions chosen in the search for cocystals in any particular system must be dictated by the relative solubility of the two components. Results show that the solubility of ASA decrease with increasing 4,4'dipy concentration, and K_{sp} can be determined by the solubility method. In order to develop the thermodynamic and kinetic aspects of cocrystallization, the crystallization technique by controlling the cooling rate and temperature was carried out based on the TPD. By controlling the operating conditions, the desired form of the cocystals can be formed in the cocystals of the zones of TPD. As for the results, the desired SAA-4,4'dipy cocystal was obtained under the conditions of slow cooling rates and high temperature. This explains the importance considering thermodynamic as well as kinetic factors when selecting cocrystallization processes and cocystal screening.

6. Summary of the conclusions

This research mainly investigated that important topics related to the process of crystallization and the development of pharmaceutical cocrystal formation. The results demonstrate the physical properties of salicylic acid cocrystals, mainly the solubility behaviour and their thermodynamics in solvents, which could benefit for a rational design of cocrystallization process as in the future. The key finding of the present work can be summarized:

- In chapter 5.1, the five novel cocrystals of salicylic acid with organic bases which contain N atoms have been produced with cooling/evaporation crystallization. The crystal structure of the cocrystals has also been determined by single crystal x-ray diffraction. The N-H...O hydrogen bonds play an important role in contributing to the stability of the compounds. The cocrystal forms of salicylic acid with coformers, that show the better properties in comparison to the pure material, can be emphasized for industrial applications.
- In chapter 5.2, the formation of SAA-4,4'-dipy cocrystal with different stoichiometry were explored by varying the solvents using solution crystallization.

In-situ studies with SAA and 4,4'-dipy using Raman spectroscopy provided a higher quantity of information on the reaction, such as identification of the end point of the reaction, the depth understanding of the formation mechanisms of cocrystals, and a more efficient design of experimental proceedings.

- The cocrystal screening of SAA-4,4'dipy and transformation behaviour have been described in chapter 5.3. Two different cocrystals including SAA-4,4'dipy cocrystals and ASA-4,4'dipy cocrystals have been identified. For a comparison of SAA-4,4'dipy cocrystals and ASA-4,4'dipy cocrystals, PXRD, DSC, microscope, and Raman spectroscopy was used with elapsing time. A solvent-mediated transformation process has been employed to prepare these cocrystals. The mechanisms of transformation from SAA-4,4'dipy cocrystals to ASA-4,4'dipy cocrystals that allowed to produce the desired cocrystal forms was explained by utilizing Raman spectroscopy which is permitted a real time monitoring. Consequently, it has been found that SAA-4,4'dipy cocrystals and ASA-4,4'dipy cocrystals, are stable and metastable forms at room temperature, respectively.

6. Summary of the conclusions

SAA-4,4'dipy cocrystals transforms to ASA-4,4'dipy cocrystals upon short periods of time of cooling at low temperature, while SAA-4,4'dipy cocrystals were stable to re-crystallization of ASA-4,4'dipy cocrystals.

- In chapter 5.4, the phase solubility behaviour of cocrystals which are formed in a 2:1 stoichiometric ratio in ethanol was explained by the relative solubility of the two components. The current study demonstrates the influence of kinetic and thermodynamic aspects on cocrystallization. Controlling the operating conditions such as cooling rate and temperature is believed to be potentially important for the formation of the desired forms in the cocrystals of the zones of TPD. SAA-4,4'dipy cocrystals which are the desired stable form were obtained under the conditions of slow cooling rates and high temperatures. Formation strategies based on the TPD were useful for stabilizing the cocrystals or controlling their transformation kinetics.

7. Summary

A first priority aim of pharmaceutical material is the successful formation and process development of pharmaceutical products because the crystal structures have influenced the physico-chemical and biopharmaceutical properties that are the molecular arrangement within the solid. In this context, pharmaceutical cocrystals, multicomponent crystalline materials with definite stoichiometries often stabilised by hydrogen bonding, has recently regarded a straightforward way to dramatically influence the solid state properties of a drug substance, particular its solubility and hence bioavailability.

The objective of this work is to improve the solubility and dissolution properties of poorly water soluble drugs. Therefore a fundamental understanding of the formation mechanisms, the solution behaviour and the solid-state properties of pharmaceutical cocrystal is required. The work covers screening of cocrystal formation in real time as well as the discovery the five novel salicylic acid cocrystals. The mechanisms of transformation of cocrystals and factors affecting cocrystal stability are reported. More specifically, the aims are to: (1) identify the factors governing the formation and characterization of cocrystals with different cofomers and stoichiometry, (2) establish a screening method of cocrystal formation using Raman spectroscopy, (3) identify the mechanisms of conversion of the cocrystals SAA-4,4'dipy to ASA-4,4'dipy using Raman spectroscopy for in-situ monitoring, (4) investigate the factors of thermodynamics and kinetics affecting cocrystals based on ternary phase diagrams, and (5) understand the solubility behaviour of cocrystals and physico-chemical advantages offered by cocrystals. Model compounds selected in this study include acetylsalicylic acid used as raw API, 4,4'-bipyridine, nicotinamide, isonicotinamide, and piperazine used as cofomer that forms cocrystals.

All of the resulting salicylic acid cocrystals, salicylic acid/ 4,4'dipyridyl (2:1), salicylic acid/ nicotinamide (1:1), salicylic acid/ isonicotinamide (1:1), salicylic acid/ piperazine (1:0.5) and salicylic acid/ N,N'-diacetylpiperazine (2:1) (derived from the reaction between aspirin and piperazine) are obtained from solution cooling/evaporation crystallization experiments. The structural analysis has shown that the well-known COOH...N heterosynthon was considered the key element in the cocrystals design strategy. The carboxylic acid-pyridine hydrogen bond is an often used as supramolecular synthon.

Raman spectroscopy which is an in-situ process analysis technology in the solution crystallization of aspirin is investigated here. The cocrystal formation behavior between

7. Summary

aspirin and 4,4'-dipyridyl in batch cooling crystallization was monitored. In addition, Raman spectroscopy provided additional information on the crystal structure of the salicylic acid-4,4'-bipy cococrystals.

An investigation of the feasibility of in-situ monitoring of the polymorphic transitions is presented. The use of an in-situ tool to monitor the transformation of cococrystals has the potential to provide information about the transformation mechanism. The purpose of this study was to investigate the mechanism of cococrystal transformation of SAA-4,4'-dipy cococrystals to ASA-4,4'-dipy cococrystals using Raman spectroscopy measurements and to design a process to produce different two cococrystals by transformation. The solvent-mediated transformation showed that SAA-4,4'-dipy cococrystals are the stable form at room temperature. Raman spectroscopy successfully distinguished between SAA-4,4'-dipy cococrystals and ASA-4,4'-dipy cococrystals, and the characteristic peak of both was observed during transformation.

The solubility behavior of SAA-4,4'-dipy cococrystals is investigated in an ethanol solvent. The solubility diagram of SAA-4,4'-dipy cococrystals was determined which are formed in a 2:1 stoichiometric ratio in ethanol. In order to improve the fundamentals of the formation mechanisms, solution behavior and solid-state properties of SAA-4,4'-dipy cococrystals, the solubility behavior and solution chemistry of cococrystals was studied. It was found that the thermodynamic stability regions of the cococrystals and its components were defined by the phase diagram. Results have shown that besides the kinetic also thermodynamic factor is important for the crystallization of cococrystals.

8. Abbreviations and symbols

Abbreviation	Meaning
4,4'dipy	4,4'dipyridyl
API	Active pharmaceutical ingredient
ASA	Acetylsalicylic acid
CDS	Cambridge structural database
DSC	Differential scanning calorimetry
EtOH	Ethanol
FT	Fourier transform
INCT	Isonicotinamide
IPA	Iso-propanol
IR	Infrared
m.p	Melting point
MeOH	Methanol
NCT	Nicotinamide
NDAP	N,N'-diacetylpiperazine
PAT	Process analytical technology
PPZ	Piperazine
PSD	Phase solubility diagram
PXRD	Powder x-ray diffractometer
SAA	Salicylic acid
SEM	Scanning electron microscopy
TPD	Ternary phase diagram
VDW	van der Waals

9. References

Symbol	Meaning	Unit
$C_{\text{SAA-4,4'dipy cocystal}}$	Concentration	[g/mL]
K	Solubility product of cocystals	[mol/L]
M_1	Pre-weighed glass vial	[g]
M_2	Weight of vial + solution	[g]
M_3	Weight of vial + evaporated solution	[g]
S	supersaturation	[-]
V	Volume	\AA^3
ΔH	Ethalpy	[J/g]
kV	Tube voltage	[-]
mA	Amperage	[mA]
2θ	Degree	[°]
K/min	Scan rate of XRD	[-]
mW	Power	[mW]
$\bar{\nu}$	Wavenumber	[cm^{-1}]
λ	Wave length	[\AA]
t	time	[s], [min]
T	temperature	[K], [°C]

9. References

- [Aak05] Aakeroy C. B., Salmon D. J., *Building co-crystals with molecular sense and supramolecular sensibility*, CrystEngComm, (2005) 7, 439-448.
- [Aak07] Aakeröy C. B., Fasulo M. E., Desper J., *Cocrystal or salt: Does it really matter?*, Mol. Pharm., (2007) 4, 317-322.
- [Ain09] Ainouz A., Authelin J-R., Billot P., Lieberman H., *Modeling and prediction of cocrystal phase diagrams*, Int. J. Pharm., 374 (2009) 82-89.
- [Air03] Airaksinen S., *Effects of excipients on hydrate formation in wet masses containing theophylline*, J. Pharm. Sci., 92 (2003) 516–528.
- [Aju09] Ajun W., Yan S., Li G., Huili L., *Preparation of aspirin and probucol in combination loaded chitosan nanoparticles and in vitro release study*, Carbohydr. Polym., 75 (2009) 566-574.
- [Aro11] Arora K. K., Tayade N. G., Suryanarayanan, R. *Unintended water mediated cocrystal formation in carbamazepine and aspirin tablets*, Mol. Pharm. (2011) 8, 982–989.
- [Aue03] Auer M. E., Griesser U. J., Sawatzki J., *Qualitative and quantitative study of polymorphic forms in drug formulations by near infrared FT-Raman spectroscopy*, J. Mol. Struct., 661 (2003) 307–317.
- [Ber08] Berry D. J., Seaton C. C., Clegg W., Harrington R. W., Coles S. J., Horton P. N., Hursthouse M. B., Storey R., Jones W., Friščić T., Blagden N., *Applying hot-stage microscopy to co-crystal screening: A study of nicotinamide with seven active pharmaceutical ingredients*, Cryst. Growth Des., (2008) 8, 1697-1712.
- [Bic11] Bica, K., Shamshina, J., Hough, W. L., MacFarlane, D. R., Rogers, R. D., *Liquid forms of pharmaceutical co-crystals: exploring the boundaries of salt formation*, Chem. Commun. (Camb), 47 (2011) 2267–2269.
- [Bon07] Bond A. D., *What is a co-crystal?*, CrystEngComm, (2007) 9, 833-834.

9. References

- [Bon07] Bond A. D., Boese R., Desiraju G. R., *On the polymorphism of aspirin*, *Angewandte Chemie International Edition*, 46 (2007) 615-617.
- [Buč09] Bučar D. K., Henry R. F., Lou X., Duerst R. W., MacGillivray L. R., Zhang G. G. Z., *Cocrystals of caffeine and hydroxybenzoic acids composed of multiple supramolecular heterosynthons: Screening via solution-mediated phase transformation and structural characterization*, *Cryst. Growth Des.*, (2009) 9, 1932-1943.
- [Car98] Carpenter J. F., Prestrelski S. J., Dong A., *Application of infrared spectroscopy to development of stable lyophilized protein formulations*, *Eur. J. Pharm. Biopharm.*, 45 (1998) 231-238.
- [Cha09] Chadwick K., Davey R., Sadiq G., Cross W., Pritchard R., *The utility of a ternary phase diagram in the discovery of new co-crystal forms*. *CrystEngComm*, (2009) 11, 412-414.
- [Che10] Cheney M. L., Weyna D. R., Shan N., Hanna M., Wojtas L., Zaworotko M. J., *Supramolecular architectures of meloxicam carboxylic acid cocrystals, a crystal engineering case study*, *Cryst. Growth Des.*, 10 (2010) 4401-4413.
- [Chi07] Childs S. L., Hardcastle K. I., *Cocrystals of piroxicam with carboxylic acids*, *Cryst. Growth Des.*, 7 (2007) 1291-1304.
- [Chi07] Childs S. L., Stahly G. P., Park A., *The salt-cocrystal continuum: The influence of crystal structure on ionization state*, *Mol. Pharm.*, 4 (2007) 323-338.
- [Chi07] Chiarella R. A., Davey R. J., Peterson M. L., *Making co-crystals the utility of ternary phase diagrams*, *Cryst. Growth Des.*, 7 (2007) 1223-1226.
- [Chi09] Childs S. L., Wood P. A., Rodríguez-Hornedo N., Reddy L. S., Hardcastle K. I., *Analysis of 50 crystal structures containing carbamazepine using the materials module of mercury csd*, *Cryst. Growth Des.*, 9 (2009) 1869-1888.
- [Cho08] Chow K., Tong H. H. Y., Lum S., Chow A. H. L., *Engineering of pharmaceutical materials: An industrial perspective*, *J. Pharm. Sci.*, 97 (2008) 2855-2877.

9. References

- [Coq14] Coquerel, G., *Crystallization of molecular systems from solution: phase diagrams, supersaturation and other basic concepts*, Chem. Soc. Rev., 43 (2014) 2286–300.
- [Cui07] Cui Y., *A material science perspective of pharmaceutical solids*, Int. J. Pharm., 339 (2007) 3-18.
- [De98] De Matas M., Edwards H. G. M., Lawson E. E., Shields L., York P., *FT-Raman spectroscopic investigation of a pseudopolymorphic transition in caffeine hydrate*, J. Mol. Struct., 440 (1998) 97–104.
- [Des95] Desiraju G. R., *Supramolecular synthons in crystal engineering—a new organic synthesis*. Angewandte Chemie International Edition in English, 34 (1995) 2311-2327.
- [Des02] Desiraju G. R., *Hydrogen bridges in crystal engineering: Interactions without borders*, Acc. Chem. Res., 35 (2002) 565-573.
- [Des03] Desiraju G. R., *Crystal engineering. From molecules to materials*, J. Mol. Struct., 656 (2003) 5-15.
- [Des03] Desiraju G. R., *Crystal and co-crystal*, CrystEngComm, (2003) 5, 466-467.
- [Don94] Dong A., Caughey W. S., *Infrared methods for study of hemoglobin reactions and structures*, Methods Enzymol., 232 (1994) 139-175.
- [Elb10] Elbagerma M. A., Edwards H. G. M., Munshi T., Hargreaves M. D., Matousek P., Scowen I. J., *Characterization of new cocrystals by raman spectroscopy, powder x-ray diffraction, differential scanning calorimetry, and transmission raman spectroscopy* Cryst. Growth Des., 10 (2010) 2360-2371.
- [Ett85] Etter M. C., *Aggregate structures of carboxylic acids and amides*, Isr. J. Chem., 25 (1985) 312-319.
- [Ett89] Etter M. C., Frankenbach G. M., *Hydrogen-bond directed cocrystallization as a tool for designing acentric organic solids*, Chem. Mater., (1989) 1, 10-12.

9. References

- [Ett90] Etter M. C., Urbanczyk-Lipkowska Z., Zia-Ebrahimi M., Panunto T. W., *Hydrogen bond-directed cocrystallization and molecular recognition properties of diarylureas*, J. Am. Chem. Soc., 112 (1990) 8415-8426.
- [Ett90] Etter M. C., *Encoding and decoding hydrogen-bond patterns of organic compounds*, Acc. Chem. Res., 23 (1990) 120-126.
- [Ett91] Etter M. C., *Hydrogen bonds as design elements in organic chemistry*, J. Phys. Chem., 95 (1991) 4601-4610.
- [Fai03] Failloux N., Bonnet I., Baron M.-H., Perrier E. *Quantitative analysis of vitamin A degradation by Raman spectroscopy*, Appl. Spectrosc., 57 (2003) 1117–1122.
- [Fáb09] Fábrián L., *Cambridge structural database analysis of molecular complementarity in cocrystals*, Cryst. Growth Des., 9 (2009) 1436-1443.
- [Fon10] Fonari M. S., Ganin E. V., Basok S. S., Lyssenko K. A., Zaworotko M. J., Kravtsov V. C., *Structural study of salicylic acid salts of a series of azacycles and azacrown ethers†*, Cryst. Growth Des., 10 (2010) 5210-5220.
- [Fle03] Fleischman S. G., Kuduva S. S., McMahon J. A., Moulton B, Bailey Walsh R. D., Rodríguez-Hornedo N., Zaworotko M. J., *Crystal engineering of the composition of pharmaceutical phases: Multiple-component crystalline solids involving carbamazepine*, Cryst. Growth Des., 3 (2003) 909-919.
- [Fri09] Friščić, T., Jones, W., *Recent Advances in Understanding the Mechanism of Cocrystal Formation via Grinding.*, Cryst. Growth Des., 9 (2009) 1621–1637.
- [Ger89] Gerrard D., Bowley H., *Instrumentation for raman spectroscopy, Practical raman spectroscopy*. Gardiner D, Graves P (Eds), Springer Berlin Heidelberg, (1989) 55-76.
- [Gho95] Ghosh, S., Grant, D. J. W., *Determination of the solubilities of crystalline solids in solvent media that induce phase changes: Solubilities of 1,2-dialkyl-3-hydroxy-4-pyridones and their formic acid solvates in formic acid and water*, Int. J. Pharm., 114 (1995) 185–196.

9. References

- [Gla01] Glaser R., Aspirin. *An ab initio quantum-mechanical study of conformational preferences and of neighboring group interactions*, J. Org. Chem., 66 (2001) 771-779.
- [Gos06] Goswami S., Jana S., Hazra A., Fun H. K., Anjum S., Atta ur R., *Recognition of creatinine by weak aromatic acids in solid phase along with their supramolecular network*, CrystEngComm, 8 (2006) 712-718.
- [Hab09] Habgood M., Deij M. A., Mazurek J., Price S. L., ter Horst J. H., *Carbamazepine co-crystallization with pyridine carboxamides: Rationalization by complementary phase diagrams and crystal energy landscapes*, Cryst. Growth Des., 10 (2009) 903-912.
- [Hat10] Hathwar V. R., Pal R., Guru Row T. N., *Charge density analysis of crystals of nicotinamide with salicylic acid and oxalic acid: An insight into the salt to cocrystal continuum*, Cryst. Growth Des., 10 (2010) 3306-3310.
- [He08] He G., Jacob C., Guo L., Chow P. S., Tan R. B., *Screening for cocrystallization tendency: The role of intermolecular interactions*, J. Phys. Chem. B, 112 (2008) 9890-9895.
- [Hu05] Hu Y., Liang J. K., Myerson A. S., Taylor L. S. *Crystallization Monitoring by Raman Spectroscopy: Simultaneous Measurement of Desupersaturation Profile and Polymorphic Form in Flufenamic Acid Systems*, Ind. Eng. Chem. Res., 44 (2005) 1233–1240.
- [Hua10] Huang N., Rodríguez-Hornedo N., *Effect of micellar solubilization on cocrystal solubility and stability*, Cryst. Growth Des., 10 (2010) 2050-2053.
- [Jet03] Jetti R. K. R., Boese R., Thallapally P. K., Desiraju G. R., *Five New Pseudopolymorphs of *sym*-Trinitrobenzene*, Cryst. Growth Des., 3 (2003) 1033–1040.
- [Kav10] Kavuru P., Aboarayas D., Arora K. K., Clarke H. D., Kennedy A., Marshall L., Ong T. T., Perman J., Pujari T., Wojtas Ł., Zaworotko M. J., *Hierarchy of supramolecular synthons: Persistent hydrogen bonds between carboxylates*

9. References

- and weakly acidic hydroxyl moieties in cocrystals of zwitterions*, Cryst. Growth Des., 10 (2010) 3568-3584.
- [Koj06] Kojima T., *Crystalline form information from multiwell plate salt screening by use of Raman microscopy*, Pharm. Res., 23 (2006) 806–812.
- [Lee10] Lee T., Wang P. Y., *Screening, manufacturing, photoluminescence, and molecular recognition of co-crystals: Cytosine with dicarboxylic acids*, Cryst. Growth Des., 10 (2010) 1419-1434.
- [Lee14] Lee K. S., Kim K. J., Ulrich J., *In-situ monitoring of cocrystallization of salicylic acid–4,4'-dipyridyl in solution using raman spectroscopy*, Cryst. Growth Des., 14 (2014) 2893-2899.
- [Lee15] Lee K. S., Kim K. J., Ulrich J., *Formation of salicylic Acid/4,4'-Dipyridyl Cocrystals Based on the Ternary Phase Diagram*, Chem. Eng. Technol., 38 (2015) 1073-1080.
- [Lei69] Leiserowitz L., Schmidt G. M. J., *Molecular packing modes. Part iii. Primary amides*, Journal of the Chemical Society A: Inorganic, Physical, Theoretical (1969) 2372-2382.
- [Lei76] Leiserowitz L., *Molecular packing modes. Carboxylic acids*, Acta Crystallogr., Sect. B: Struct. Sci, 32 (1976) 775-802.
- [Lim97] Limmatvapirat S., Yamaguchi K., Yonemochi E., Oguchi T., Yamamoto K., *A 1:1 deoxycholic acid-salicylic acid complex* Acta Crystallogr., Sect. C: Cryst. Struct. Commun., 53 (1997) 803-805.
- [Lor01] Lorenz, H., Sheehan, P., Seidel-Morgenstern, A., *Coupling of simulated moving bed chromatography and fractional crystallisation for efficient enantioseparation.*, J. Chromatogr. A, 908 (2001) 201–214.
- [Lu08] Lu E., Rodriguez-Hornedo N., Suryanarayanan R., *A rapid thermal method for cocrystal screening*, CrystEngComm, 10 (2008) 665-668.
- [Lu09] Lu J., Rohani S., *Preparation and characterization of theophylline–nicotinamide cocrystal*, Org. Process Res. Dev., 13 (2009) 1269-

9. References

- 1275.
- [Lu12] Lu Y., Qi J., Wu W., *Absorption, disposition and pharmacokinetics of nanoemulsions*, *Curr. Drug Metab.*, 13 (2012) 396–417.
- [Mac00] Mackowiak P. A., *Brief history of antipyretic therapy*, *Clinical Infectious Diseases*, 31 (2000) (Supplement 5): S154-S156.
- [Mah09] Maheshwari C., Jayasankar A., Khan N. A., Amidon G. E., Rodriguez-Hornedo N., *Factors that influence the spontaneous formation of pharmaceutical cocrystals by simply mixing solid reactants*, *CrystEngComm*, 11 (2009) 493-500.
- [McN06] McNamara D. P., Childs S. L., Giordano J., Iarriccio A., Cassidy J., Shet M. S., Mannion R., O'Donnell E., Park A., *Use of a glutaric acid cocrystal to improve oral bioavailability of a low solubility api*, *Pharm Res*, 23 (2006) 1888-1897.
- [Mit67] Mitchell A. G., Saville D. J., *The dissolution of aspirin and aspirin tablets**, *J. Pharm. Pharmacol.*, 19 (1967) 729-734.
- [Moh11] Mohammad M. A., Alhalaweh A., Velaga S. P., *Hansen solubility parameter as a tool to predict cocrystal formation*, *Int. J. Pharm.*, 407 (2011) 63-71.
- [Muk13] Mukherjee A., Tothadi S., Chakraborty S., Ganguly S., Desiraju G. R., *Synthon identification in co-crystals and polymorphs with IR spectroscopy. Primary amides as a case study*, *CrystEngComm*, 15 (2013) 4640-4654.
- [Neh05] Nehm S. J., Rodríguez-Spong B., Rodríguez-Hornedo N., *Phase solubility diagrams of cocrystals are explained by solubility product and solution complexation*, *Cryst. Growth Des.*, 6 (2005) 592-600.
- [Ném05] Németh Z., Hegedűs B., Szánta, C., Sztatisz J., Pokol G., *Pressurization effects on the polymorphic forms of famotidine*, *Thermochim. Acta*, 430 (2005) 35–41.
- [Nor06] Nordström F. L., Rasmuson Å. C., *Solubility and melting properties of salicylic acid*, *J. Chem. Eng. Data*, 51 (2006) 1668-1671.
- [O'Br04] O'Brien L. E., Timmins P., Williams A. C., York P., *Use of in-situ FT-Raman*

9. References

- spectroscopy to study the kinetics of the transformation of carbamazepine polymorphs*, J. Pharm. Biomed. Anal., 36 (2004) 335–340.
- [Ouv04] Ouvrard C., Price S. L., *Toward crystal structure prediction for conformationally flexible molecules: The headaches illustrated by aspirin*, Cryst. Growth Des., 4 (2004) 1119-1127.
- [Pra02] Pratiwi D., Fawcett J. P., Gordon K. C., Rades T., *Quantitative analysis of polymorphic mixtures of ranitidine hydrochloride by Raman spectroscopy and principal components analysis*, Eur. J. Pharm. Biopharm., 54 (2002) 337–341.
- [Qia13] Qiao N., Wang K., Schlindwein W., Davies A., Li M., *In-situ monitoring of carbamazepine-nicotinamide cocrystal intrinsic dissolution behavior*, Eur. J. Pharm. Biopharm., 83 (2013) 415–26.
- [Rag09] Rager T., Hilfiker R., *Stability domains of multi-component crystals in ternary phase diagrams*, Zeitschrift für Physikalische Chemie International journal of research in physical chemistry and chemical physics, 223 (2009) 793.
- [Rod06] Rodríguez-Hornedo N., Nehm S. J., Seefeldt K. F., Pagán-Torres Y., Falkiewicz C. J., *Reaction crystallization of pharmaceutical molecular complexes*, Mol. Pharm., (2006) 3, 362-367.
- [Sch09] Schartman R. R., *On the thermodynamics of cocrystal formation*, Int. J. Pharm., 365 (2009) 77-80.
- [Sch09] Schultheiss N., Newman A., *Pharmaceutical cocrystals and their physicochemical properties*, Cryst. Growth Des., 9 (2009) 2950-2967.
- [Sim81] Simon B., Boistelle R., *Crystal growth from low temperature solutions*, J. Cryst. Growth, 52 (1981) 779–788.
- [Sin74] Singh T. P., Vijayan M., *Structural studies of analgesics and their interactions. li. The crystal structure of a 1:1 complex between antipyrine and salicylic acid (salipyrine)*, Acta Crystallogr., Sect. B: Struct. Sci, 30 (1974) 557-562.
- [Sko03] Skoulika S. G., Georgiou C. A., *Rapid, noninvasive quantitative determination of acyclovir in pharmaceutical solid dosage forms through their poly(vinyl*

9. References

- chloride) blister package by solid-state Fourier transform Raman spectroscopy*, Appl. Spectrosc., 57 (2003) 407–412.
- [Sko09] Skovsgaard S., Bond A. D., *Co-crystallisation of benzoic acid derivatives with n-containing bases in solution and by mechanical grinding: Stoichiometric variants, polymorphism and twinning*, CrystEngComm, 11, (2009) 444-453.
- [Sta02] Starbuck C., *Process Optimization of a Complex Pharmaceutical Polymorphic System via In-situ Raman Spectroscopy*, Cryst. Growth Des., 2 (2002) 515–522.
- [Ste10] Stevens J. S., Byard S. J., Schroeder S. L., *Salt or co-crystal? Determination of protonation state by x-ray photoelectron spectroscopy (xps)*, J. Pharm. Sci., 99 (2010) 4453-4457.
- [Sve99] Svensson O., Josefson M., Langkilde F. W., *Reaction monitoring using Raman spectroscopy and chemometrics*, Chemom. Intell., Lab. Syst. 49 (1999) 49–66.
- [Tak08] Takata N., Shiraki K., Takano R., Hayashi Y., Terada K., *Cocrystal screening of stanolone and mestanolone using slurry crystallization*, Cryst. Growth Des., 8, (2008), 3032-3037
- [Tra05] Trask A. V., Motherwell W. D. S., Jones W., *Pharmaceutical cocrystallization: Engineering a remedy for caffeine hydration*, Cryst. Growth Des., 5 (2005) 1013-1021.
- [Taw68] Tawashi R., *Aspirin: dissolution rates of two polymorphic forms*, Science 160 (1968) 76.
- [Tay00] Taylor L. S., Langkilde F. W., *Evaluation of solid-state forms present in tablets by Raman spectroscopy*, J. Pharm. Sci., 89 (2000) 1342–1353.
- [Tra05] Trask A. V., Motherwell W. D. S., Jones W., *Pharmaceutical cocrystallization: Engineering a remedy for caffeine hydration*, Cryst. Growth Des., 5 (2005) 1013-1021.

9. References

- [Tra06] Trask A. V., Motherwell W. D. S., Jones W., *Physical stability enhancement of theophylline via cocrystallization*, Int. J. Pharm., 320 (2006) 114-123.
- [Tra07] Trask A. V., *An overview of pharmaceutical cocrystals as intellectual property*, Mol. Pharm., (2007) 4, 301-309.
- [Van90] Vane J.R., Flower R. J., Botting R. M., *History of aspirin and its mechanism of action*, Stroke; a journal of cerebral circulation, 21 (1990) 12-23.
- [Ver02] Vergote G. J., Vervaet C., Remon J. P., Haemers T., Verpoort F. *Near-infrared FT-Raman spectroscopy as a rapid analytical tool for the determination of diltiazem hydrochloride in tablets*, Eur. J. Pharm. Sci., 16 (2002) 63–67.
- [Vip01] Vippagunta S. R., Brittain H. G., Grant D. J., *Crystalline solids*, Adv. Drug Delivery Rev., 48 (2001) 3-26.
- [Vis06] Vishweshwar P., McMahon J. A., Bis J. A., Zaworotko M. J., *Pharmaceutical co-crystals*, J. Pharm. Sci., 95 (2006) 499-516.
- [Wal03] Walsh R. D. B., Bradner M. W., Fleischman S., Morales L. A., Moulton B., Rodriguez-Hornedo N., Zaworotko M. J., *Crystal engineering of the composition of pharmaceutical phases*, Chem. Commun., (2003) 2, 186-187.
- [Wan00] Wang F., Wachter J. A., Antosz F. J., Berglund K. A. *An Investigation of Solvent-Mediated Polymorphic Transformation of Progesterone Using in-situ Raman Spectroscopy*, Org. Process Res. Dev., (2000) 4, 391–395.
- [War05] Wartewig S., Neubert R. H. H. *Pharmaceutical applications of Mid-IR and Raman spectroscopy*, Adv. Drug Deliv. Rev., 57 (2005) 1144–1170.
- [Wey09] Weyna D. R., Shattock T., Vishweshwar P., Zaworotko M. J., *Synthesis and structural characterization of cocrystals and pharmaceutical cocrystals: Mechanochemistry vs slow evaporation from solution*, Cryst. Growth Des., 9 (2009) 1106-1123.
- [Zha07] Zhang G. G., Henry R. F., Borchardt T. B., Lou X., *Efficient co-crystal screening using solution-mediated phase transformation*, J. Pharm. Sci., 96 (2007) 990-995.

9. References

- [Zhu97] Zhu, H., Khankari, R. K., Padden, B. E., Munson, E. J., Gleason, W. B., Grant, D. J., *Physicochemical characterization of nedocromil bivalent metal salt hydrates. 1. Nedocromil magnesium*, J. Pharm. Sci., 86 (1996) 1026–34.
- [Zhu97] Zhu, H., Halfen, J. A., Young, V. G., Padden, B. E., Munson, E. J., Menon, V., Grant, D. J., *Physicochemical characterization of nedocromil bivalent metal salt hydrates. 3. Nedocromil calcium*, J. Pharm. Sci., 86 (1997) 1439–47.

10. Declaration

I declare that I have not completed or initiated a doctorate procedure at any other university with this dissertation topic. It is a compilation of the results of work carried out by my own by students under my supervision. The used resources and tools or previously cited information have been distinguished by quotation marks.

Halle (Saale), 30/11/2015

M. Sc. Kyeongsill Lee

Curriculum vitae

Kyeongsill Lee

First Name: Kyeongsill

Last Name: Lee

Gender: Female

Date of birth: 04/10/1984

Place of birth: Daejeon

Country of birth: South Korea

Nationality: Korean

E-mail: baanmo@nate.com

Mobile Number: (+82)10-2846-1320

Education Experiences:

- | | |
|-------------------|--|
| 03/2010 - Present | PhD at the chair of Thermal Process Technology, Martin Luther University Halle-Wittenberg, in Germany
PhD thesis with the title:
Cocrystal Formation –Thermodynamic and Kinetics - |
| 03/2008 - 02/2010 | Holder of M.Sc. degree in chemical engineering in Hanbat National University, in Korea
Master thesis with the title:
Control of Yield and Purity of Pharmaceutical ingredient in Salting-out Crystallization |
| 03/2003 – 02/2008 | Holder of B.Sc. degree in chemical engineering in Hanbat National University, in Korea. |

Scientific works

- 10/2012 - Present Formation of co-crystal of pharmaceutical ingredients by using solution crystallization : Thermodynamics and kinetics
- 03/2010 – 09/2012 Product design by crystallization processes: Sugar coating on APIs by cooling crystallization
- 02/2009 – 02/2010 Upgrading purity and yield of pharmaceutical ingredient by salting-out crystallization
- 03/2008 - 01/2009 Treatment of wastewater containing organic solvent using layer melt crystallization & Separation acetic acid and pure water by melting crystallization

Peer Reviewed Publications in Journals and Proceedings:

- 2015 Lee K. S., Kim K. J., Ulrich J.: Formation of Salicylic Acid/4,4'-Dipyridyl Cocrystals Based on the Ternary Phase Diagram. **Chemical Engineering & Technology** 2015, 38 (6), 1073-1080.
- 2014 Lee K. S., Kim K. J., Ulrich J.: N-H...O, O-H...O hydrogen bonded supramolecular formation in the cocrystal of salicylic acid with N-containing bases, in proceeding of ISIC 19 (19th International Symposium on Industrial Crystallization), Toulouse, edited by Biscans B., Mazzotti M., 2014, p.340-343.
- 2014 Lee K. S., Kim K. J., Ulrich J.: Formation of salicylic acid/4,4'-dipyridyl cocrystal based on the ternary phase diagram, in proceeding of BIWIC 21 (21st International Workshop on Industrial Crystallization), Rouen, edited by Gérard C., Yohann C., Nicolas C., 2014, p. 35-41.
- 2014 Lee K. S., Kim K. J., Ulrich J.: In situ monitoring of cocrystallization of salicylic acid-4,4'-dipyridyl in solution using raman spectroscopy. **Crystal Growth & Design** 2014, 14 (6), 2893-2899.
- 2012 Lydia Helmdach, Dan Pertig, Stefanie Rüdiger, Kyeong-Sill Lee, Torsten Stelzer, Joachim Ulrich,: *Bubbles - Trouble-Makers in Crystallizers Classical Problems*

during *Inline Measurements*, **Chemical Engineering & Technology 2011**, 35 (6), 1017-1023.

- 2012 Lee K. S., Kim K. J., Ulrich J.: Coating of pharmaceutical ingredient using crystallization, in proceeding of BIWIC 19 (19th International Workshop on Industrial Crystallization), Tianjin, edited by Sha Z., Yin Q., Chen J., Xie C., 2012, p. 652-657.
- 2012 Lee K. S., Kim K. J., Ulrich J.: Sugar crystallization in ethanol-water mixture by drowning-out crystallization, in proceeding of HIW 2012 (Hanbat International Workshop on Industrial and Pharmaceutical Crystallization), Daejeon, edited by Kim K.J., 2012, P. 105-112.
- 2012 Lee K. S., Kim K. J., Ulrich J.: Development of sugar coating method on pharmaceutical ingredient using cooling crystallization, in proceeding of HIW 2012 (Hanbat International Workshop on Industrial and Pharmaceutical Crystallization), Daejeon, edited by Kim K.J., 2012, P. 105-112.
- 2011 Lee K. S., Ulrich J.: Formation of crystalline coatings by solution crystallization, in proceeding of ISIC 18 (18th International Symposium on Industrial Crystallization), Zürich, edited by Biscans B., Mazzotti M., 2011, p. 363-364.

Patents:

Kwang-Joo Kim, Kyeong-sill Lee: Process for Preparation and Conversion of Taltirelin Crystalline Form α , Korea Patent Application 10-2013-0168997, filed December 31, 2013.

Oral presentations:

- 09/2014 Lee K. S., Kim K. J., Ulrich J.: Formation of salicylic acid/4,4'dipyridyl cocrystal based on the ternary phase diagram, BIWIC 2014 (21st International Workshop on Industrial Crystallization), Rouen, (10-12, September 2014).
- 09/2012 Lee K. S., Kim K. J., Ulrich J.: Development of sugar coating method on pharmaceutical ingredient using cooling crystallization, HIW 2012, Daejeon (5-6 September 2012).
- 06/2012 Lee K. S., Ulrich J.: Coating of pharmaceutical ingredient using crystallization,

ACHEMA 2012, Frankfurt am Main (18-22 June 2012).

10/2011 University of Szeged Faculty of pharmacy department in Hungary: Formation of crystalline coatings by solution crystallization, (11-12 October 2011).

Poster:

10-11/2014 Cocystal formation of aspirin/4,4'dipyridyl: crystallization pathway by monitoring of solute concentration based on ternary phase diagram
ICSST14 (10th International conference on Separation Science and Technology)
Nara City, 30.10-01.11.2014

09/2014 N-H...O, O-H...O hydrogen bonded supramolecular formation in the cocystal of salicylic acid with N-containing bases
ISIC 19 (19th International Symposium on Industrial Crystallization)
Toulouse, 16-19.09.2014

06/2014 In situ monitoring of the transformation of aspirin cocystal using Raman spectroscopy
ACTS-2014 & CGOM 11 (Joint Congress of Asian Crystallization Technology Symposium-2014 and 11th international Workshop on Crystal Growth of Organic materials)
Nara City, 17-20.06.2014

11/2013 Control of co-crystal and polymorphs of pharmaceuticals by solution crystallization
AIChE 2013 (American institute of Chemical Engineers)
San Francisco, 3-8.11.2013

04/2013 Sugar coating on pharmaceutical ingredient using solution crystallization
KCS 2013 (111st Korean Chemical Society)
Ilsan, 17-19.04.2013

09/2012 Coating of pharmaceutical ingredient using crystallization
BIWIC 2012 (19th international Workshop on Industrial Crystallization)
Tainjin, 7-9.09.2012

Curriculum vitae

09/2011 Sugar crystallization in ethanol-water mixture by drowning-out crystallization
HIW 2012 (Hanbat International Workshop on Industrial and Pharmaceutical
Crystallization)
Daejeon, 5-6.09.2012

09/ 2011 Formation of crystalline coatings by solution crystallization
ISIC 2011 (18th International Symposium on Industrial Crystallization)
Zürich, 15.09.2011

30/11/2015

Kyeongsill Lee

Declaration under Oath

Declaration under Oath

I declare under oath that this thesis is my own work entirely and has been written without any help from other people. I used only the sources mentioned and included all the citations correctly both in word or content.

30/11/2015

Kyeongsill Lee